Universidade de Aveiro: Departamento de Ciências Médicas
Ano 2019

Vasco de Almeida Lucas

Redes metabólicas no envelhecimento e doenças relacionadas com o envelhecimento

Metabolic networks in aging and age-related diseases

This work was supported by projects pAGE (CENTRO2020 CENTRO-01-0145-FEDER-000003) and iBiMED (UID/BIM/04501/2019, project POCI-01-0145-FEDER-007628)

Universidade de Aveiro: Departamento de Ciências Médicas
Ano 2019

Vasco de Almeida Lucas

Redes metabólicas no envelhecimento e doenças relacionadas com o envelhecimento

Metabolic networks in aging and age-related diseases

Tese apresentada à Universidade de Aveiro para cumprimento dos requisitos necessários à obtenção do grau de Mestre em Biomedicina Molecular, realizada sob a orientação científica do Doutora Raquel M Silva, Investigadora Auxiliar, Universidade Católica Portuguesa

This work was supported by projects pAGE (CENTRO2020 CENTRO-01-0145-FEDER-000003) and iBiMED (UID/BIM/04501/2019, project POCI-01-0145-FEDER-007628)

O júri

President

Prof. Doutor Ramiro Almeida
professor Auxiliar do Departamento de Ciências Médicas da Universidade de Aveiro

Prof. Doutora Ana Cristina de Fraga Esteves
professora Auxiliar, Universidade Católica Portuguesa

Prof. Doutora Raquel M. Silva

investigadora Auxiliar, Universidade Católica Portuguesa

Agradecimentos

This work would not be possible without some people and institutions to whom I want to express my gratitude.

Firstly, for accepting and providing all de condition necessary to the development of this work, I want to thank Aveiro University specially to the Medical Sciences Department, the Institute of Biomedicine and the Institute of Electronic and Telematic Engineering of Aveiro, IEETA.

To **Dra. Raquel Silva** for all the effort invested in this work, all the conditions, arrangements and considerations, all the teachings, advices and guidance that allowed me to make my way through all this process.

To **Diogo Neves** for all the patience, time and effort invested in teaching me and developing this work. For always be willing to spare some of his time in order to clarify any question that would come up, and for doing it with a consistent patience and sympathy.

To **Ana Teixeira** and **Sara Duarte-Pereira** for introducing me to laboratory and bioinformatic work respectively.

To **Dr. Sérgio Matos** from IEETA department for creating the Egas datasets and for giving me access to this software,

To **Dr. Nuno Neves** for giving me a ride to Aveiro every time he could making it possible to conciliate every aspect of my life with the elaboration of this thesis and the academic challenges offered by the master's degree in **Molecular Biomedicine,**

To **Ludmilla Blaschikoff** for listening to my day to day chattering, for supporting and encouraging me to put all the effort in this work and for always being available to help with every problem that came up,

To **João Guilherme Silva (JG)** for being my confident, for listening and enduring all my frustrations and for being a cheering force throughout this whole process,

To **Alexandre Nunes** for all the small talk chats, helping me take my mind of the day to day stress specially during lunch time and for always answering my unusual silly questions.

To my uncle **José Manuel Ruas** for always providing transportation, place and conditions to stay in Aveiro whenever I needed, making it possible to always comply with the day to day academical demands, and for and always willing to help me with every problem that would come up.

To all my family specially to my aunts **Paula Lucas** and **Maria Manuela Ruas** for always be willing to help with every matter;

And finally, to my mother **Maria Augusta Faria de Almeida Ruas** and father **Paulo Jorge Dias Lucas** and my sister **Marta de Almeida Lucas** whose presence, love and dedication are of the most importance not only to elaboration of this thesis but also to every aspect of my life.

Palvras-Chave

NAD^+, NAMPT, NAPRT, FK866, Envelhecimento, Doenças associadas ao envelhecimento, Proteostase, EGAS, Cytoscape, ClueGo, Redes proteicas

Resumo

O envelhecimento é um processo fisiológico natural, contudo as suas causas específicas não são totalmente compreendidas ao nível molecular. Durante o envelhecimento, os níveis do cofator redox Nicotinamida Adenina Dinucleotídeo (NAD^+) diminuem. Esta molécula é essencial para a produção de energia por parte da célula e também é um substrato para uma variedade de enzimas que regulam a expressão genética e a sobrevivência celular.

Para obter informações sobre as redes metabólicas de doenças relacionadas com o envelhecimento, adotamos uma combinação de abordagens bioinformática e molecular. Utilizamos métodos de extração de texto para extrair dados de interação proteica de 1500 resumos de artigos da PubMed contendo palavras-chave relacionadas com proteostase, envelhecimento e doenças relacionadas com o envelhecimento. As redes de proteínas foram obtidas com o Cytoscape e submetidas a uma análise baseada em parâmetros. Seguiu-se uma análise de enriquecimento usando o ClueGo um plug-in do Cytoscape. A análise de parâmetros revelou APP como a proteína mais central e influente na rede e a análise de enriquecimento retratou uma predominância de termos relacionados com o sistema imunológico, juntamente com a regulação do ciclo celular.

Como modelo celular, usamos um inibidor do metabolismo do NAD^+ em células de neuroblastoma SH-SY5Y para imitar o declínio do NAD^+ durante o envelhecimento. Em diferentes momentos (8h, 24h, 48h e 72h), medimos a viabilidade celular juntamente com os níveis de expressão de NAMPT e NAPRT, as enzimas limitadoras de taxa das vias Salvage de Nicotinamida e Preiss-Handler, respetivamente, ambas vias de produtoras de NAD^+. Os Nossos resultados mostram uma diminuição de 50% na viabilidade celular às 48h, juntamente com uma diminuição na expressão proteica de NAPRT. Não foram registadas alterações nos níveis de proteína NAMPT em nenhum momento. É possível que outras vias de biossíntese do NAD^+ estejam ativas, de maneira que outros estudos com o objetivo de elucidar esta questão são necessários.

Keywords

NAD^+, NAMPT, NAPRT, FK866, Aging, Aging-related diseases, Proteostasis, EGAS, Cytoscape, ClueGo, Protein Networks

Abstract

Aging is a natural physiological process, but its specific causes are not entirely understood at the molecular level. During aging, the levels of the redox cofactor Nicotinamide Adenine Dinucleotide (NAD) decrease. This molecule is essential for energy production by the cell and is also a substrate to a range of enzymes that regulate gene expression and cell survival.

To gain insight into the metabolic networks of age-related disorders, we took a combined bioinformatics and molecular approach. We used text-mining methods to extract protein interaction data from 1500 PubMed abstracts containing keywords related to proteostasis, aging and age-related diseases. Protein networks were obtained with Cytoscape and were submitted to parameter-based analysis. An enrichment analysis using the cytoscape plug-in ClueGo was followed. Parameter analysis revealed APP as the most central and influential protein in the network and enrichment analysis depicted a predominance of terms related to Immune system along with Cancer and Cell Cycle regulation.

As a cellular model, we have used a NAD metabolism inhibitor in SH-SY5Y neuroblastoma cells to mimic the NAD decline during aging. At different time points (8h, 24h, and 48h) we measured cell viability along with the expression levels of NAMPT and NAPRT, the rate-limiting enzymes from the NAD biosynthetic nicotinamide salvage pathway and the Preiss handler pathway respectively. Our results show a 50% decrease in cell viability at 48h along with a decrease in NAPRT protein expression. No alterations in NAMPT protein levels were recorded in any measured time point. It is possible that other NAD biosynthesis pathways are activated, so further studies intended to elucidate question are required.

Outline

Figures List

Table List

List of Abbreviations:

NAD^+: Nicotinamide Adenine Dinucleotide

NADP: Nicotinamide Adenine Dinucleotide Phosphate

PARP-1: Poly (ADP-ribose) polymerase-1

NA: Nicotinic acid

NAM: Nicotinamide

NR: Nicotinamide riboside

NMN: Nicotinamide Mononucleotide

ACMS: α-amino-β-carboxymuconate-ε-semialdehyde

QPRT: Quinolinate phosphoribosyltransferase

AMS: α-amino-β-muconate-ε-semialdehyde

ACMSD: α-amino-β-carboxymuconate-ε-semialdehyde decarboxylase

PARPs: Poly-ADP-ribose polymerases

NAMPT: Nicotinamide Phosphoribosyltransferase

NMNAT: Nicotinamide Mononucleotide Adenylyltransferase

NAMN: Nicotinic acid mononucleotide

NAAD: Nicotinic Acid Adenine Dinucleotide

NMRK1: Nicotinamide Riboside Kinase 1

NMRK2: Nicotinamide Riboside Kinase 2

ADP: Adenosine diphosphate

ARTs: ADP-ribosyltransferases

SIRT: Sirtuin

NF-kB: Nuclear factor kappa-light-chain-enhancer of activated B cells

FoxO3: Forkhead box O3

TNF-α: Tumor necrosis factor alpha

MAPK: Mitogen-activated protein kinase

JNK: c-Jun N-terminal kinase

ATP: Adenosine triphosphate

IL-6: Interleukin 6

HTT: Huntingtin

APOE: Apolipoprotein E

STAT3: Signal transducer and activator of transcription 3

PPARD: Peroxisome proliferator-activated receptor delta

PTEN: Phosphatase and tensin homolog

ER: Endoplasmic reticulum

HSP: Heat shock proteins

ROS: Reactive oxygen species

UPS: Ubiquitin-Proteasome System

ERAD: ER-associated degradation

IRE1: Inositol-requiring enzyme 1

ATF6: Activating transcription factor-6

PERK: Protein kinase RNA (PKR)-like ER kinase

XBP1: X-box binding protein 1

UPR: Unfolded Protein Response

sHSP: Small HSP

AA´s: Antibiotic-Antimycotic

BCA: Bison Kinetic Acid Assay

P3: Proteostasis 3 first 200 articles

P4: Proteostasis 4 first 200 articles

P4T: Proteostasis 4 1500 articles

MAPT: Microtubule-associated protein tau

CLU: Clusterin

IGFLR1: IGF like family receptor 1

RELN: include Reelin

EIF2S1: Eukaryotic translation initiation factor 2 subunit 1

SCNA: Alpha-synuclein

RHBDF2: Rhomboid family member 2

BACE1: β-secretase 1

sAPPα: Amyloid precursor protein-α

sAPPβ: Amyloid precursor protein-β

NMDA: N-methyl-d-aspartate

CREB: cAMP response element-binding protein

ESC: Embryonic stem cells

GTP: Guanosine triphosphate

HIF-1α: Hypoxia inducible factor-1α

DAMPs: Danger-associated molecular patterns

TLR2: Toll-like receptor 2

IL-1β: Interleukin-1β

CARD: Caspase activation and recruitment domains

IL-4: Interleukin-4

ARG1: Arginase-1

IDE: insulin-degrading enzyme

POCD: Postoperative cognitive dysfunction

IL17A: Interleukin17A

TGFβ: Transforming growth factor-β

CX3CR1: G-protein coupled receptor 13

CX3CL1: Chemokine C-X3-C motif ligand 1

MPTP: 1-methyl-4-phenyl-1,2,3,6-tetrahydropyridine

VEGF: Vascular endothelial growth factor

1.Introduction

1.1. Nicotinamide Adenine Dinucleotide (NAD^+)

The discovery of the Nicotinamide Adenine Dinucleotide (NAD^+) molecule dates back to the beginning of the 20th century, after the British biochemists Arthur Harden and William John Young [1] noticed the presence of a fermentation stimulator molecule in boiled yeast extracts, which they later named Cozymase. It was only in 1930 that its chemical composition was discovered by a Swedish chemist named Hans von Euler-Chelpin [2], who described it as a nucleotide sugar phosphate. Later in 1936, Otto Heinrich Warburg discovered the role of Cozymase in the several redox reactions, which consist of the transfer of hydride from one molecule to another, performed by the nicotinamide ring [3]

NAD^+ is composed by two ribose ringed nucleotides (nicotinamide and adenine) that are linked by two phosphate groups. NAD^+ participates in several redox reactions given its ability to bind electrons and, as a result, reducing NAD^+ to NADH which can then be used as a reducing agent to donate electrons. This co-enzyme is associated with several cellular catabolic processes including beta-oxidation of fatty acids, tricarboxylic acid cycle, and glycolysis. NAD^+ can also be converted into nicotinamide adenine dinucleotide phosphate ($NADP^+$) by the addition of a phosphate group in the second position of the adenine moiety ribose ring by NAD kinases. This is a crucial cofactor in very important anabolic reactions, such as the pentose phosphate pathway, which requires NADPH (the reduced form of $NADP^+$) as a reducing agent as well as in cholesterol synthesis and fatty acid chain elongation [4].

1.2. NAD^+ biosynthetic pathways

In mammals, NAD^+ levels tend to rise or fall depending on the cellular functions [5]. Biosynthesis of NAD^+ can be made from several molecules that are able to activate respective NAD^+ biosynthesis pathways called NAD^+ precursors. Two examples are nicotinic acid (NA) and nicotinamide (NAM), which together are also called niacin. These molecules were firstly identified by an American biochemist, Conrad Elvehjemby in 1938 [6]. Other more recently discovered NAD^+ precursor is nicotinamide riboside (NR), described by Charles Brenner and co-workers in 2004 [7]. All these molecules can contribute to NAD^+ production [8] and are part of the vitamin B3 complex usually obtained from diet. The impairment in NAD^+ production is particularly linked to the development of a pathology called pellagra that can result in symptoms like diarrhea, dermatitis, dementia and ultimately can lead to death [9].

In addition to niacin, the amino acid L-tryptophan can also trigger the production of NAD^+ through a NAD^+ biosynthesis pathway called the de novo pathway. The first reaction of this pathway consists essentially in the conversion of tryptophan into N-formylkynurenine catalyzed by either Indoleamine 2,3-dioxygenase, induced by inflammatory stimuli [10] [11], or Tryptophan 2,3-dioxygenase activated by tryptophan and glucocorticoids [12] [13]. Although they have similar functions, these enzymes are found in different amounts in different tissues. Tryptophan 2,3-dioxygenase is primarily found in liver tissue where it is reported to have highest activity, in contrast to Indoleamine 2,3-dioxygenase that is more prominent in extrahepatic tissues having its highest activity in the intestine, lung and spleen [14] [15]

N-formylkynurenine is converted into kynurenine by Kynurenine formamidase (AFMID), which is then transformed into 3-OH kynurenine by the action of the enzyme kynurenine 3-monooxygenase. Kynureninase acts on 3-OH kynurenine, transforming it in 3-hydroxyanthranilate that finaly is coverted into α-amino-β-carboxymuconate-ε-semialdehyde (ACMS) by 3-hydroxyanthranilate 3,4-dioxygenase [9].

From this stage, ACMS can go on to form NAD^+ after its conversion into quinolinic acid by spontaneous cyclization and consequently formation of NAMN after condensation with 5-phospho-α-D-ribose 1-diphosphate, a process catalyzed by the enzyme Quinolinate phosphoribosyltransferase (QPRT) [16]. NAMN is then inserted in the Preiss-Handler pathway leading to the formation of NAD^+. This whole process can only take place if the ACMS cellular stock fails to meet the quantity required for an enzymatic reaction, otherwise α-amino-β-carboxymuconate-ε-semialdehyde decarboxylase (ACMSD) converts it into α-amino-β-muconate-ε-semialdehyde (AMS) (**Figure 1**).

NAM salvage pathway begins when NAM is transformed in Nicotinamide mononucleotide (NMN) by the enzyme Nicotinamide phosphoribosyltransferase (NAMPT), a protein that was discovered and named pre-B enhancing colony factor, because it was thought to function as a cytokine [17]. NMN is then transformed in NAD^+ in a reaction catalyzed by Nicotinamide mononucleotide adenylyltransferase (NMNAT) (**Figure 1**), which is described to have three different isoforms present in different cell organelles: NMNAT1 is present in the nucleus [18] [19] [20], NMNAT2 can be found in both the cytosol and Golgi apparatus [21] [20], and NMNAT3 can be detected in the mitochondria [22] [20].

NAD^+ can also be produced from NA through the Preiss-Handler pathway, which begins with the production of Nicotinic Acid Mononucleotide (NAMN) from NA. Similarly to NMN, NAMN is also

recognized by NMNATs converting it in Nicotinic Acid Adenine Dinucleotide (NAAD) which is then transformed into NAD^+ by NAD synthase [23] (**Figure 1**).

NR was firstly described as a NAD^+ precursor in bacteria not able to perform the Preiss-Handler and *de novo* pathways due to the lack of intermediate enzymes [24] [25] [26]. In mammals, NR is transformed into NMN by the phosphorylating activity of the Nicotinamide riboside kinase 1 (NMRK1) or Nicotinamide riboside kinase 2 (NMRK2) enzymes. These are mostly expressed in liver, skeletal muscle, heart and brown adipose tissue [5]. NMN is then converted to NAD^+ by the NMNATs (**Figure 1**).

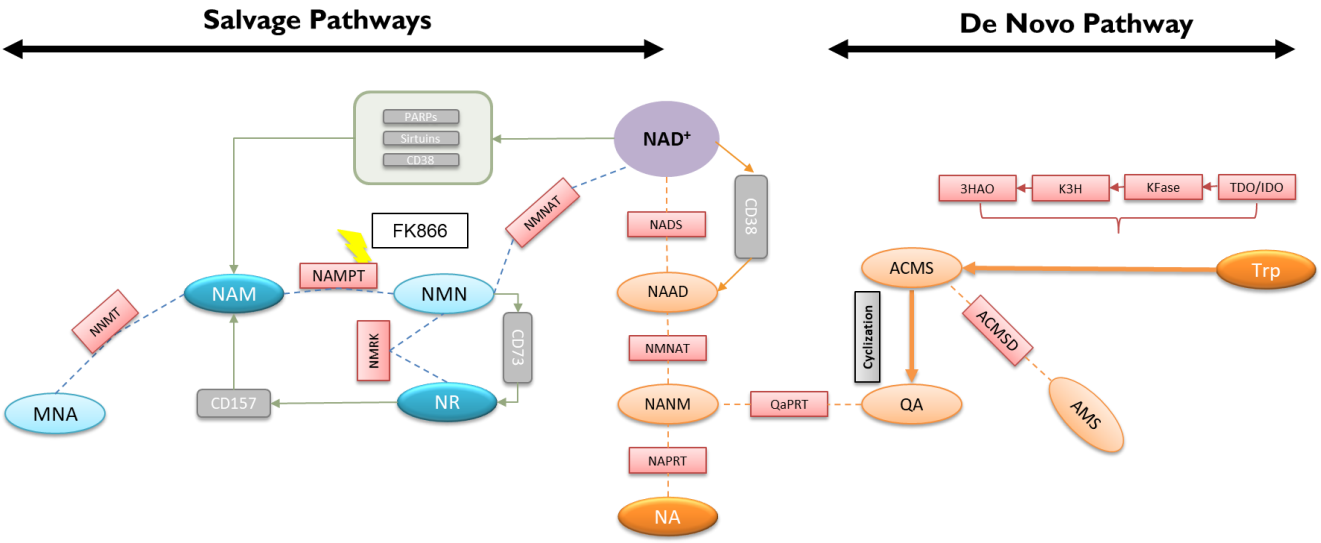

***Figure 1**- Metabolic network of in NAD^+ in mammals: To the left are represented the intermediates from the NAM & NR salvage Pathways, on the right the intermediates from the Preiss-Handler & de novo Pathways. NAD+ biosynthesis enzymes are depicted in red color and NAD consuming enzymes are shown in gray.*

.

1.3. NAD^+ consuming enzymes

NAD^+ is not just limited to serve as coenzyme in redox reactions performed by hydride transfer enzymes, several NAD^+ consuming enzymes that break the glycosidic bond between the NAM moiety and the Adenosine diphosphate (ADP) ribose moiety, have recently been discovered [8]. This type of enzymes includes: The Poly-ADP-ribose polymerases (PARPs), sirtuins [27], ADP-ribosyltransferases (ARTs) and the Cyclic ADP-ribose synthases and ADP-ribosyl cyclases, such as CD38/157 ectoenzymes [28].

1.3.1. Sirtuins

This family of enzymes is mainly characterized by their ability to remove acetyl and malonyl groups from proteins lysine residues. They cleave NAD^+ between NAM and ADP-ribose and transfer the removed acetyl group to the latter generating O-acetyl-ADP-ribose. Their name originates from the Silent Information Regulator 2 *(SIR2)*, a gene found in budding yeast that in the late 1990s was shown to be associated with the extension of life span in this organism by repressing genome instability [29] [30] [31]. Several other similar genes called Sirtuins are present in other organisms such as animals, plants, and bacteria [32]. In humans, this family is composed of seven NAD^+ dependent deacetylases (SIRT1–7) [5], that deacetylate histones and transcription factors to regulate cell stress, metabolism, and survival pathways, DNA repair and circadian rhythm, among other cellular processes [33] [34] [35] [36]. Activation of these genes either by as Calorie restriction or pharmacological means, is reported to be associated with the increase in either the life span or health span of several organisms [37] [38] [34]. Sirtuins differ from each other in their biological function, enzymatic activities, substrates and molecules to which they bind, expression patterns and cellular location [37] [39] [40]. All sirtuins preform deacetylase reactions, with the exception of SIRT4 that has ADP-ribosyltransferase activity [37]. SIRT1, the human ortholog of Sir2 [41] and the most studied enzyme within this family, is associated with several therapeutic and preventive interventions for several metabolic, cardiovascular, neurodegenerative diseases and cancer, mainly associated with aging [42].

Several studies have emerged indicating the activation of SIRT1 as a result of the implementation of the Calorie restriction diet, a conditioning described in the literature as a method of increasing life span in bacteria and fungi [43] [44] [45]. Studies suggest an association between Calorie restriction and the increase in muscle mitochondrial biogenesis in healthy humans through SIRT1 and activation of Peroxisome proliferator-activated receptor gamma coactivator 1-alpha [46], and the enhancement of cell adaptation to hypoxia through SIRT1-dependent mitochondrial autophagy in mouse aged kidney [47]. Several activators of SIRT1, such as resveratrol, have been described as having Calorie restriction mimetic properties displaying potential therapeutics for the treatment of type 2 diabetes, decreasing insulin resistance, increasing mitochondrial content and prolonging survival in mice fed with a high-fat diet [48] [49].

SIRT1 has also been correlated to innate inflammatory regulation. With aging, adaptive immunity tends to decrease in effectiveness in contrast to innate immunity that undergoes an over-activation. This process called inflammaging has been identified as one of the great factors

associated with aging [50] [51] [52]. Many studies indicate SIRT1 as an inflammatory suppressor in various tissues acting on the Nuclear factor kappa B (NF-kB) system, one of the major and most evolutionarily conserved regulators of innate immunity. NF-κB is a pleiotropic transcription factor that controls transcription of DNA, cytokine production and cell survival. Forkhead box O3 (FoxO3) is another protein described in the regulation of immune system homeostasis and is a mammalian homolog of DAF-16, reported to be a key factor in the longevity in *C. elegans* [53] [54] [55] [56] [57]. Upon oxidative stress in mammalian cells, FoxO3 forms a complex with SIRT1 leading to its deacetylation, proportionating an increasing resistance to oxidative stress or inducing cell cycle arrest [58]. This process might be attributed to FoxO3 inhibitory capacity of NF-kB system, preventing Tumor necrosis factor alpha (TNF-α) activation [55]. The decline of SIRT1 activation during aging and consequent overactivation of NF-kB system along with the inhibition of oxidative stress response, is a supportive evidence of the inflammaging theory establishing a bridge between the aging process and the increase of innate inflammatory response [59].

1.3.2. Poly-ADP-ribose polymerases (PARPS)

Another large family of NAD^+-dependent enzymes called Poly (ADP ribose) polymerases (PARPs) share the ability to catalyze the transfer of ADP-ribose to target proteins. This family of 18 enzymes, cleave NAD^+ into NAM and ADP-ribose and are involved in several major cell processes such as DNA repair, genomic stability, and programmed cell death. In the last decade, the interest in the role of these individual proteins in cellular functions has increased, therefore many members of this protein family, like PARP1 and PARP2 have been specifically related to several functions such as modulation of chromatin structure, transcription, replication, recombination, DNA repair and even in metabolic regulation by influencing mitochondrial function and oxidative metabolism [60] [61] [62].

Because SIRT1 and the PARP family share the same coenzyme (NAD^+) it is been reported by [63] that *PARP-1−/−* mice (Mice with deletion of *PARP1* gene leading to PARP1 levels depletion) present a substantial increase in SIRT1 activity in brown adipose tissue and muscle reporting a higher mitochondrial content, increased energy expenditure, and protection against metabolic disease. Furthermore, they verified that drug-based inhibition of PARP both *in vitro* and *in vivo* increased NAD^+ intracellular levels, oxidative metabolism and SIRT1 activity.

Since PARP proteins are deeply involved in the mechanisms of DNA self-repair, many authors have been exploring their use in oncology since some tumors rely solely on PARP-mediated DNA repair for survival. One example is hormone receptor- and ERBB2-negative ("triple-negative") BRCA1-deficient mammary carcinomas which are reported by [64] to be sensitive to PARP1 inhibitor AZD2281 in mice, stopping tumor growth without signs of toxicity and resulting in strongly increased survival. On the other hand, PARP1 hyperactivation has been correlated with a series of outcomes such as a specific programmed cell death pathway characterized by loss of mitochondrial membrane potential, Adenosine triphosphate (ATP) and NAD^+ depletion, the activation of the calcium-dependent non-lysosomal cysteine proteases μ-calpain and the release of apoptosis inducing factor. This apoptosis inducing effect has been explored by several authors in cancer treatment like Bey who used β-lapachone to provoke a PARP1 hyperactivation and as a consequence, killing Non-small-cell lung carcinoma cells (NSCLC) [65]. Apart from PARP1 and PARP2, not much is known about the other members of the PARP family, with the exception of tankyrase 1 also known as PARP5a, a protein that is responsible for enhancing telomere elongation by telomerase in some types of cancer cells and therefore has been pointed as a potential target in cancer therapy [66] [67].

1.3.3. cADPR synthases, CD38 & CD157

CD38 and CD157 are membrane proteins that are important in the regulation of intracellular Ca^{2+}, mediated by their main function of forming molecules such as cyclic ADP ribose, NAADP and ADP-ribose by the cleavage of NAD^+ and $NADP^+$ [68]. The catalytic efficiency of CD38 is significantly higher than CD157 [69]. Several studies characterize CD38 as a very important factor in immune responses, metabolic disturbances like obesity and diabetes, and also in some immunodeficiency virus infections, chronic lymphocytic leukemia and myelomas [70] [68] [71] [72] [73] [69]. CD38 is the major NAD^+ consuming enzyme involved in energy metabolism in many mice tissues, including liver, brain, heart, and kidney [74] [75], therefore, CD38-deficient mice fed high-fat diet were reported by [70] to present an increase in NAD^+ levels in different tissues along with a higher metabolic rate compared to control mice. This resistance to diet-induced obesity was concluded to be caused by the overactivation of the NAD-dependent SIRT-PGC1α axis given the high levels of NAD^+ in the tissues making CD38 a regulator of body weight in mice during a high-fat diet. PARP1

and CD38 increase are considered to be the main causes of age-associated NAD^+ levels reduction in tissues [76] [77] [78].

1.4. Age related changes in NAD^+ metabolism

During aging the NAD^+ levels of an organism tend to decrease. This observation was first made in a study of mice called BESTO, which were genetically programmed to overexpress SIRT1 in pancreatic cells. In these mice, insulin hypersecretion was recorded, however as they aged the levels of SIRT1, and insulin secretion decreased. In a successful attempt to counteract this decline, a precursor of NAD^+, NMN, was given to these mice which led the authors to conclude that the decrease in NAD^+ levels were the cause of the loss of the BESTO phenotype [79]. Following this study, others confirmed that NAD^+ levels decreased over time in different tissues and organs. Furthermore, age-related decrease in NAD^+ biosynthesis and increased NAD^+ consumption was correlated with several human age-related pathologies [77] [34] [80] [81] [79].

One of the major causes of NAD^+ decline with age may be the overactivation of NAD^+ consuming enzymes PARPs and CD38. During the aging process there is an accumulation in DNA damage, that is thought to result in the increase in PARP1 activation. Also, age-related increase in CD38 expression and activity has been associated, through a SIRT3-Dependent Mechanism, with mitochondrial dysfunction [63] [76] [82] [83] [78]. The overactivation of these enzymes causes an excessive degradation of NAD^+ which leads to a decrease in SIRT1 activity. This was confirmed in a study involving PARP1 inhibitors and *PARP1* gene knockout, that when administrated to mice, caused an increase in SIRT1 activation and consequently several beneficial metabolic phenotypes [63]. Furthermore, it was concluded that PARP2 directly regulates SIRT1 expression with PARP-2 deficiency increasing SIRT1 activity in cultured myotubes and mice [63].

Another probable cause to the decrease in NAD^+ levels during aging, is the decline in NAMPT expression in several tissues. As already mentioned above, NAMPT is a very important enzyme for NAD^+ production, being responsible for the conversion of NAM into NMN in the first step of the NAM salvage pathway. With the depletion of this enzyme, the NAD^+ production gets compromised leading to a decrease in the several NAD^+ dependent cell functions such as activity of the NAD^+ dependent enzymes and the chain of redox reactions [84] [81] [85] [86].

1.5. Therapeutic potential of NAD^+ bosting molecules in aging

To solve the slow decrease in NAD^+ levels throughout aging, many authors attempted to raise the NAD^+ levels in several organisms such as mice and yeast through the administration of NAD^+ precursors. As a result, an increase in lifespan and/or healthspan in these groups of individuals was registered, in comparison with the control groups [87] [43] [77] [55] [88] [89].

1.5.1. Metabolic disorders

Although the molecular causes of aging have not yet been clarified, some metabolic alterations associated with the development of some age-related pathologies have been attributed to the decreasing levels of NAD^+. In contrast, the rise in cellular levels of this molecule has been the answer to treat these diseases in several model organisms [90] [91] [92]. Diabetes is one example given its association with SIRT1 activity. According to [93], SIRT1 regulates insulin secretion by repressing Mitochondrial uncoupling protein 2 in pancreatic β cells, in addition to preventing the development of insulin resistance in various peripheral tissues [94]. Therefore, with the natural age-associated decease in NAD^+ levels, the regulatory function of SIRT1 becomes inefficient.

Sirtuins also appear to be involved in another pathophysiology mechanism known as Non-alcoholic fatty liver disease. This pathology is caused by excessive storage of fat in the liver (steatosis) without the patient displaying any habits of excessive alcohol consumption or any other secondary cause. It consists in a gradual process linked with Insulin resistance and metabolic syndrome, which can start as a Non-alcoholic steatosis but quickly develop into a non-alcoholic steatohepatitis and consequently hepatic fibrosis, hepatic cirrhosis and hepatoma [95].

1.5.2. Neurodegeneration

Age-related neurodegenerative diseases make up one of the leading causes of death in developed countries. In the last 20 years the interest in studying the relation of pathophysiological processes related to these diseases with the metabolism of NAD^+ has increased.

Wallerian degeneration is a mechanism that consists of nerve cells axon degeneration after a cutting or smashing lesion. This process has been often correlated with several peripheral neuropathies such as Alzheimer and Parkinson's disease, traumatic brain injury, and inflammatory disorders like Multiple sclerosis [96] [97] [98] [99]. The expression of a fusion protein, named

"Wallerian degeneration slow", is reported to prevent axons degeneration, [100] [101]. This unusual chimeric protein is composed by 70 amino acid N-terminal sequence from the Ubiquitin conjugation factor E4 B multiubiquitination factor and the NMNAT1 protein, requiring both domains to protect axons from degeneration [102]. Wallerian degeneration slow mutation protects against neuronal insults, including Parkinson's disease, hypoxic-ischemic injury, toxic neuropathy (taxol), and others [103].

Aminopropyl carbazole, termed P7C3 is reported to activate NAMPT and consequently increasing NAD^+ levels [104] promoting an increase in the process of neurogenesis [105] and providing neuroprotective effects in mouse models of brain injury [106] and several diseases such as Parkinson's disease and amyotrophic lateral sclerosis [107] [108] [109] [104].

NAD^+ levels of degenerative axons tend to be smaller compared to healthy axons. In addition, restoration of NAD^+ to normal levels, either by its artificial supplementation, the administration of some of its precursors such as NAM, NA, NMN or NR, or by overexpression of the enzymes involved in the synthesis of NAD^+ such as NMNATs, is reported to delayed axonal degeneration [110] [111] [112] [113]. Also, SIRT1 activation through administration of resveratrol along with injection of SIRT1 lentivirus in the hippocampus, promoted neuronal survival in p25 model mice of Alzheimer disease and tauopathies, reducing neurodegeneration in the hippocampus, preventing learning impairment, and decreasing the acetylation of the known SIRT1 substrates PGC-1α and p53 [114]. Relatively to α-synuclein related pathologies such as Parkinson's disease and Lewy bodies dementia, Donmez reported that the overexpression of SIRT1 in mouse model with A53T α-synuclein mutation, improved its lifespan [115]. To SIRT1 is also suggested a protective role to the neuronal tissue in some models of Huntington's disease [116] [117]. NAD^+ boosting does not just have beneficial effects in the central nervous system, [118] reports that administration of NR protects against noise-induced hearing loss and degeneration of spiral ganglia neurites. Also, in a recent study it was demonstrated that administration of NAM and overexpression of NMNAT1 prevented mitochondrial dysfunction resulting in a reduced vulnerability of DBA/2J mice to glaucoma [89]. Other examples of neurodegenerative diseases that have been recently correlated to NAD^+ metabolism, are the Cockayne syndrome group B and Ataxia-telangiectasia [119] [120].

1.5.3. Cardiovascular disorders

In the last century, cardiovascular diseases have risen to the top major cause of death in developed countries with aging being its most prominent risk factor. Even elderly individuals without any type

of cardiovascular disease display characteristic arterial wall changes including stiffening, dilation and intimal thickening. Aging of vascular cells often cause compromising changes in function and structure of blood vessels that may result in several critical consequences such as high blood pressure, heart attacks, and strokes [121].

NMN administration to aged mice is reported to have a beneficial effect on vascular function due to increased activation of SIRT1 [88]. In addition, SIRT1 activation was reported to prevent endothelial cells senescence induced by disturbed flow [122] and protect vascular smooth muscle against DNA damage, medial degeneration, and atherosclerosis [123]. Depletion of SIRT3 was associated with mitochondrial dysfunction which is correlated to the development of several cardiovascular pathological processed such as heart failure, hypertrophic and dilated cardiomyopathy, pulmonary hypertension and endothelial dysfunction in early atherogenesis. [124] [125] [126] [127].

1.6. FK866

Destabilization of NAD^+ levels can lead to cell death especially in those that rely highly on this molecule to satisfy its homeostatic requirements, such as tumoral cells that are known for high cell division rates [128]. Several studies report a significant overexpression of NAMPT in various types of cancer cells [129] [130] [131] [132] implying a particular dependency of this molecule to maintain NAD^+ intracellular levels. Therefore, lately, NAMPT has been approached by many authors as a potential target for cancer treatment leading to the emergence of several compounds capable of targeting this molecule. One in particular, (E)-N-[4-(1-benzoylpiperidin-4-yl) butyl]-3-(pyridin3-yl) acrylamide also known as FK866 or APO866, is known to inhibit NAMPT activity (**Figure 1**). This compound decreases both NAD^+ and ATP levels in several cell lines leading to a decrease in cell viability as a consequence [133] [134] [135], and is currently under clinical trials for evaluation as synergetic cancer-treating drug [136]. Besides the NAD^+ biosynthesis-related apoptotic effect, FK866 is also reported to modulate the apoptotic cascade by activation of the caspase protein cascade and negatively altering the membrane potential of mitochondria [137] [133]. Increased cell death as a result of FK866 administration, is also correlated with the increase in autophagy according to some authors [134]. NAMPT activity in known to promote cell proliferation and survival by providing a constant supply of NAD^+ [138] [139] confirmed by the fact that its inhibition or Knockdown was reported to inhibit the growth of differentiated cancer cells through autophagy [140].

1.7. Proteostasis

One of the hallmarks of aging is the loss in protein homeostasis (proteostasis). Endoplasmic reticulum (ER) is considered to be the protein production house of a cell, in this organelle there are several machineries by which it can fold and package the proteins properly and can send it to the Golgi apparatus.

Upon their synthesis in the ER-associated ribosomes, proteins must be subject to a number of post-translational modifications. These modifications include protein folding, a process that occur in the ER cytosol where a series of enzymes like chaperones, oxidoreductases, and a special kind of chaperones named holdases and foldases that respectively perform their activity ATP-independently and dependently, engage together to give proteins their three-dimensional native structure. Failure to complete this process usually gives origin to inactive proteins, however in some cases, misfolded proteins can adopt or interfere with several cellular functions or even generate cytotoxic components such as free radicals and reactive oxygen species (ROS) which ultimately can result in a pathological process. In fact, several common neurodegenerative pathologies such as Huntington's disease, Alzheimer disease, Parkinson's disease, and Amyotrophic lateral sclerosis have been correlated with abnormal protein folding [141] [142] [143] [144]. In order to maintain proteostasis and prevent the overall effect of these misfolded proteins on cellular integrity, cells adopt a combination of several distinct response mechanisms and factors which include the Ubiquitin-Proteasome System (UPS), autophagy, Heat-shock response and chaperones, ER-associated degradation (ERAD) and the Unfolded Protein Response (UPR). Many studies reveal that with advanced cells age, these response mechanisms gradually start to fail leading to a disruption of cellular proteostasis which is thought to contribute to many age-related cytological alterations. When the protein-folding capacity is overwhelmed by protein-folding demand in the ER, misfolded proteins tend to accumulate over time. At certain point, a signal transduction pathway called the UPR is triggered initiating a reaction that culminates in a reduction in protein synthesis and enhanced degradation of misfolded proteins and later, the transcriptional upregulation of several target genes related to proteostasis monitoring. The UPR consists of a complex network of interconnected signaling pathways that begin with the activation of three signal traducing ER receptors which are known as Inositol-requiring enzyme 1 (IRE1) (α and β), Activating transcription factor-6 (ATF6 (α and β)) and Protein kinase RNA (PKR)-like ER kinase (PERK). Usually IRE1α is found in its inactive form distributed in great amounts along the ER membrane linked to the ER chaperone Binding immunoglobulin protein the ATPase domain. Upon excessive unfolded protein

accumulation in the ER, luminal domain self-associates, which leads IRE1α to its dimerization and trans-autophosphorylation inducing a conformational change that activates its RNase domain to catalyze excision of a 26-nt intron within the X-box binding protein 1 (XBP1) mRNA, [145]. Also in mammals, misfolded proteins can bind to the substrate binding domain of Binding immunoglobulin protein leading to its dissociation from IRE1α triggering its dimerization and auto-transphosphorylation. The unconventional mRNA splicing of *XBP1* that ultimately leads to the synthesis of XBP1s, a transcription factor that promotes the transcription of several UPR-related genes associated with protein folding, secretion, ERAD, and lipid synthesis [146] [147] [148]. The ERAD besides functioning as an ER unfolded protein clearance mechanism, is also known to have a regulation role in the levels of specific enzymes or signaling molecules in response to perturbed metabolic states. ERAD was discovered in late 1980s, after several groups reported that many incorrectly folded polypeptides or unassembled subunits of protein complexes formed in the ER were targeted for rapid degradation and did not stayed stable for long suggesting the existence of an ER protein degradative pathway [149]. The ERAD system is activated when abnormal unfolded protein aggregates overwhelm the UPR in the ER. Unfolded proteins are transported through the ER membrane into the cytosol by a process known as retro-translocation where they are marked by ubiquitin-conjugating enzymes and latter degraded in the proteasome [150]. Since the discovery of this mechanism many of the associated pathways, intermediaries and activators have been unveiled along with the mechanism of its articulation with the UPS.

PERK is a type I transmembrane kinase that upon acute ER stress oligomerizes and trans-auto phosphorylates. This generates an activating signal by the phosphorylation of the Eukaryotic translation initiator factor-2 at serine 51 of the α-subunit which leads to protein translation inhibition that eventually will decrease the flux of protein to the ER lumen [151], and the increase translation of the Activating transcription factor 4 (ATF4) responsible for the stimulation of several unfolded protein stress defense mechanisms such as the augmentation in the folding capacity of the ER by the upregulation of the transcription of chaperones and foldases, the stimulation of the macroautophagy process, and the incrementation of the antioxidant response. If the ER stress is prolonged, ATF4 will promote the expression of apoptosis inducing factors.

ATF6α and ATF6β, both isomerases of ATF6 factor are 90-kDa ER type II transmembrane glycoproteins that are constitutively expressed as precursor forms designated pATF6α(P) and pATF6β(P) [152]. Upon accumulation of misfolded proteins in the ER, these two migrate to the Golgi apparatus, where they are cleaved by the proteases S1P and S2P causing the release of their

cytosolic domains designated pATF6α(N) and pATF6β(N) that will function as nuclear transcription factors [152]. According to Yamamoto pATF6α(N) can promote an upregulation of a handful of UPR related genes that include genes coding for chaperones and ERAD pathway components [153]. This last one results from heterodimerization with XBP1s that as already mentioned is responsible for the activation of the ERAD system ultimately leading to the degradation of the stress causing misfolding proteins by the UPS [154].

The UPS is composed of two phases: In the first phase, the target protein has to undergo a process known as ubiquitination, which consists in the conjugation of polyubiquitin chains to proteins, and is performed in three different steps (activation, conjugation, and ligation) by three different enzymes (ubiquitin-activating enzymes (E1s), ubiquitin-conjugating enzymes (E2s), and ubiquitin ligases (E3s), respectively). In the second phase, the tagged protein is degraded by the 26S proteasome complex and the ubiquitin chains are removed by the deubiquitinating enzymes for latter to be reused [155] [156]. UPS activity is shown to be decreased not only in healthy aged cells and organisms [157] but also in several aging associated pathologies such as, cancer [158] Alzheimer and Parkinson diseases [159].

The mammalian 26S Proteasome is a protein structure with a weight of about 2000 kilodaltons (kDa) constituted by two components, one of them being 20S, the catalytic component formed by four heptameric rings, with its two outer rings being composed of seven α structural subunits that allow proteins to enter the component and the two inner ones being formed by homologous seven distinct β catalytic subunits that forms an enclosed cavity with three proteolytic activities (trypsin-like, caspase-like and chymotrypsin-like activity) where proteins are degraded. The other component, denominated by 19S, is directly connected to the α ring of the 20S core and is responsible for the regulation of its activity along with the unfolding and translocation of the ubiquitinated substrates into the catalytic cavity. In eukaryotes this component is known to be formed by nineteen proteins that are divided in a nine-protein subunit that include an AAA Family ATPase hexametric ring, and a ten protein subunit that forms a lid like structure to the hole component. The proteasome complex can only be assembled after ATP binding to these ATPase proteins and can only start protein degradation upon ATP hydrolysis [155] [160].

Despite the proteasome capability for protein degradation in the cell, some protein aggregates are too large to pass through the central pore of the 20S core. To remedy this situation, several specialized molecular chaperone machines are employed to disassociate misfolded proteins from aggregates and orient them to proteasome where they are individually degraded [161]. If the

inclusion happens to be too large, the cell can activate the process of autophagy that results the inclusion being degraded by the nonspecific proteases in the lysosome. There are three ways this process engages with the UPS which are known as macroautophagy, microautophagy and Chaperone-mediated autophagy. The first route is characterized by capture of entire organelles or parts of the cytosol into an autophagosome, a spherical vesicle structure with double layer membranes, that is then directed and fused to the lysosome that will degrade its content. This process has been described to have important physiological roles in human health and disease. In the second route the lysosome directly encompasses the cytosol and, in the Chaperone-mediated autophagy, Heat shock cognate 71 kDa protein (HSC70) chaperones transport unfolded proteins to the interior of the lysosome through the Lysosome-associated membrane protein 2 receptor [162] [163]. The already mentioned term “chaperone” was first mentioned in the literature in 1978 by Ron Laskey, who attributed it to a nuclear protein named nucleoplasmin that demonstrated to prevent histone aggregation with DNA during nucleosome formation [164]. In 1987 R. John Ellis generalized the concept to all proteins that were responsible for the post-translational assembly of protein complexes [165]. In fact, [166] defines chaperones as proteins able to help in the assembly or folding of other proteins, not composing their final structure. Chaperones can perform their function alone or with the help of different cochaperones that allow a more robust regulation of the ongoing process. Initially. many chaperones were named according to their molecular weight as is the case of Hsp40s, Hsp60s, Hsp70s, Hsp90s, Hsp100s, and the Small (Hsps) [166]. Today molecular chaperones are grouped in HSP70, HSP90, DNAJ/HSP40, chaperonin/HSP60, and small HSP (sHSP) families [141]. The most studied families are the HSP70 and HSP90 families with 15 and 4 mammalian homologs respectively and with levels estimated to make up 1–2% of the total protein in some cells [167]. Their activity depends on ATP which is hydrolyzed causing a conformational change proper for substrate binding.

1.8. Text Mining

The continuous publication of biomedical studies causes an increase in data accumulation in written formats. As a consequence, there is a need to develop and use bioinformatic tools to analyze such data. Text mining tools can process and interpret the meaning of unstructured text at small and large scale, automatically identify and extract concepts, as well as relationships between concepts or between concepts and intended questions. Example of these text mining biocurating tools include the following:

i) Brat, an intuitive web-based tool for text annotation able to perform concept normalization, integrate automatic annotation services, search capabilities and document comparison;

ii) TagTog annotation tool, that provides automatic annotation services complemented with manual editing based on chosen pre-defined concepts along with a user's revision-based system for update the machine-learning annotation models;

iii) MyMiner, complete web-based solution tool for biocuration that provides features such as supporting document triage, automatic concept recognition and document comparison;

iv) and EGAS, a web-based platform for biomedical text mining and collaborative curation that allows users to annotate and distinguish different types of concepts and highlight relations between those annotated concepts. This software allows importation of data in its standard text formats such as BioC, RAW and A1 or from PubMed or PubMed Central through identifier matching and remote search query. After data importation, datasets can be submitted to automatic annotation by a concept recognition tool which can manually be altered by curators by removing or adding new annotations [168].

Examples of EGAS application include: [168] where EGAS text mining-assisted curation capacity was tested by execution of a planned task that focused on the identification of human inherited gene mutations and associated clinical attributes in sorted PubMed abstracts. Results from this study support the importance of EGAS text mining automatic concept recognition in dataset curation given the enhanced annotation quality and reduced time required to annotation assignment compared with non-automatically curated datasets.

Another study performed by [169], consisted in a search for protein–protein interactions, protein expression and post-translational modifications performed in 100 selected PubMed abstracts related to neuropathological disorders. This study also reports that application of the EGAS text mining annotation algorithm significantly contributed to reduced curation time.

2. OBJECTIVES

The increase in published studies about aging and age-related pathologies in the last years is resulting in a continuous accumulation of information regarding specific topics within those areas. Due to the immensity of accumulated information related to these themes, with this study we aim:

-To extract information of Proteins, Cellular processes and their interactions from published studies, using a bioinformatic approach.

- To find novel links between Biological Processes or Cellular Pathways altered during aging and age-related pathologies (Neurodegenerative, Cardiovascular and Metabolic diseases), associated with proteostasis.

- To study NAD^+ metabolism's relation with aging, using FK866 to establish a cellular model of aging.

3. Methods & Materials

3.1. Bioinformatic Analysis of EGAS Datasets Protein Interaction Networks

3.1.1. Extraction of Interaction Networks from EGAS datasets

The Proteostasis 3 dataset in total is composed of 1523 articles selected according to the keywords: proteostasis, aging, Neurodegenerative Diseases, Cardiovascular Diseases, Metabolic Diseases (age-related diseases) and organized in a crescent manner according to their Pubmed ID. The same articles were prioritized according to the number of annotations forming the dataset Proteostasis 4. From the total number of articles in Proteostasis 3 (1523) and Proteostasis 4 (1508), (given that some articles were removed), the first 200 articles were analyzed and 417 and 554 interactions were registered, respectively. The total number of articles from Proteostasis 4 was also annotated, from which 1165 interactions were recorded. All sets of interactions (Proteostasis 3 first 200 articles (P3), Proteostasis 4 first 200 articles (P4) and Proteostasis 4 1500 (P4T)) were subsequently separated into 3 categories that distinguished between Protein-Bioprocess interactions, Protein-Drug Interactions, and standard Protein-Protein interactions. Only Standard Protein-Protein interactions were used in subsequent analysis, with each protein represented by a HGNC ID. After filtration, from P3, P4 and PT4, only 22, 116 and 321 interactions respectively, remained. Retrieve/ID mapping tool from UniProt was used to convert from HGNC to UniProt ID, allowing to match each ID with each protein name. Using the Cytoscape version 3.7.0 software, schematic representations of these 3 interaction networks were obtained.

3.1.2. Parameter-based Network Analysis

In order to evaluate the importance of each node in the network, we performed a parameter-based analysis using Cytoscape to evaluate the following:

Degree distribution: Number of edges connected to each node;

Closeness centrality: Measures how close a node is to any other node, and its capacity to affect all the other nodes in the network

Average Shortest Path Length: Contrast with Closeness centrality by measuring the average of the distance (measured in edges) from n to every other node.

Betweenness centrality: Represents the number of times a node function as bridge along the shortest path between other nodes in the network

Stress centrality: The number of shortest paths passing through a node.

Neighborhood connectivity: The average number of neighbor nodes from the neighbor nodes of n.

To better understand every parameter individual value for each node, their relationship and its overall effect on the network we used Parameter Visualization Tool of Cytoscape software to create similar networks with a visual representation base on size and color, of the parameters value for each node.

3.1.3. ClueGo Enrichment analysis

In order to extend the analysis of all proteins extracted from the datasets beyond the network parameter evaluation, we sought to perform an enrichment analysis to highlight the roles and the influence that these proteins have on a range of cellular processes. To do this we used a Cytoscape plug-in called ClueGo that is able to represent associations between Gene ontology (GO) /pathway terms related to lists of genes and proteins, creating groups according to their biological role. These relationships between terms are measured based on their shared genes that are defined using kappa statistics. To access terms association, a binary gene to term matrix (matching between selected terms and their associated genes) is created. Terms are then compared to each other under kappa statistics-based assessment, resulting in a network like visual representation where nodes represent terms and are linked to each other according to their kappa score level that represents the number of shared genes between the two linked terms. The score threshold can be manually modified to values between 0 to 1 which consequently, in case of value augmentation will increase network connectivity and decrease in case of value diminution.

GO is used to describe specific and established relationships between genes and physiological processes within a living organism. This includes a set of well-defined and relatable terms that are continuously updated and expanded by expert curators and can be represented through gene clusters enrichment analysis. ClueGo extracts and continually update GO terms through the Gene ontology Consortium where they are registered according to a well-accepted system of common nomenclatures and associated with describing information that is available for consultation. This platform is able to store, in a hierarchically structured way, the increasing large amount of information regarding every sequenced gene and known functionalities within biological system ranging from their associated biological processes and molecular function to their cellular component. Molecular Function of a gene or gene product consists in their potential biochemical

function within cell that describe how they impact all other cell entities. Biological processes terms comprise a series of molecular functions usually performed by a series of gene products that ultimately leads to a particular impact in cell physiological state. The hierarchically structured way of GO term storing is comprised of terms with higher general definition, associated to a higher number of genes and hierarchically closer to the root that branch into more specific with less associated genes terms. The ClueGo analysis programing box in the contains options that allow the user to select the terms required minimum number and percentage of associated genes and the target interval levels considered relevant for the analysis which will exclude terms included in higher or lower levels

ClueGo precompiled annotation files also include Reactome, a free, open-source, curated and peer-reviewed pathway database that include reactions and biological processes; BioCarta, a large collection of maps that include information of over 120,000 genes from multiple species known to interact to form common metabolic pathways, signal transduction pathway, and other biochemical pathways; and also the Kyoto Encyclopedia of Genes and Genomes (KEGG), a collection of databases that integrates genes according to experimental knowledge into high-level functions and their relationship with the biological system, representing them in manually drawn KEGG pathway maps. From this interface, ClueGo can create a functionally organized GO/pathway term network which also can be submitted to customized parameter adjustments.

The results analyzed in this thesis are extracted from ClueGo enrichment analysis of the 22 proteins that integrate the P3 network, the 104 proteins from P4 network and the 224 proteins from the P4T network. All assessments were performed under the following GO/Pathways parameters:

Pathways Shown: pV ≤ 0.05 significance

GO tree interval: Minimum level: 11 & Maximum level: 20

Go Term /Pathways selection at Cluster #1: 4

Minimum percentage of associated genes: 5% Genes

GO Term/Pathway Network Connectivity (Kappa score): 0,4

3.2. FK866 Experiments

3.2.1. Cell culture

Human neuroblastoma SH-SY5Y cells were obtained from the iBiMED cell culture bank, cultured in MEM:F12 10% FBS [F12 (Gibco, Invitrogen), MEM (Gibco, Invitrogen), $NaHCO_3$ (SIGMA), Sodium pyruvate (SIGMA), Antibiotic-Antimycotic (AA´s) 1% (100U/mL) Streptomycin, Penicilin and Amphotericin (Gibco, Invitrogen), L-glutamine, 10% FBS and H_2O], and were maintained in a humidified incubator supplied with 5% CO2/95% air at 37°C. Plate washing was done with Phosphate Buffered Saline (PBS) and for cell detachment 2mL trypsin-0,5% EDTA was used for 3 minutes at 37ºC. Centrifugations were performed at 1000 rpm, for 3 minutes at 22ºC using a Thermo scientific Heraeus Multifuge X1R Centrifuge. Only cells between passage numbers 11 to 20 were used at about 80% confluence. Cells were treated with the fresh media containing indicated reagents and later collected for further experiments.

3.2.2. Chemical treatments

Cultured SH-SY5Y cells were treated with the NAMPT inhibitor FK866 at 10nM and 100nM for 8h, 24h, 48h and 72h. FK866 was dissolved in MEM F12 10% FBS in a 1µl per 1ml proportion and then added according to the amount of MEM F12 10% FBS needed to fill each plate. The same quantity of MEM F12 10% FBS was added to control plates in order to make up the total volume of the FK866 treated plates

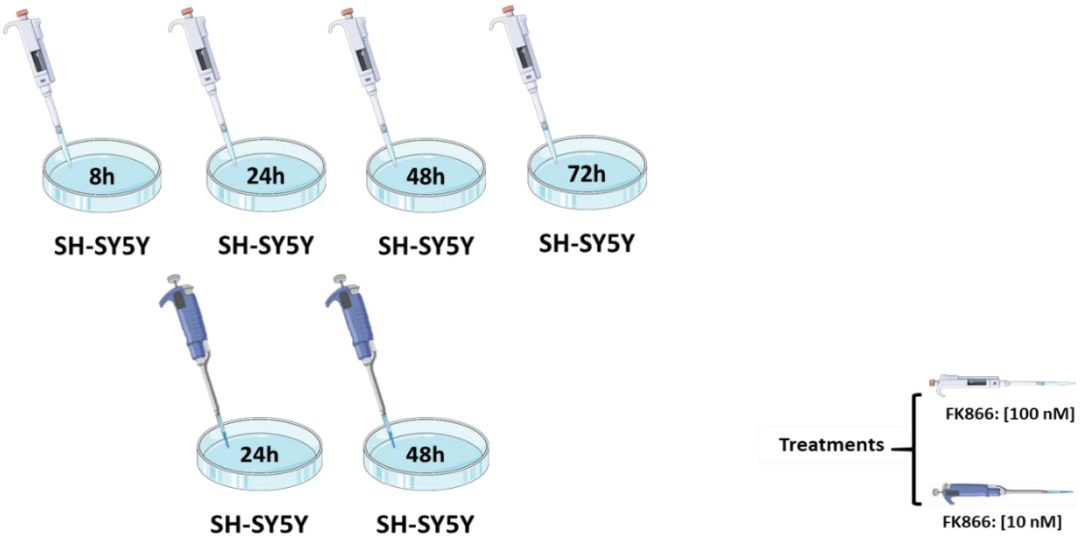

***Figure 2**- Experimental Plan*

3.2.3. Western Blot

Cells were lysed in ice cold RIPA buffer [NaCl 150mM (1,5ml); Np-40 1% (0,1ml), Sodium Deoxycholate 0,5% (0,05ml); SDS 0,1% (0,01ml); Tris 25mM, ph 7,4 (5ml); dH2O] supplemented with protease inhibitors and sonicated at Amplitude 60º in room temperature (two series of five strokes). Protein was quantified by spectrophotometer absorbance measurement using the Thermo Scientific™ Pierce™ Bison Kinetic Acid Assay (BCA) Protein Assay Kit, under a BSA pattern curve. Fifteen µg of protein were loaded with Laemmli Buffer and Stacking gel buffer (0.5M Tris-HCL buffer, ph 6.8), separated by SDS-polyacrylamide gel electrophoresis (**Table 1**) and electro-transferred onto a nitrocellulose membrane.

***Table 1**- Resolving and Stacking Gel used for SDS-PAGE Western Blot*

	Resolving Gel 12,5%	**Stacking gel 4%**
H_2O	1,6 ml	1,732ml
SDS 10%	50µl	25µl
0.5M Tris HCL ph 8,8	1,875ml	250µl
Acrylamide 27:1	1,5ml	250µl
TEMED	5µl	5µl
APS 10%	25µl	25µl

Monitoring for equal protein loading was carried out by using control antibodies for Actin detection. Membranes were left blocking overnight (16h) at 4ºC in TBS-T 5% low-fat milk (NAMPT and NAPRT) and 5% BSA (Actin). For protein detection, anti-rabbit primary NAMPT (HPA047776-100UL SIGMA) and NAPRT (HPA024017-100UL SIGMA) antibodies were incubated for 2h, both diluted at 1:2000 in 1% TBS-T 1x 1% low-fat milk, and anti-mouse primary Actin antibodies incubated for 1h diluted at 1:10000 in 1% BSA. For NAMPT and NAPRT, incubation with HRP-linked anti-rabbit secondary antibodies (16770745) diluted 1:5000 in 1% TBS-T 1x 1%low-fat milk was carried out for 1h, while HRP-linked anti-mouse secondary antibody (16770765) diluted 1:5000 in 1% BSA was used for Actin in an incubation period of 30 mins. For signal detection, ECL prime RPN2236 Amersham™ was added to the membrane and image acquisition was performed using ChemiDoc™ Touch Imaging System.

3.2.4. Viability assay with Trypan blue exclusion method

To evaluate the effect of FK866 on cell viability, Trypan blue assay was the method of choice. This azo dye also known as (3Z,3'Z)-3,3'-[(3,3'-dimethylbiphenyl-4,4'-diyl)di(1Z)hydrazin-2-yl-1-ylidene]bis(5-amino-4-oxo-3,4-dihydronaphthalene-2,7-disulfonic acid) can only enter the cell when the integrity of the cell membrane is compromised, which is a typical trait of dying cells. SH-SY5Y cells were added to 35mm plates along with MEM-F12 10% FBS. Cell medium was removed from the plates and conserved in a separate Eppendorf. Trypsin-EDTA 0.05% was added to detach cells from the plate surface and after incubation for 3 minutes at 37ºC, the previously kept medium was re-added to inactivate Trypsin-EDTA 0.05% followed by of 3 minutes centrifugation 1000 RPM at 22ºC. Supernatant was discarded and the pellet was conserved and resuspended with 10ml of new MEM-F12 10% (**Figure 3**). 100 µl was separated to an Eppendorf along with 10 µl of Trypan Blue. Cell were counted under inverted optical microscope LEICA.

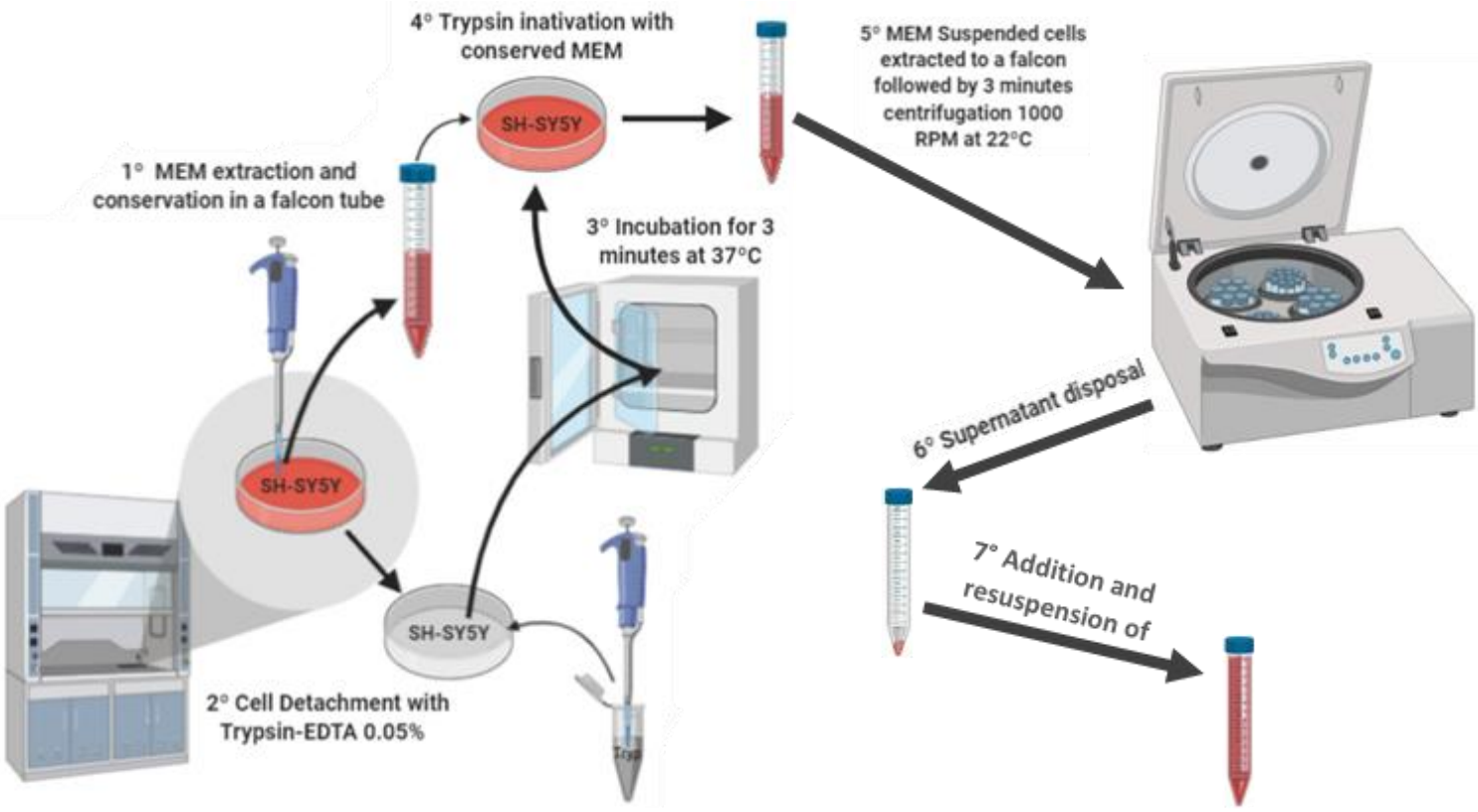

Figure 3- Representation of the first part of the Typan Blue Viability assay protocol

4. Results & Discussion

4.1. Parameter-based Analysis of EGAS extracted Networks using Cytoscape Software

4.1.1. P3 Network Parameter Evaluation

Network analysis parameters are listed in **Table 2**. As it can be seen in the P3 network representation shown in **Figure 4**, this network is mostly formed of isolated clusters so it is not meaningful to use the Closeness Centrality score. However, two clusters stand out, formed by the interactions mediated by APP and HSF1. APP has the highest level of Degree distribution, followed by HSF1, which reflects the number of edges in these two nodes. This can be verified by **Figure 5** that contrasts Closeness Centrality with Degree distribution measured by node size and color, respectively. In **Figure 5,** F7, TFPI, VWF, ADAMTS13, HSP26 and HSP104 show large size which indicates high Closeness centrality, and a bright reddish color meaning low degree distribution. Despite not having such a large size as the others, APP is represented with a blue color meaning high degree distribution. These results indicate that APP has higher centrality compared with the other proteins in the network that display a maximum value of both Average Shortest Path Length and Closeness centrality.

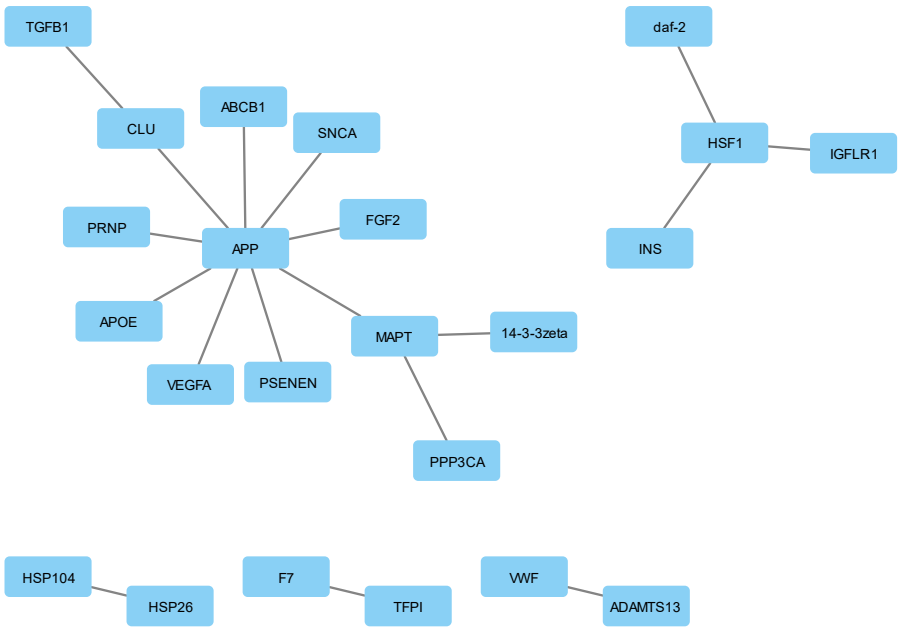

***Figure 4**- Representation on Cytoscape software of P3 Network*

Considering the parameter Betweenness centrality, values reveal that HSF1, APP, Microtubule-associated protein tau (MAPT) and Clusterin (CLU) have important bridging function between nodes

in the network given that only their score is different than zero (**Table 2**). The same nodes are distinguished by the Stress value that, as already mentioned in the methods section, measures the number of short paths that pass through a node. However, despite displaying a higher Betweenness Centrality score than the other three proteins, HSF1 has a lower Stress value compared to CLU, MAPT and APP. This can be justified by the fact that HSF1 is the central node of an isolated cluster that only links Insulin, IGF like family receptor 1 (IGFLR1) and daf-2, the insulin-like growth factor 1 homolog in the worm *C. elegans*, explaining its Degree distribution score of 3, the reduced Stress centrality score of 6 (short paths) and its maximum score of Betweenness centrality given that it is the bridging point of all nodes in the cluster. Furthermore, looking at **Figure 6**, we can see a distinct blue color representing high Betweenness Centrality of both APP and HSF1 compared to MAPT and CLU, which display a bright yellow and a dark grey color, respectively, and the rest of the nodes with a Betweenness Centrality value of 0 represented by the red color.

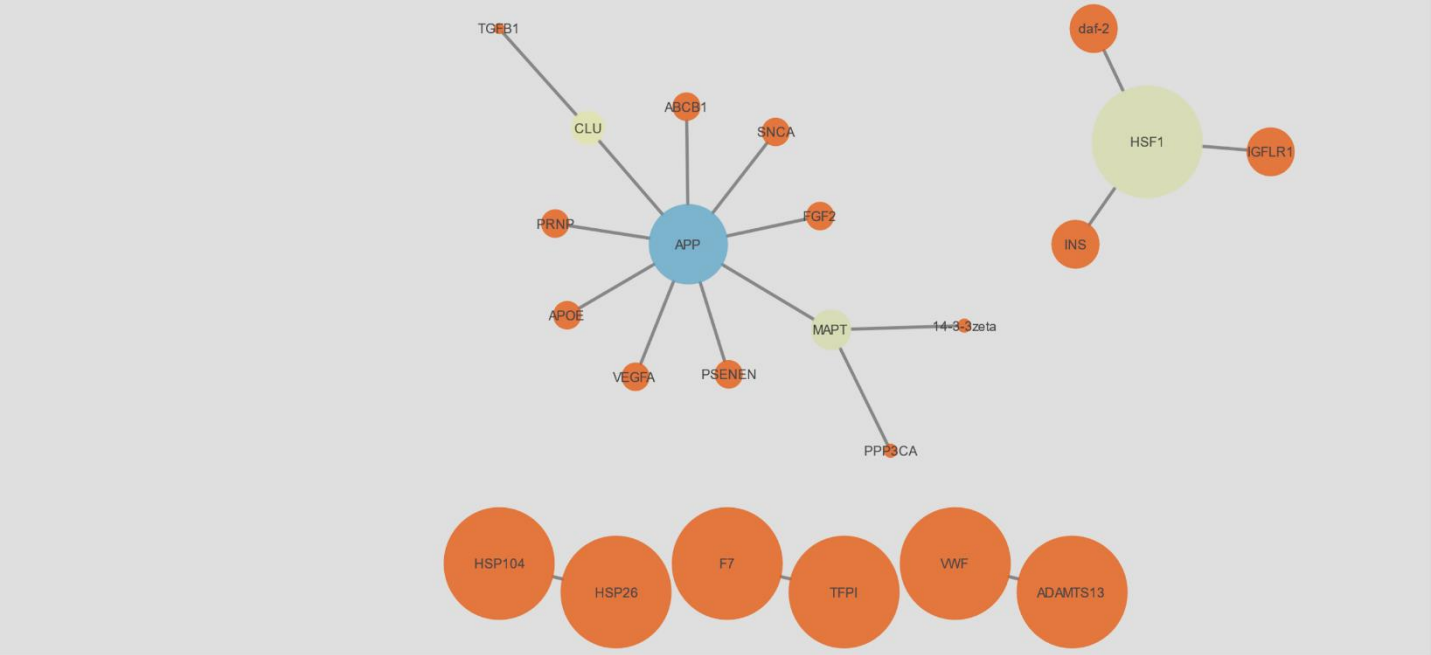

***Figure 5**- Representation of P3 network using Parameter visualization tool of Cytoscape software, Closeness Centrality values are represented according to node size (Low values to small sizes) and Degree distribution values according to nodes color (Low values to bright colors)(Blue color depicted as maximum, red color depicted as minimum)*

From **Figure 6,** we can also note a great difference in Neighborhood connectivity, represented by the node sizes, between APP directly linked nodes (with the exception of MAPT and CLU that are also linked to other nodes, having lower Neighborhood connectivity value as a consequence), and the remaining nodes. This is another indicator of the centrality dominance of APP in this network

since every node directly linked to it is rated among the highest scores. In conclusion, from the results of the parameter analysis of P3, APP stands out as the most significant, influential and connected node of this network. Since articles included in the Proteostasis 3 dataset were selected according to keywords related to aging, pathologies associated with aging and proteostasis, the results are not surprising, given the number of articles published relating APP with all these processes.

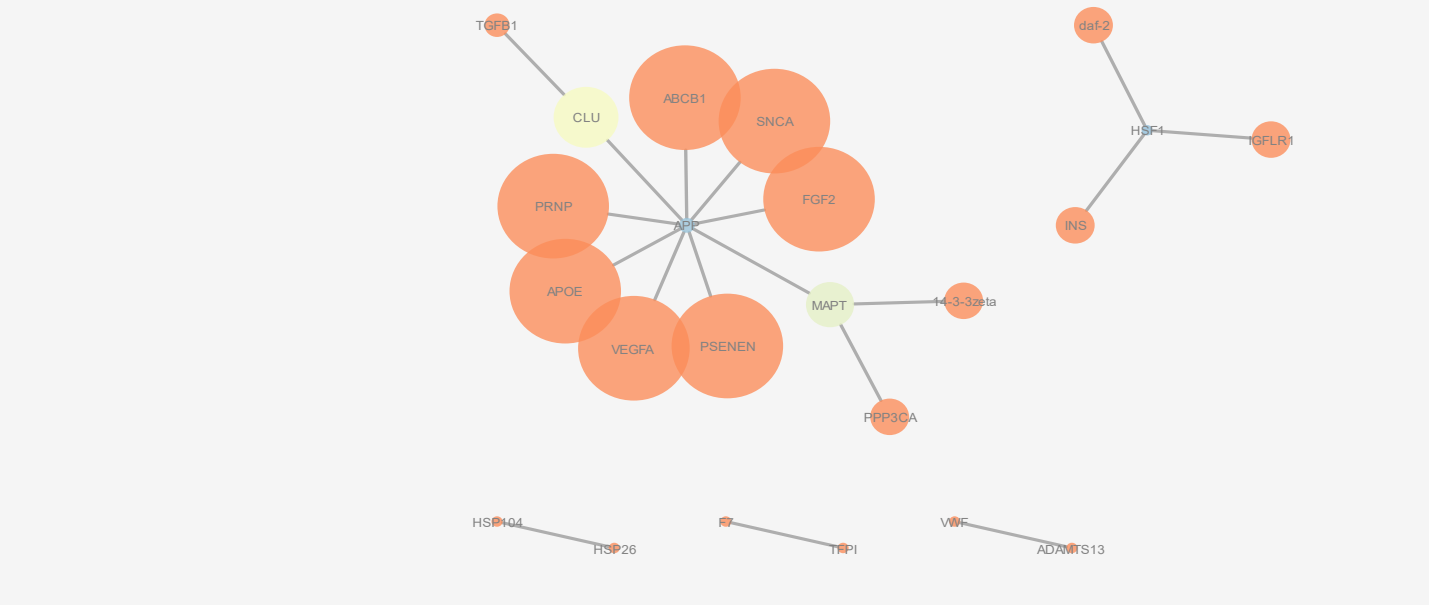

***Figure 6**- Representation of P3 network using Parameter visualization tool of Cytoscape software, Neighborhood Connectivity values are represented according to node size (Low values to small sizes) and Betweenness Centrality values according to nodes color (Low values to bright colors)(Blue color depicted as maximum, red color depicted as minimum)*

***Table 2**- Parameter analysis of P3 network (Parameters evaluated: Average Shortest Path Length, Betweenness centrality, Closeness centrality, Clustering coefficients, Degree distributions, Neighborhood connectivity and Stress centrality (Only shown the first 23 genes of each parameter(values are sorted in a decrescent way))*

AverageShortestPathLength		BetweennessCentrality		ClosenessCentrality		Degree		NeighborhoodConnectivity		Stress	
Gene	Value	Gene	Value	Gene	Value	Gene	Value	Gene	Value	Gene	Value
HSF1	1.0	HSF1	1.0	HSF1	1.0	APP	9	PRNP	9.0	APP	124
ADAMTS13	1.0	APP	0.93939394	ADAMTS13	1.0	HSF1	3	VEGFA	9.0	MAPT	42
VWF	1.0	MAPT	0.31818182	VWF	1.0	MAPT	3	SNCA	9.0	CLU	22
TFPI	1.0	CLU	0.16666667	TFPI	1.0	CLU	2	ABCB1	9.0	HSF1	6
F7	1.0	INS	0.0	F7	1.0	INS	1	FGF2	9.0	INS	0
HSP26	1.0	ADAMTS13	0.0	HSP26	1.0	ADAMTS1	1	APOE	9.0	ADAMTS1	0
HSP104	1.0	VWF	0.0	HSP104	1.0	VWF	1	PSENEN	9.0	VWF	0
APP	1.25	PRNP	0.0	APP	0.8	PRNP	1	CLU	5.0	PRNP	0
INS	1.66666667	VEGFA	0.0	INS	0.6	VEGFA	1	MAPT	3.66666667	VEGFA	0
daf-2	1.66666667	SNCA	0.0	daf-2	0.6	SNCA	1	INS	3.0	SNCA	0
IGFLR1	1.66666667	ABCB1	0.0	IGFLR1	0.6	ABCB1	1	14-3-3zeta	3.0	ABCB1	0
MAPT	1.83333333	TFPI	0.0	MAPT	0.54545455	TFPI	1	PPP3CA	3.0	TFPI	0
CLU	2.0	F7	0.0	CLU	0.5	F7	1	daf-2	3.0	F7	0
PRNP	2.16666667	FGF2	0.0	PRNP	0.46153846	FGF2	1	IGFLR1	3.0	FGF2	0
VEGFA	2.16666667	14-3-3zeta	0.0	VEGFA	0.46153846	14-3-3zeta	1	TGFB1	2.0	14-3-3zeta	0
SNCA	2.16666667	PPP3CA	0.0	SNCA	0.46153846	PPP3CA	1	APP	1.33333333	PPP3CA	0
ABCB1	2.16666667	TGFB1	0.0	ABCB1	0.46153846	TGFB1	1	HSF1	1.0	TGFB1	0
FGF2	2.16666667	APOE	0.0	FGF2	0.46153846	APOE	1	ADAMTS13	1.0	APOE	0
APOE	2.16666667	HSP26	0.0	APOE	0.46153846	HSP26	1	VWF	1.0	HSP26	0
PSENEN	2.16666667	HSP104	0.0	PSENEN	0.46153846	HSP104	1	TFPI	1.0	HSP104	0
14-3-3zeta	2.75	daf-2	0.0	14-3-3zeta	0.36363636	daf-2	1	F7	1.0	daf-2	0
PPP3CA	2.75	IGFLR1	0.0	PPP3CA	0.36363636	IGFLR1	1	HSP26	1.0	IGFLR1	0
TGFB1	2.91666667	PSENEN	0.0	TGFB1	0.34285714	PSENEN	1	HSP104	1.0	PSENEN	0

4.1.2. P4 Network Parameter Evaluation

As already mentioned in the methods section above, Proteostasis 3 articles were classified and sorted from the highest to the lowest number of annotations, hence creating a new dataset that we called Proteostasis 4. A similar analysis to the first 200 articles of the Proteostasis 3 dataset was performed to the first 200 articles of the Proteostasis 4 group. As expected, a higher number of Proteins (104) and interactions (116) were recorded in the first 200 articles of the Proteostasis 4 compared to the first 200 of the Proteostasis 3, as it can be observed by the presence of a higher number of nodes in the resulting network represented in **Figure 7.** Compared to **Figure 4**, a denser network was obtained with two major clusters formed by APP and SNCA that are also connected, while HSF1 is now a minor player as evidenced by parameter analysis.

***Figure 7**- Representation on Cytoscape software of P4 Network*

The Average Shortest Path Length and Closeness Centrality assessment highlight eleven nodes with the maximum score (1.0) in each category (**Table 3**) that include Reelin (RELN), TFPI, peroxisome proliferative activated receptor delta (PPARD) and Eukaryotic translation initiation factor 2 subunit 1 (EIF2S1), which are also featured with the maximum value (1.0) in the Betweenness Centrality category. This is shown in both **Figure 8** and **Figure 9,** where we see these represented by the largest nodes in the network along with other 7 nodes that do not show

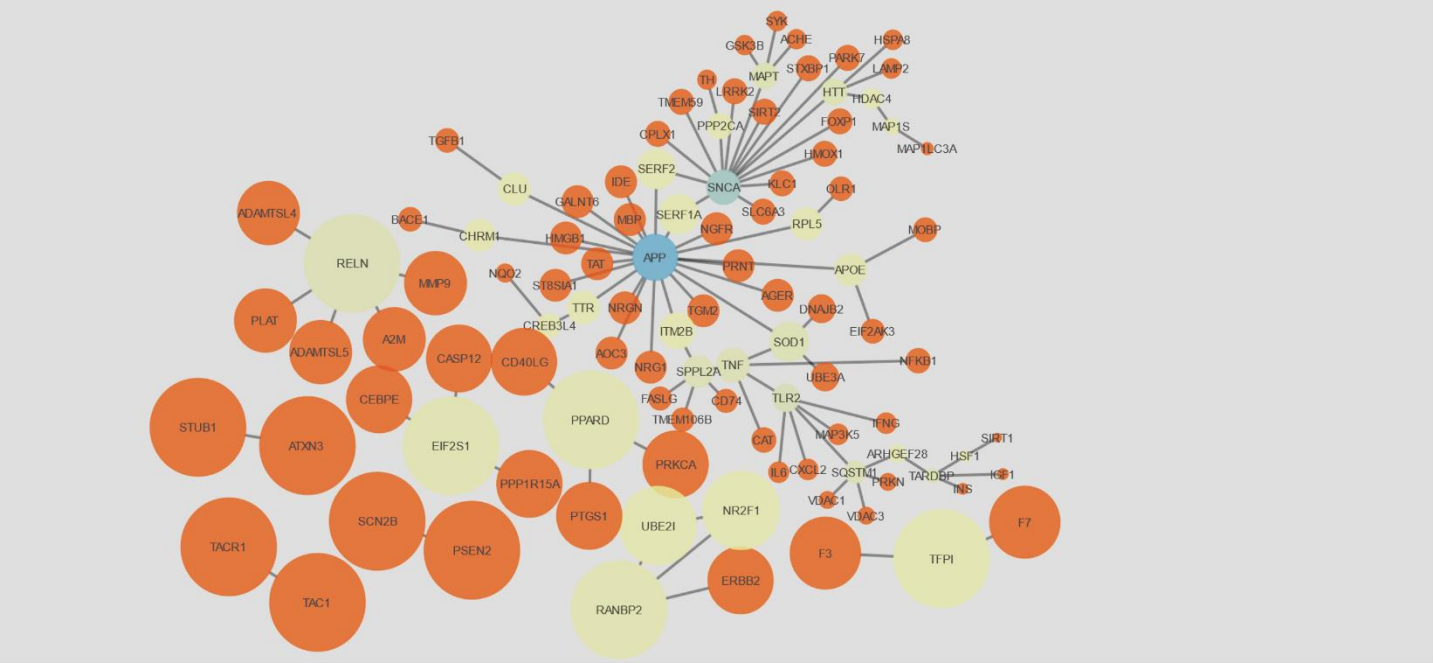

Figure 8- *Representation of P4 network using Parameter visualization tool of Cytoscape software, Closeness Centrality values are represented according to node size (Low values to small sizes) and Degree distribution values according to nodes color (Low values to bright colors)(Blue color depicted as maximum, red color depicted as minimum)*

the same maximum value in Betweenness Centrality parameter (1.0) as RELN, TFPI, PPARD and EIF2S1 (**Table 3**). This is not only an indicator of these nodes' high centrality in the network but also of the bridging function that they exert in this network. However, according to the Degree distribution parameter represented in **Figure 8,** APP appears to be the node with highest number of edges connected to it, with 22 linked edges as registered in **Table 2**.

Degree distribution values of RELN (5), PPARD (3), EIF2S1 (3) and TFPI (2) despite not being the lowest amongst the 104 genes in this network, are low compared to APP value, highlighted as the most influential node in this network. These values can be explained because RELN, TFPI, PPARD and EIF2S1 are central nodes of their own isolated cluster. This arguably explains the high values in Closeness Centrality, Average Shortest Path Length and Betweenness Centrality obtained for these

4 genes that, therefore, cannot be considered viable positive indicators of these nodes' network centrality. Stress centrality values also indicate APP as the node crossed with more short paths, with a value of 6785. It is also worth mention that Alpha-synuclein (SCNA) possesses a Stress Centrality value of 5084 and a Degree distribution of 15, also indicating a high centrality. Additionally, as we can see in both **Figure 9** and **Table 3,** several nodes that are solely directly linked to APP or SCNA display the highest Neighborhood Connectivity values in the network confirming them as the central nodes of this network.

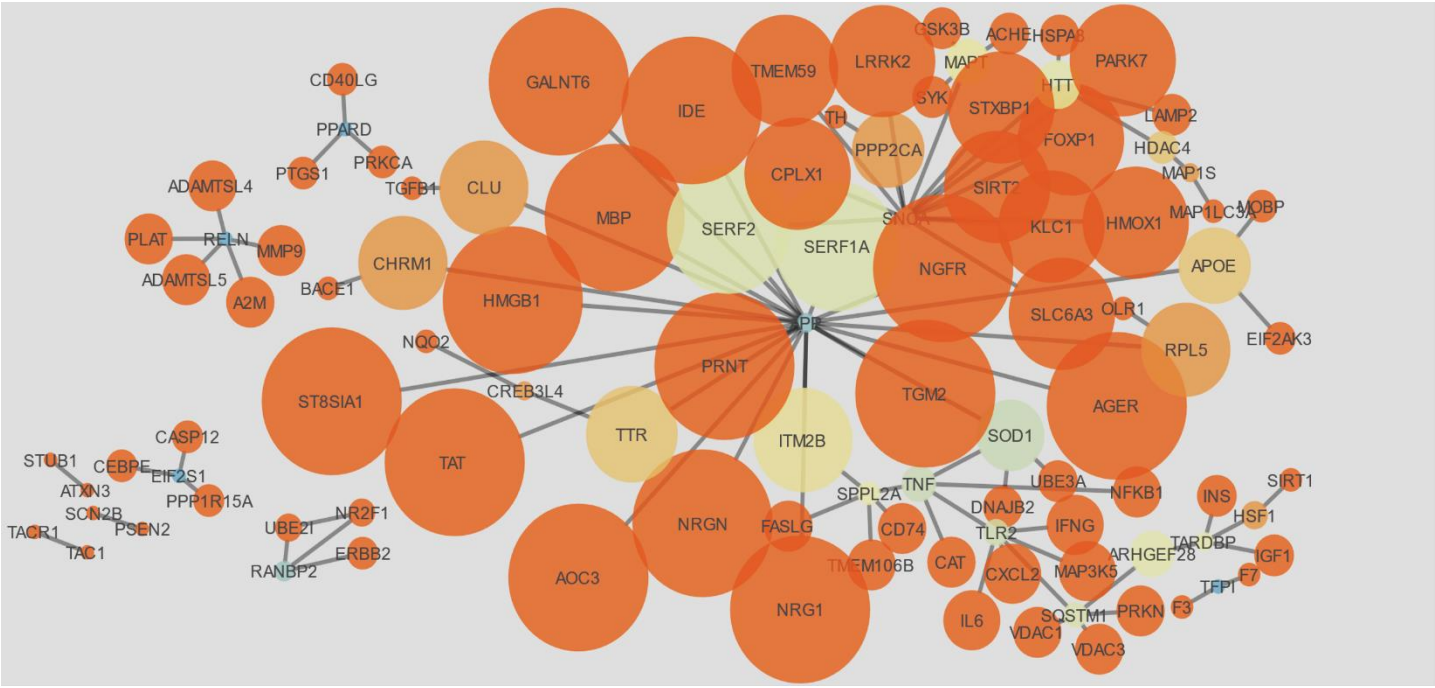

***Figure 9**- Representation of P4 network using Parameter visualization tool of Cytoscape software, Neighborhood Connectivity values are represented according to node size (Low values to small sizes) and Betweenness Centrality values according to nodes color (Low values to bright colors)(Blue color depicted as maximum, red color depicted as minimum)*

P4 network as we can recall, was obtained through the rearrangement of the articles composing P3 according to the number of annotations, therefore , we could record a higher number of nodes and edges, and a different network structure essentially supported not only by APP as in P3, but also by SCNA. Similarly to APP, there are many studies relating SCNA to aging, associated pathologies and proteostasis. Specifically, SNCA aggregation inside neurons leads to the formation of insoluble fibrils that originate Lewy bodies during age-related pathological conditions called synucleinopathies, which include Parkinson's disease, Lewy bodies dementia, Multiple system atrophy and other rare diseases. Also, looking at both **Table 2 and 3,** we note that P4 has 8 times more proteins than P3 with values of Betweenness Centrality different that 0 indicating a more

branched network. This can be visually confirmed when comparing **Figure 6** with F**igure 9.** In conclusion, our parameter analysis of P4 reveals APP and SCNA as the most significant, influential and connected nodes in the network. From P4 more annotations were extracted resulting in a more robust and connected network than P3.

***Table 3**- Parameter analysis of P4 network (Parameters evaluated: Average Shortest Path Length, Betweenness centrality, Closeness centrality, Clustering coefficients, Degree distributions, Neighborhood connectivity and Stress centrality (Only shown the first 23 genes of each parameter(values are sorted in a decrescent way))*

Average Shortest Path Length		Betweenness Centrality		Closeness Centrality		Degree		NeighborhoodConnectivity		Stress	
Gene	Value	Gene	Value	Gene	Value	Gene	Value	Gene	Value	Gene	Value
PSEN2	1.0	RELN	1.0	PSEN2	1.0	APP	22	IDE	22.0	APP	6786
SCN2B	1.0	TFPI	1.0	SCN2B	1.0	SNCA	15	GALNT6	22.0	SNCA	5084
RELN	1.0	PPARD	1.0	RELN	1.0	TLR2	6	ST8SIA1	22.0	SOD1	3054
RANBP2	1.0	EIF2S1	1.0	RANBP2	1.0	TNF	5	NGFR	22.0	TNF	2874
TFPI	1.0	APP	0.77877193	TFPI	1.0	RELN	5	AGER	22.0	TLR2	2472
TAC1	1.0	RANBP2	0.66666667	TAC1	1.0	SQSTM1	5	HMGB1	22.0	SERF1A	2392
TACR1	1.0	SNCA	0.49035088	TACR1	1.0	SPPL2A	5	NRGN	22.0	SERF2	2392
PPARD	1.0	SOD1	0.37438596	PPARD	1.0	SOD1	4	AOC3	22.0	SQSTM1	1662
STUB1	1.0	TNF	0.36701754	STUB1	1.0	HTT	4	TAT	22.0	HTT	1244
ATXN3	1.0	TLR2	0.32070175	ATXN3	1.0	MAPT	4	TGM2	22.0	ARHGEF28	940
EIF2S1	1.0	SQSTM1	0.21894737	EIF2S1	1.0	TARDBP	4	PRNT	22.0	TARDBP	770
NR2F1	1.33333333	SERF1A	0.20982456	NR2F1	0.75	APOE	3	MBP	22.0	MAPT	756
UBE2I	1.33333333	SERF2	0.20982456	UBE2I	0.75	RANBP2	3	NRG1	22.0	SPPL2A	618
F3	1.5	HTT	0.12701754	F3	0.66666667	PPARD	3	SERF1A	18.5	ITM2B	592
F7	1.5	ARHGEF28	0.1245614	F7	0.66666667	EIF2S1	3	SERF2	18.5	HDAC4	504
ERBB2	1.66666667	TARDBP	0.10280702	ERBB2	0.6	RPL5	2	LRRK2	15.0	APOE	390
PRKCA	1.66666667	SPPL2A	0.08421053	PRKCA	0.6	NR2F1	2	CPLX1	15.0	TTR	388
PTGS1	1.66666667	MAPT	0.07789474	PTGS1	0.6	UBE2I	2	FOXP1	15.0	MAP1S	254
CD40LG	1.66666667	ITM2B	0.07157895	CD40LG	0.6	CHRM1	2	STXBP1	15.0	PPP2CA	254
PPP1R15A	1.66666667	APOE	0.0522807	PPP1R15A	0.6	TFPI	2	HMOX1	15.0	RPL5	196
CASP12	1.66666667	HDAC4	0.05192982	CASP12	0.6	MAP1S	2	SLC6A3	15.0	CHRM1	196
CEBPE	1.66666667	TTR	0.05192982	CEBPE	0.6	HDAC4	2	PARK7	15.0	HSF1	196
ADAMTSL5	1.8	RPL5	0.02631579	ADAMTSL	0.55555556	ITM2B	2	SIRT2	15.0	CLU	196

4.1.3. P4T Network Parameter Evaluation

From the 1500 articles included in the Proteostasis 4 dataset we were able to extract the network shown in **Figure 10,** composed of 224 proteins (nodes) and 321 interactions (edges). In this analysis, it was obtained 3 times the number of nodes with maximum Average Shortest Path Length and Closeness Centrality compared to the parameter analysis of the first 200 articles of this dataset. However, as we can see in **Figure 11,** similarly to the P4, all the nodes that display high values of these two parameters are part of small isolated clusters with limited influence in the whole network. Furthermore, 4 proteins (Rhomboid family member 2 (RHBDF2), WWF and also PPARD and EIF2S1) distinguish themselves in the Betweenness Centrality parameter with maximum value. Again, looking at **Figure 10** we can see that this is justified by the fact that these nodes are central points in small isolated clusters.

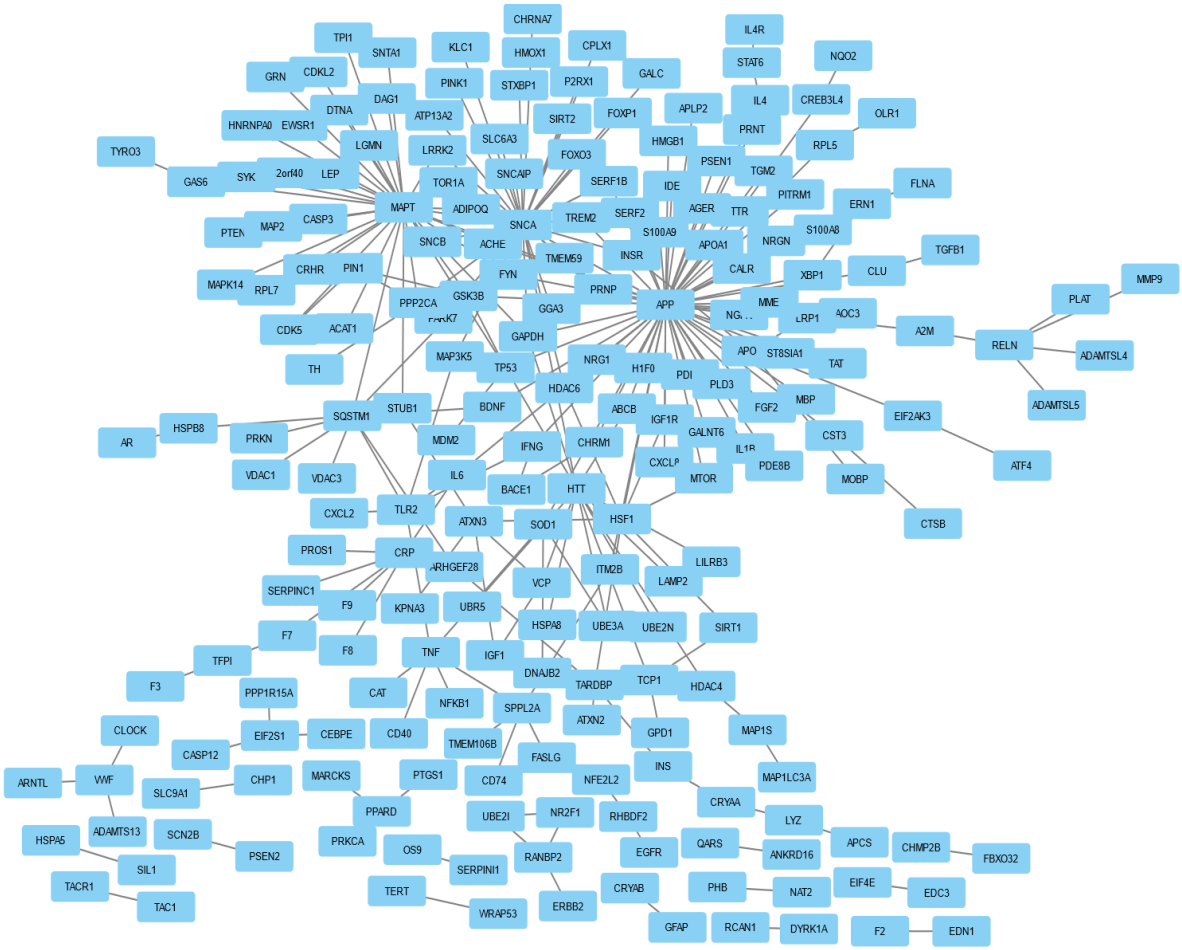

***Figure 10**- Representation on Cytoscape software of P4T Network*

From **Figure 11** we can also see that, similarly to P4, both APP and SNCA appear to be among the highest values of Degree Distribution, however, two additional clusters formed by nodes MAPT and Huntingtin (HTT) distinguish themselves from the rest of the network, also displaying high degree values. Looking at **Table 3** we can see that these same genes are ranked with the 4 highest values of Stress Centrality in the same order as Degree Distribution values (1st APP: 32554, 2ndMAPT: 13346, 3rd SNCA: 12012 4th HTT: 11590). In both **Figure 12** and **Table 4** we can see that as expected, the Neighborhood Connectivity values are the highest for the nodes solely and directly linked to APP, MAPT, SCNA or HTT. It is also worth mentioning that many high Neighborhood Centrality value nodes are linked to more than one of the 4 proteins mentioned.

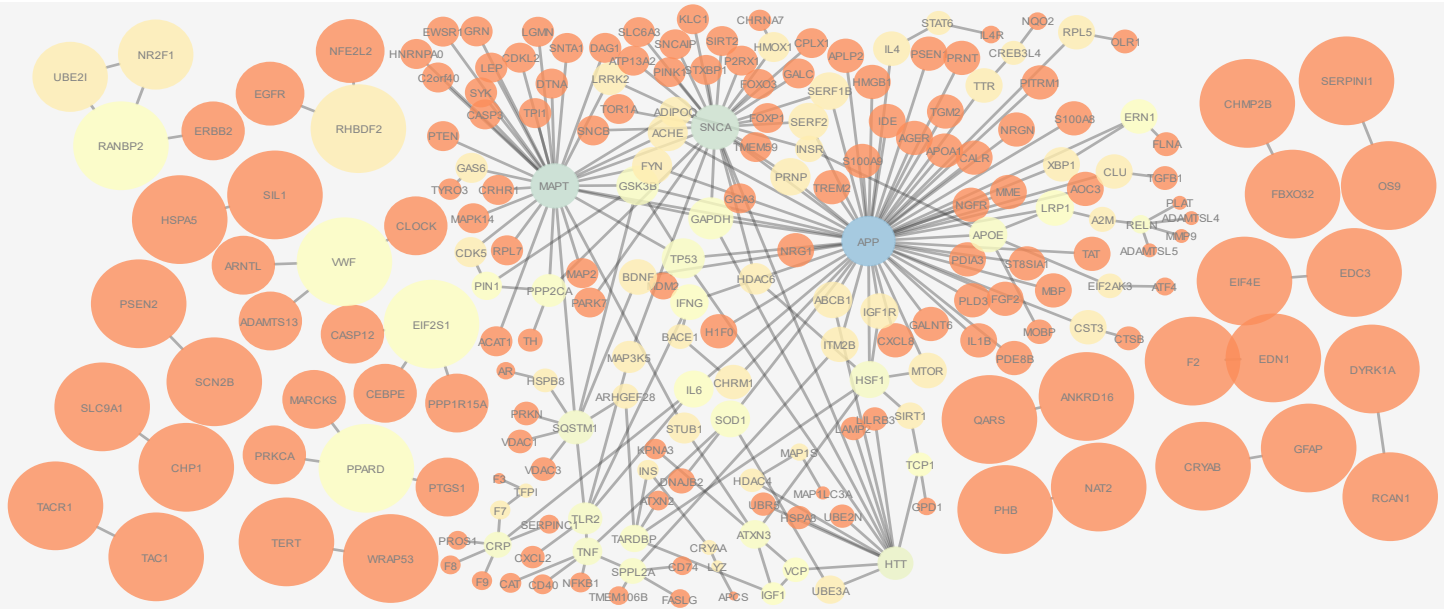

***Figure 11**- Representation of P4T network using Parameter visualization tool of Cytoscape software, Closeness Centrality values are represented according to node size (Low values to small sizes) and Degree distribution values according to nodes color (Low values to bright colors)(Blue color depicted as maximum, red color depicted as minimum)*

All evidences suggest that APP, MAPT, SCNA and HTT are the most central, influential and significant nodes in the network. These proteins have all been related with several age-related neurodegenerative diseases that are characterized by the formation of aggregates from altered forms of the proteins in the neuronal tissue. With this analysis, we can conclude that these 4 proteins are related with a large number of other proteins that might be part of important cellular pathways to maintain proteostasis. Therefore, in order to identify underlying biological processes and cellular pathways, we submitted protein clusters extracted from all three networks to an enrichment analysis using ClueGo as discussed in the next chapter. Dataset reorganization resulted in a wider and more connected network, however networks obtained with the first 200 articles are not representative of the final 1500 network. Nevertheless, if it were possible to elect one representative protein, the clear choice would be APP given its consistency across the three networks.

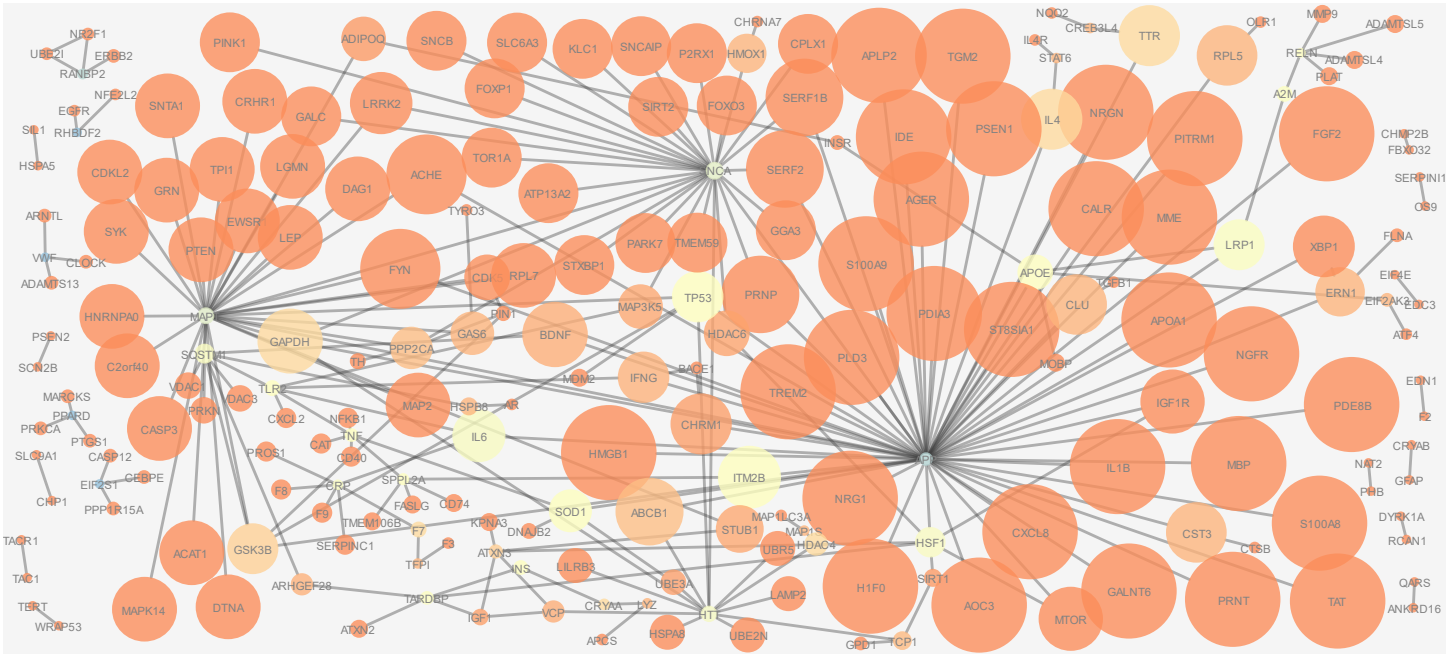

Figure 12- *Representation of P4T network using Parameter visualization tool of Cytoscape software, Neighborhood Connectivity values are represented according to node size (Low values to small sizes) and Betweenness Centrality distribution values according to nodes color (Low values to bright colors)(Blue color depicted as maximum, red color depicted as minimum)*

Table 4- *Parameter analysis of P4T network (Parameters evaluated: Average Shortest Path Length, Betweenness centrality, Closeness centrality, Clustering coefficients, Degree distributions, Neighborhood connectivity and Stress centrality (Only shown the first 23 genes of each parameter(values are sorted in a decrescent way))*

AverageShortestPathLength		BetweennessCentrality		ClosenessCentrality		Degree		NeighborhoodConnectivity		Stress	
Gene	Value	Gene	Value	Gene	Value	Gene	Value	Gene	Value	Gene	Value
PSEN2	1.0	PPARD	1.0	PSEN2	1.0	APP	58	IDE	58.0	APP	32554
SCN2B	1.0	EIF2S1	1.0	SCN2B	1.0	MAPT	33	GALNT6	58.0	MAPT	13346
RANBP2	1.0	VWF	1.0	RANBP2	1.0	SNCA	29	ST8SIA1	58.0	SNCA	12012
TAC1	1.0	RHBDF2	1.0	TAC1	1.0	HTT	13	NGFR	58.0	HTT	11590
TACR1	1.0	APP	0.70237477	TACR1	1.0	SQSTM1	9	AGER	58.0	SQSTM1	5210
PPARD	1.0	RANBP2	0.66666667	PPARD	1.0	HSF1	7	HMGB1	58.0	HSF1	4314
EIF2S1	1.0	MAPT	0.29867834	EIF2S1	1.0	TNF	6	NRGN	58.0	IL6	3800
EDN1	1.0	SNCA	0.26201801	EDN1	1.0	TLR2	6	AOC3	58.0	TP53	3544
F2	1.0	HTT	0.12431926	F2	1.0	CRP	6	TAT	58.0	CRP	3116
VWF	1.0	IL6	0.09176407	VWF	1.0	APOE	5	TGM2	58.0	GAPDH	2822
NAT2	1.0	HSF1	0.08736364	NAT2	1.0	RELN	5	PRNT	58.0	TARDBP	2818
PHB	1.0	SQSTM1	0.08140097	PHB	1.0	SPPL2A	5	MBP	58.0	LRP1	2796
GFAP	1.0	CRP	0.07798701	GFAP	1.0	TARDBP	5	NRG1	58.0	A2M	2340
CRYAB	1.0	LRP1	0.06623377	CRYAB	1.0	GSK3B	5	H1F0	58.0	HDAC4	2032
DYRK1A	1.0	TARDBP	0.06134632	DYRK1A	1.0	ATXN3	5	PSEN1	58.0	SOD1	2010
RCAN1	1.0	A2M	0.05551948	RCAN1	1.0	TP53	5	PDE8B	58.0	ABCB1	1926
OS9	1.0	SOD1	0.04837013	OS9	1.0	SOD1	4	IL1B	58.0	RELN	1892
SERPINI1	1.0	RELN	0.04506494	SERPINI1	1.0	PPP2CA	4	CXCL8	58.0	TNF	1802
WRAP53	1.0	APOE	0.04154968	WRAP53	1.0	GAPDH	4	FGF2	58.0	APOE	1790
TERT	1.0	TNF	0.04002922	TERT	1.0	RANBP2	3	APOA1	58.0	TLR2	1624
RHBDF2	1.0	ITM2B	0.03827706	RHBDF2	1.0	IL6	3	PLD3	58.0	ITM2B	1600
CHP1	1.0	TP53	0.0364724	CHP1	1.0	IFNG	3	MME	58.0	GSK3B	1516
SLC9A1	1.0	TLR2	0.03449675	SLC9A1	1.0	IGF1	3	PDIA3	58.0	SPPL2A	1464

4.2. ClueGo Enrichment Analysis results

4.2.1. Enrichment analysis of P3 network

Extracted from bioprocess enrichment analysis**, Figure 13** represents the group of terms associated to the proteins that make up the P3 interaction network. Regulation of long-term synaptic potentiation stands out as the only associated term, which according to the literature may be related to APP, the central node in the P3 network. Indeed, studies have established a correlation between APP pathological metabolism and long-term synaptic potentiation [170] [171] revealing that high levels of β-secretase 1 , an enzyme that initiates the production of Aβ from APP, reduces Protein kinase A expression in the mouse brain, a major regulator of long-term synaptic potentiation in the hippocampus through upregulation of synaptic vesicle release in presynaptic terminal [87]. Non-pathological cleavage of APP performed by α-secretase also known as ADAM-10, results in the release of secreted amyloid precursor protein-α (sAPPα) [172] which has been associated with multiple neuroprotective and neurotrophic mechanisms [173]. Its peptide structure is similar to the secreted amyloid precursor protein-β (sAPPβ) produced after β-secretase 1 pathological associated cleavage of APP, however sAPPα possess an additional fragment of 16 amino acids in the C-terminal. Curiously, the same extra fragment is associated with enhancement of LTP in the hippocampus, in a transgenic mouse model of Alzheimer disease [173, 174].

***Figure 13**- Enrichment analysis performed with Cytoscape plug-in ClueGo for P3 related Bioprocesses. Analysis was performed through the European Bioinformatics Institute (EMBLE-EBI)-Uniprot-Gene Ontology Annotation (GOA) with Go Term /Pathways selection at Cluster #1- 4 and 5% Genes, Kappa score= 0,4*

Also, results from Gene Associated Pathway analysis represented by **Figure 14** reveal that under the selected parameters, complement and coagulation cascades are the only pathways associated with this protein cluster. The relationship between amyloid-beta formation and both coagulation and complement cascades is extensively described throughout the literature. A study performed by Wyss-Coray suggest that activation of the complement prevents the neurotoxicity caused by Aβ and might reduce/impede the accumulation or induce the clearance of degenerating or amyloid affected neuronal cells [175].

Figure 14*- Enrichment analysis performed with the Cytoscape plug-in ClueGo for P3 genes related KEGG Cellular Pathways. Analysis was preformed through KEGG data base with a 0.05 significance and Go Term /Pathways selection at Cluster #1- 4 and 5% Genes, Kappa score= 0,4*

Furthermore, in experiments performed by Yin in Apolipoprotein E (ApoE) (included in the P3 network) deficient mice, the classical complement cascade was activated upon reacting to oxidized lipids leading to leukocyte infiltration of the choroid plexus contrasting its inhibition upon expression of all human ApoE isoforms through the formation of ApoE-C1q complexes [176]. Zamolodchikov reported the activation of the coagulation cascade in human plasma by Aβ through the activation of Plasma protein factor XII that leads to activation of factor XI [177]

4.2.2. Enrichment analysis of P4 network

Upon GO Term Bioprocess enrichment analysis under the same parameters, a considerable higher diversity of terms is associated with P4 (48 terms) compared to P3 network (1 term, as above). Looking at **Figure 15,** the larger groups are represented by the following Terms: Regulation of T cell differentiation (20,34%), Positive regulation of cardiac muscle differentiation (21,88%), Activation of MAP kinase activity (9,38%), Positive regulation of cysteine-type endopeptidase activity (9,38%),

Regulation of proteasomal ubiquitin-dependent protein catabolic process (9,38%), Regulation of pre-miRNA transcription by RNA polymerase II (6,25%) and Regulation of long-term synaptic potentiation (6,25%). As suggested by many studies all these processes have a role or are affected during aging or age-related pathological processes.

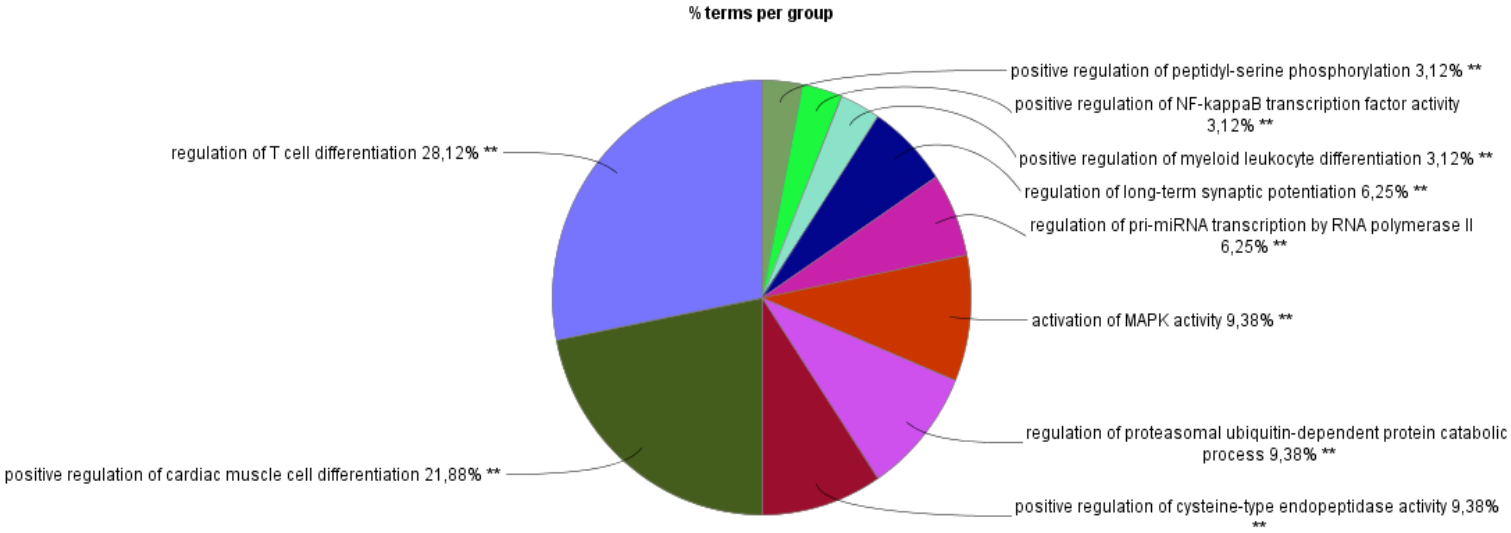

Figure 15*- Pie Chart representation of each group terms' percentage relatively to total number of terms obtained through the related GO Bioprocesses enrichment analysis of P4 gene cluster performed with the Cytoscape plug-in ClueGo. Analysis was preformed through the European Bioinformatics Institute (EMBLE-EBI)-Uniprot-Gene Ontology Annotation (GOA) data bases with Go Term/Pathways selection at Cluster #1- 5 and 5% Genes, GO tree interval of 7 min level and 15 max level, Kappa score= 0,4*

It has been already described in the literature the association of MAPK pathways with processes in human T-cells, particularly during the aging process. In a study performed by Lanna the increased number of Human T cells that display senescence-like traits during aging was attributed to non-canonical activation of the MAPK pathway [178]. This study revealed that sestrins, a family of poorly understood stress sensing proteins composed of *Sesn1*, *Sesn2* and *Sesn3,* display a pro-aging effect in T lymphocytes after binding to Erk, Jnk or p38. These are the three main separately regulated subgroups of the signal transducing enzymes from the MAPK pathway, involved in a series of mammalian physiologic processes such as aging, senescence and metabolism. This protein association, possible along with several other scaffolding proteins, form the sestrin-MAPK Activation Complex that simultaneously activates Erk, Jnk and p38 leading to T cell aging and senescence [179].

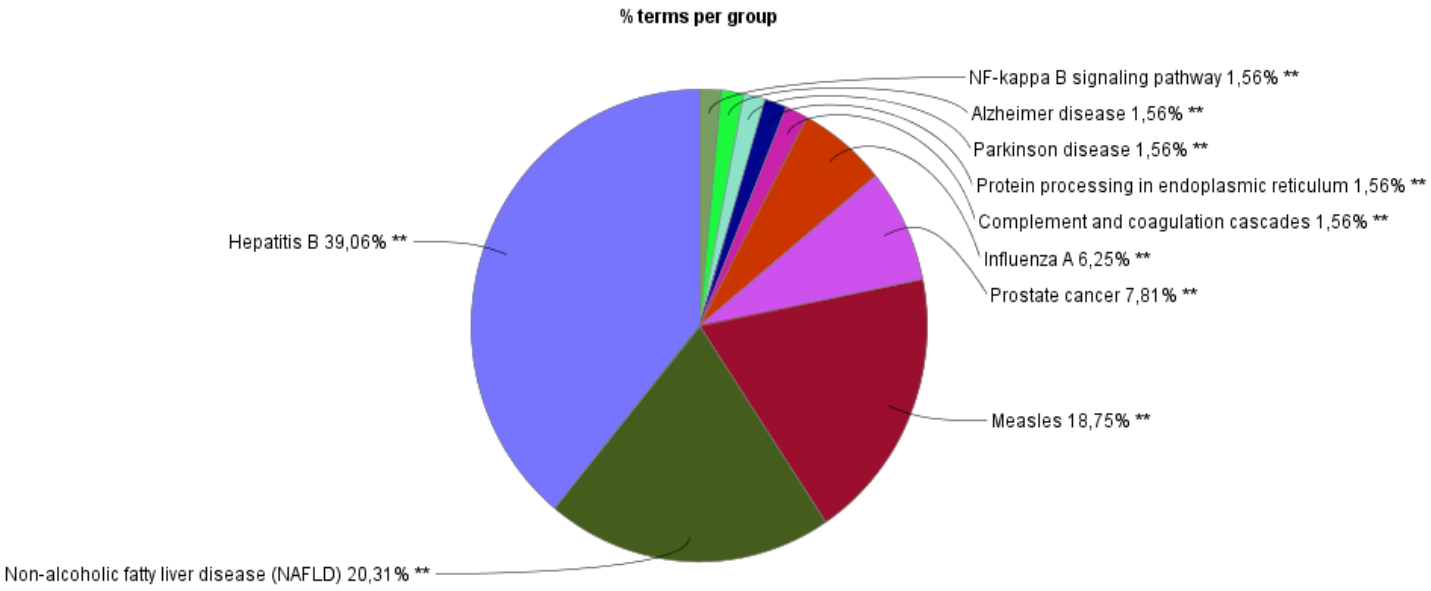

Figure 16- *Pie Chart representation of each group terms' percentage relatively to total number of terms obtained through the related KEGG Cellular Pathways enrichment analysis of P4 gene cluster performed with the Cytoscape plug-in ClueGo. Analysis was preformed through KEGG data base with a 0.05 significance and Go Term /Pathways selection a Cluster #1- 4 and 5% Genes, Kappa score= 0,4*

According to Veng, aging results in an increase in the voltage-gated calcium channel altering specific cell signaling. This causes a decrease in LTP-dependent memory storage by the activation of the N-methyl-d-aspartate (NMDA) receptors that cause a disruption in the influx of calcium to the intracellular space which can result in the activation of intracellular signaling pathways that alters protein synthesis and gene expression, ultimately leading to decrease in the LTP activation [180]. One example is described by Foster that reports that age-related memory loss in mice is associated with increase in both expression and activity of the Ca^{2+} dependent protein phosphatase calcineurin (CaN) in the hippocampus [181]. This is accompanied by augmented activation (not expression) of CaN-regulated protein phosphatase 1 along with a dephosphorylation of CaN substrates with a role in cell survival such as Bcl-2-associated death protein and cAMP response element-binding protein (CREB). Curiously, in the dentate gyrus (a region of the hippocampus thought to have a role in the production of new episodic memories) from adult male Sprague Dawley rats, an up-regulation of CREB transcription factors zif/268 and members of the activator protein-1 transcription factor complex, caused by NMDA receptor activation, occurred upon induction of LTP at perforant path synapses [182] [183].

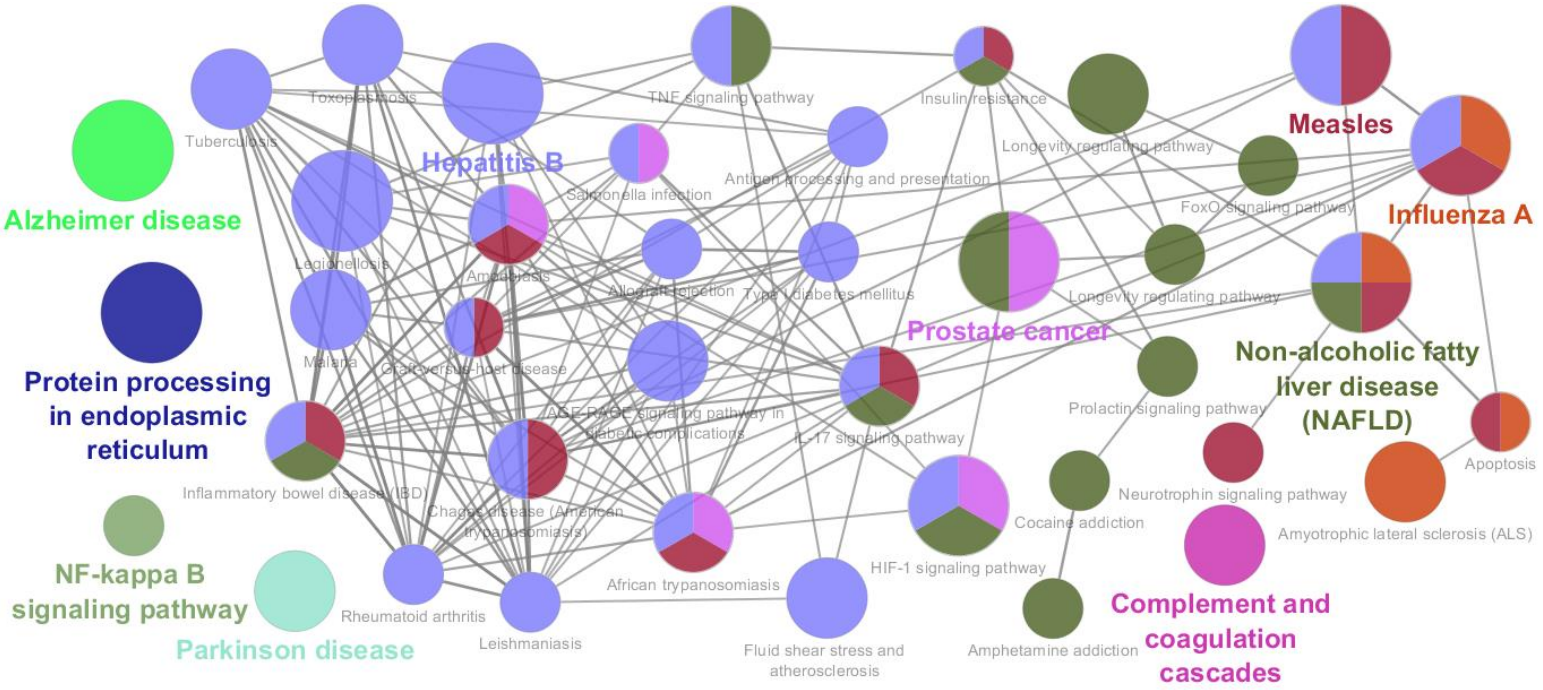

***Figure 17**- Network representation of an enrichment analysis for P4 genes related Bioprocesses performed with Cytoscape in ClueGo. Analysis was preformed through the European Bioinformatics Institute (EMBLE-EBI)-Uniprot-Gene Ontology Annotation (GOA) data bases with a 0.05 significance and Go Term /Pathways selection at Cluster #1- 3 and 5% Genes, GO interval of 11 min level and 20 max level, Kappa score= 0,4*

As referred earlier, one category used for article selection was age-related cardiovascular pathologies, therefore it does not come as a surprise to find genes involved in the positive regulation of cardiac muscle cell differentiation. Several age-associated alterations in the cardiovascular system have been depicted as important driving forces for the development of cardiovascular diseases in advanced ages. One example relatable to the results obtained in this enrichment analysis, is a study performed by Glass that highlighted the differentiation inducing role of miR-1 in transfected embryonic stem cells (ESC) in C57BL/6 mice infarcted myocardium along with the decrease in apoptotic rate through the activation of p-AKT and inhibition of caspase-3, Phosphatase and Tensin homolog (PTEN) and superoxide production [184]. Furthermore, a reduction in the fibrosis of interstitial and vascular tissue interstitial and vascular fibrosis was verified for the miR-1-ESC and ESC transplanted groups in comparison with the control, however, miR-1-ESC and ESC groups did not display statistical significance differences. Also, post-MI miR-1-ESC transplanted mice showed increased heart function compared with the control groups. Looking at **Figure 16** our analysis confirms the existence of a relationship between the activation of p-AKT

(referred to as Protein kinase B) and the positive regulation of cardiac muscle cell differentiation. In another approach, Morissette shows the inhibitory effect of high levels of the protein myostatin on both p38 MAPK and the serine-threonine kinase Akt resulting in the impairment of cardiomyocyte growth in mice [185]. As concluded by Morissette, his study presents itself as an evidence of the role of the age-related increase in serum myostatin levels in the development of cardiovascular diseases mediated by both Akt and p38 MAPK [185]. Despite not including myostatin, our enrichment analysis depicts a series of genes related to activation MAPK activity namely the Mitogen-activated protein kinase kinase kinase 5 (MAP3K5) known to be an upstream activator of the MKK/JNK signal transduction cascade and the p38 MAPK signal transduction cascade. These results can be considered further evidences of the role of aging associated alterations in cardiovascular structure and function in the development of cardiovascular pathologies and the associated mediating role of MAPK signaling pathways.

4.2.3. Enrichment analysis of P4T

In this chapter are displayed the results from the enrichment analysis (under the defined parameters) of the proteins from P4T network, that as already mentioned, was formed by the totality of interactions extracted from the entire Proteostasis 4 dataset. In concordance with previous analysis, both GO Bioprocess Terms and KEGG pathways were searched, obtaining in total 159 representative GO bioprocess Terms and 112 associated KEGG pathways. Compared to the number of GO Bioprocess Terms and KEGG Pathways obtained for P4 (48 and 40 respectively), these numbers show themselves to be considerably higher. This may be due to the higher number of proteins extracted from P4T (222) compared to the number of proteins extracted from P4 (104). The overall analysis (GO Terms and KEGG Pathways), reveals Cell Cycle and Cancer as the predominant functional role in the P4T protein network. However, similarly to the P4, there is a great number of genes associated with the Immune system functions such as the IL-17 signaling pathway and immune response to a range of infectious diseases along with known longevity pathways such as the FoxO and HIF-1 signaling pathways. The Highest Cell cycle related Bioprocess GO Terms Group are represented by the following terms: CD4-positive, alpha-beta T cell differentiation involved in immune response (9,32%), activation of protein kinase B activity (9,32%), regulation of MAPK activity (7,45%) and positive regulation of MAPK cascade (6,21%) while

examples of related KEGG pathways include: IL-17 signaling pathway (32,43%), HIF-1 signaling pathway, MAPK signaling pathway (6,76%) and PI3K-AKT signaling pathway.

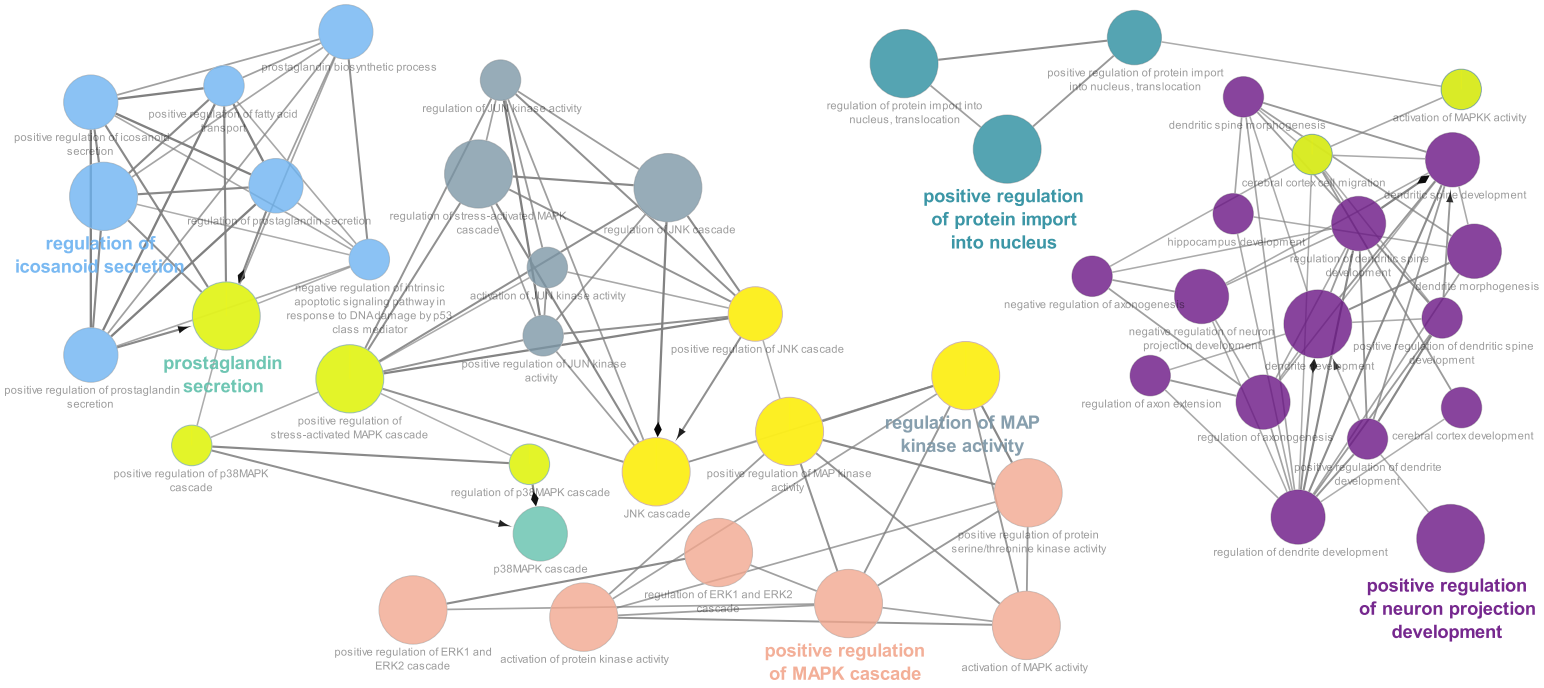

***Figure 18**- Network representation of an enrichment analysis for P4T genes related Bioprocesses performed with Cytoscape plug-in ClueGo. Analysis was preformed through the European Bioinformatics Institute (EMBLE-EBI)-Uniprot-Gene Ontology Annotation (GOA) data bases with a 0.05 significance and Go Term /Pathways selection at Cluster #1- 3 and 5% Genes, GO tree interval of 11 min level and 20 max level, Kappa score= 0,4 (Only connected Groups represented)*

In the results from both P4 and P4T Bioprocess GO Term enrichment analysis (**Figures 15, 17, 18, 19**) along with P4T KEGG pathway analysis (**Figures 16, 20, 21**), the already mentioned MAPK signaling pathway is represented by a considerable amount of terms revealing it to be closely associated with the P4 and P4T protein networks. This pathway constitutes a cell stimuli translational mechanism known to regulate over 160 cytosolic and nuclear proteins that in mammals are involved in several processes such as cell proliferation, differentiation, survival but also apoptosis, cell migration and development, metabolism and inflammation. The activation of the pathway happens through the activation of tyrosine kinases receptors such as EGFR (although G Protein-Coupled Receptors can also serve as activators) [186] upon stimulation by growth factors, hormones, neurotransmitters, inflammatory cytokines or physical stress, consequently this leads to the activation of small GTPase Ras through at least two known distinct mechanisms that activate different MAPK signaling cascades. This GTPase has three forms (HRAS, KRAS, and NRAS) all

appearing mutated in various cancers. Upon mutated, these proteins lose their enzymatic properties, allowing it to remain bound to guanosine triphosphate (GTP) and hence continuously activated [187]. The activation of Ras generates a phosphorylation cascade that culminates in the activation of ERK1 or ERK2 also known as MAPK3 and MAPK1 respectively. The best characterized mammalian MAP3K is Raf with tree identified mammalian isoforms Raf (or Raf-1), B-Raf, and A-Raf and was originally identified as a retroviral oncogene. In fact, the high incidence of both Ras and Raf mutation in human cancers was the first indicator of MAPK roles in proliferation and oncogenic growth [188]. A study performed by Tang concluded that this pathway also activates HSF-1, suggesting the existence of an interaction between the MAPK signaling pathway and the proteotoxic stress [189].

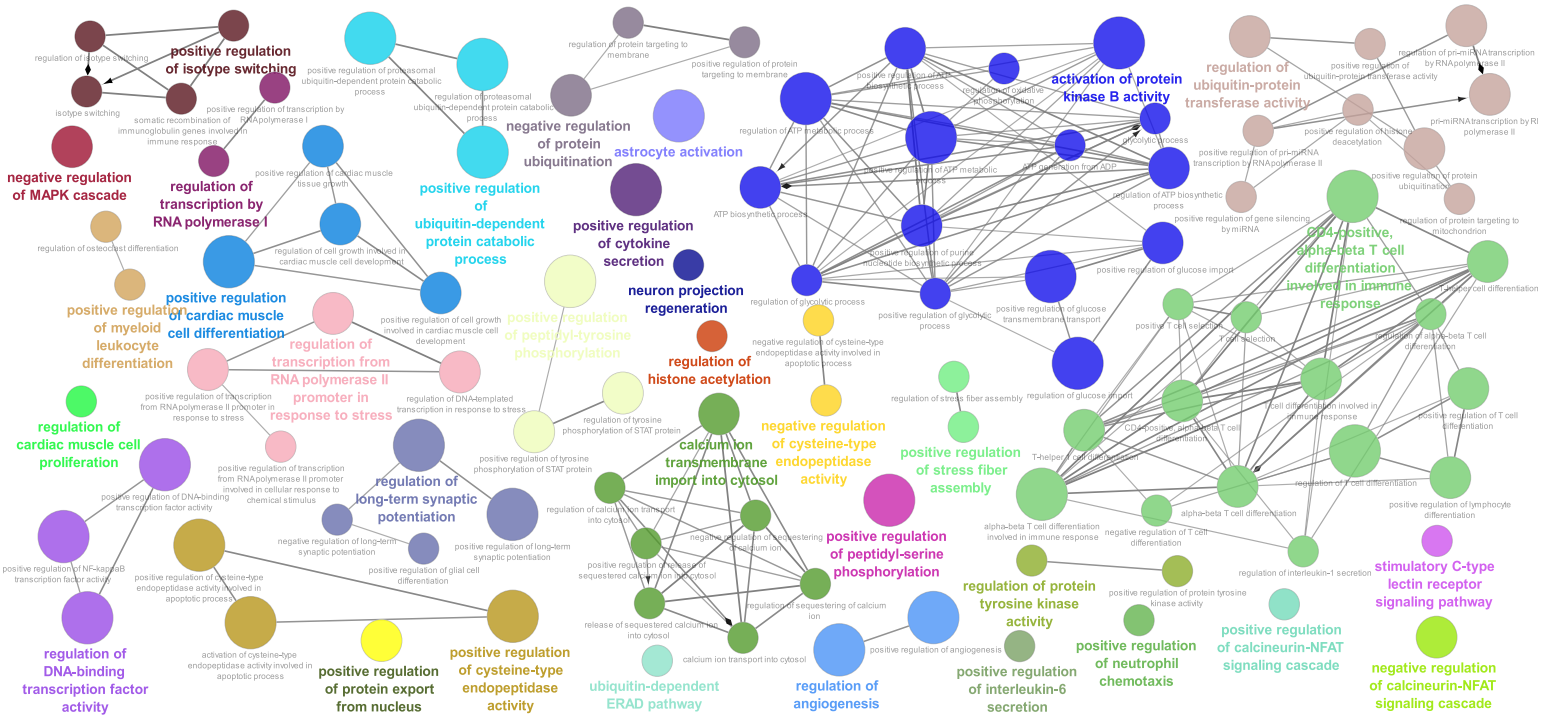

***Figure 19**- Network representation of an enrichment analysis for P4T genes related Bioprocesses performed with Cytoscape plug-in ClueGo. Analysis was preformed through the European Bioinformatics Institute (EMBLE-EBI)-Uniprot-Gene Ontology Annotation (GOA) data bases with a 0.05 significance and Go Term /Pathways selection at Cluster #1- 3 and 5% Genes, GO tree interval of 11 min level and 20 max level, Kappa score= 0,4 (Only unconnected Groups represented*

A role of MAPK signaling pathway in prostate cancer (depicted in both P4 and P4T KEGG pathway enrichment analysis) has also been found in several studies such as [190] that concludes that the activation of the MAPK signaling pathway potentiates the mutant PTEN/PI3K/AKT axis associated

progression and metastasis. Additionally, MAPK signaling inhibition by the MEK inhibitor PD325901, significantly reduced the metastatic progression initiated from transplanted stem/progenitor cells [190]. An evidenced interaction in the P4T Bioprocess KEGG pathway enrichment analysis is the MAPK signaling pathway-Proteoglycans in cancer. This interaction is also described in a study performed by [191]. This study, revealed that elevated expression of melanoma chondroitin sulfate proteoglycan (an early cell surface melanoma progression marker involved in the stimulation of tumor cell proliferation) in early tumors may facilitate melanoma progression by augmenting the activation of Focal adhesion kinase (FAK) (an known integrator of both growth factor and adhesion-related signaling pathways), ERK1 and ERK2 through distinct mechanisms.

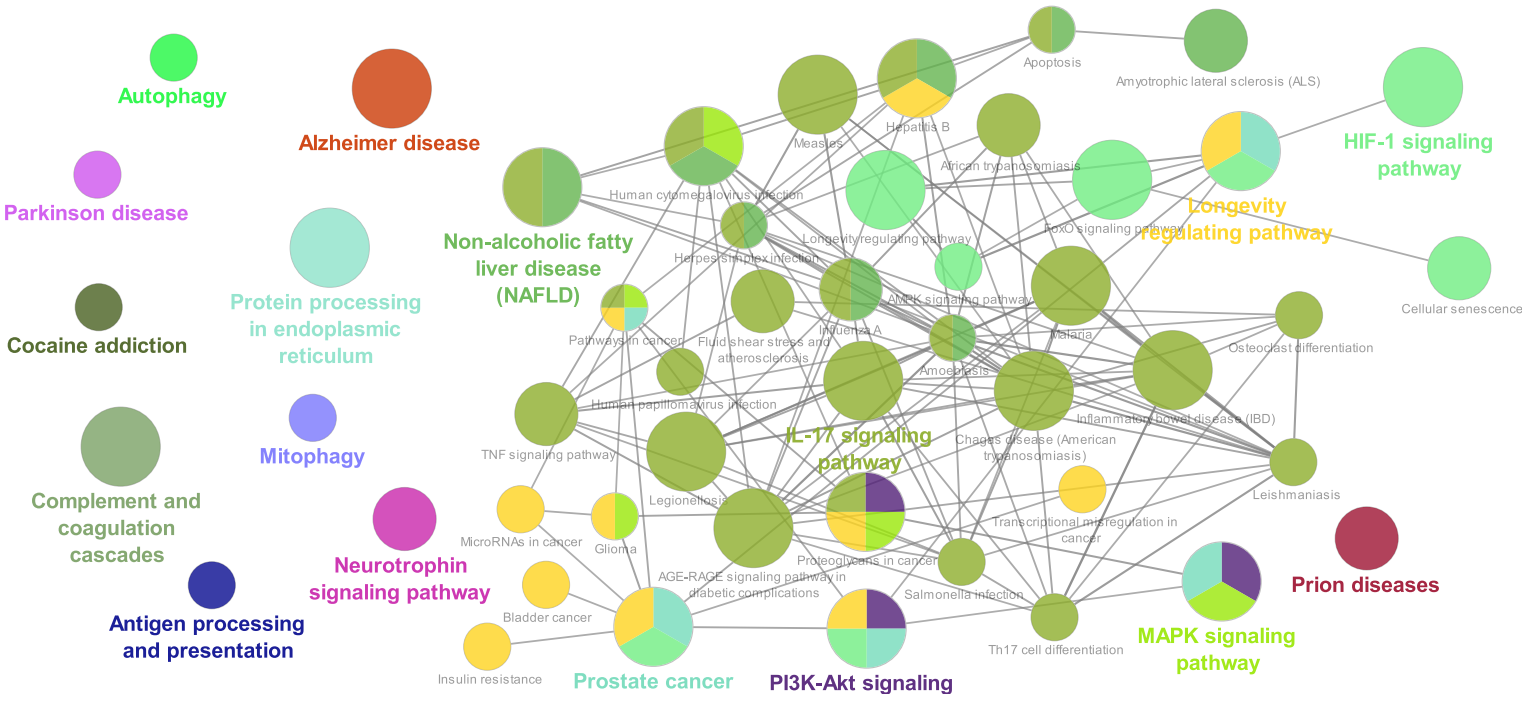

***Figure 20**- Network representation of an enrichment analysis for P4T genes related KEGG cellular pathways performed with Cytoscape plug-in ClueGo. Analysis was performed under a 0.05 significance and Go Term /Pathways selection at Cluster #1- 3 and 5% Genes, GO tree interval of 11 min level and 20 max level, Kappa score= 0,4*

Other cell cycle related pathways evidenced in our analysis include the PI3K-Akt and the HIF-1 signaling pathways. Akt or Protein kinase B, is a seronine/threonine-specific protein kinase known to be an oncogene and to possesses three isoforms. Akt1 is associated with cell surviving given its capacity to inhibit apoptotic processes and both skeletal muscle hypertrophy and general tissue

growth in mice [192]. Akt2 is known to be involved in the insulin signaling pathway and Akt3 regulates many processes including metabolism, proliferation, cell survival, growth and angiogenesis. It also plays a role in brain development and has been reported to increase malignant glioma cells proliferation and to be required to mitochondrial biogenesis stimulation through Vascular endothelial growth factor (VEGF) [193] [194]. In fact, according to Xu, Stat3 signaling is a crucial inducer of PI3K-Akt-dependent expression of hypoxia inducible factor-1α (HIF-1α) resulting in VEGF upregulation and promotion of tumor growth/survival [195]. This interaction between PI3K/Akt pathway and HIF-1α signaling described in literature might explain both results obtained in GO term Bioprocess and KEGG pathway enrichment analysis given the high number of proteins and associated terms related to both HIF-1α signaling and positive regulation of Akt signaling.

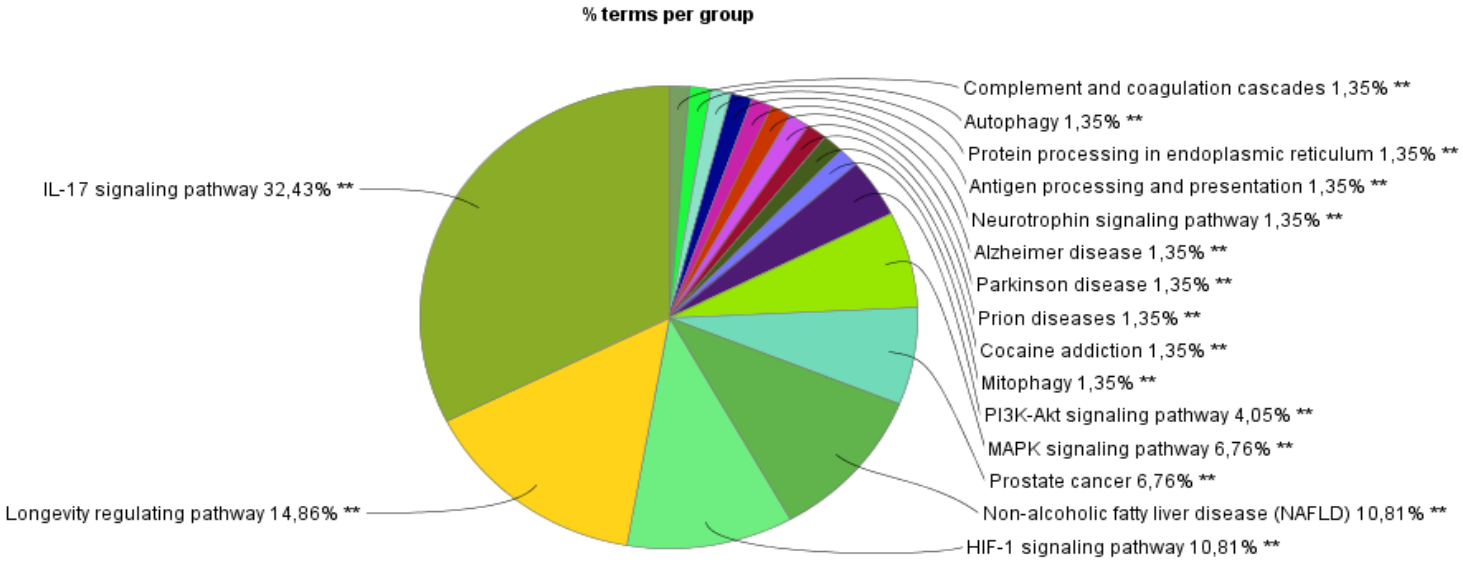

***Figure 21**- Pie Chart representation of each group terms' percentage relatively to total number of terms obtained through the related KEGG Cellular Pathways enrichment analysis of P4T gene cluster performed with the Cytoscape plug-in ClueGo. Analysis was preformed through KEGG data base with a 0.05 significance and Go Term /Pathways selection at Cluster #1-4 and 5% Genes, Kappa score= 0,4*

4.4. Neuroinflammation

The network analysis of P4T revealed APP, MAPT, SCNA and HTT as the central nodes in the network. It is well described in literature the relationship between these proteins and a range of age-related neurodegenerative diseases. As already mentioned, the enrichment analysis identified a relationship between these proteins and several components and functions of the immune

system. Therefore, in this chapter, we discuss some of the existing reports in literature correlating the neuroinflammation with each of these four proteins along with its role in the development of the associated pathology [196] [197] [198] [199].

The brain is known to express specialized pattern recognition receptors (PRRs) that upon detecting microbial molecules known as pathogen-associated molecular patterns (PAMPs), trigger an innate immune response. Besides PAMPs, PRRs are also able to recognize self-inherent molecules named danger-associated molecular patterns (DAMPs) that consequently trigger neuroinflammation. These molecules are increased in diseased brains in several forms that include misfolded proteins, aggregated peptides and mislocalized nucleic acids. Various types of cells in the brain including astrocytes, neurons and endothelial cells possess PRR and are able to induce an innate immune response through the recognition of DAMPs or PAMPs in addition to expressing receptors for cytokines and other inflammatory mediators involved in coordination of inflammatory responses in the brain. However, microglia cells stand out as the most important immune regulating cells in the brain. These cells are able to recognize DAMPs and PAMPs through highly expressed PRR in their membrane such as Toll-like receptor 2 (TLR2), TLR4 and TLR6 supported by co-receptors such as CD36 (also known as platelet glycoprotein 4), CD14 and CD47, and initiate an immune response [200] [201] [202]. Because of the significant overlap between both PAMPs and DAMPs activated signaling pathways, microglial cells may not be able to distinguish between self and microorganisms' originated molecules which might lead to the activation of immune responses upon recognition of some endogenous molecules such as aggregated amyloid-β and α-synuclein, mutant huntingtin (HTT) and superoxide dismutase 1, the S100A9–S100A8 complex (also known as MRP14–MRP8) and chromogranin A. The immune response to these molecules might result in chronic neurodegeneration leading to the development of several known age-related neurodegenerative pathologies such as Alzheimer disease, Parkinson's disease, frontotemporal dementia and Lewy body dementia. Microglial cell can be activated in two ways resulting in two different responses. The first, "M1-like" usually results in reduction in the secretion of neurotrophic factors along with the expression of inducible nitric oxide synthase and the production of reactive oxygen species (ROS) and the pro-forms of the pro-inflammatory cytokines such as members of the interleukin-1β (IL-1β) like IL-1β and IL-18. This ultimately might lead to chronic brain Inflammation, structural damage to neuron and neuronal dysfunction [196]. The sensor molecules from the NOD-like receptor family are cytosolic receptors that are constituted by a ligand interaction involved domain called Leucine-rich repeat bonded to a NACHT domain that possess an ATPase-like activity and is thought to be involved in the oligomerization of the proteins, which in turn bind to either a

Caspase activation and recruitment domains (CARD) NOD-like receptor or pyrin domain (NLRP). The most studied NOD-like receptor is NLRP3 that is usually blocked by specific Leucine-rich repeat-binding chaperon proteins. Upon activation, NRLP bind to the adaptor proteins composed of a pyrin domain and a CARD domain, through its own pyrin domain. CARD domain attracts and binds Procaspase-1 monomers forming at last a specialized structure called the inflammasome. This structure is able to cleave the pro-forms of like IL-1β and IL-18 through the activation of caspase 1 and 8 [203]. The 'M2-like' activation of microglia is relatable to the secretion of neurotrophic factors and proteases, the production of interleukin-4 (IL-4), the expression of the enzymes Arginase-1 (ARG1) and insulin-degrading enzyme (IDE) (Included in P4), and enhanced phagocytic activity. M2-microglia cells are subjected to both states of alternative activation and acquired deactivation promoted by IL-4/IL-13 and IL-10/TGF- β, respectively. M2 microglia can aid in the phagocytosis process of misfolded proteins and cell debris, promote tissue repair along with ECM reconstruction and neuron survival through neurotrophic factors. M2 microglia response ultimately antagonize the M1 pro-inflammatory responses resulting in immunosuppression and neuron protection [204].

APP association to IL-17 signaling pathway is related to Postoperative cognitive dysfunction (POCD), a pathological condition that develops in some patients submitted to surgical intervention. This condition is more frequent in elderly patients and consists in the decline in cognitive function mainly in memory and executive functions that usually last from 1–12 months after surgery but can extend to longer periods. The role of cytokine interleukin 17A (IL17A) in POCD and associated signaling pathways in mice is explored in a study performed by Tian [205]. They concluded that cognitive decline related to in POCD is related to IL-17A-associated hippocampal damage through TGFβ/Smad pathway dependent Aβ1–42 accumulation and activation of astrocytes in old mice, upon finding that after hepatectomy in mice, an increase in levels of IL17A in the hippocampus was coincident with the development of cognitive impairment, that was correlated with the increase in the production of β-amyloid 1-42 (Aβ1–42) along with several other featuring pathological traits of Alzheimer disease such as activation of astrocytes, increased phosphorylation of Signaling mother against decapentaplegic peptide 3 (Smad3) protein and upregulation of transforming growth factor-β (TGFβ) the hippocampus. Furthermore the mediating role of IL-17A in POCD was confirmed through the pre-surgery administration of IL-17A monoclonal antibody to mice that averted any alteration in the Aβ1–42 and TGFβ/Smad signaling, and the development of cognitive impairment along with a receptor small interfering RNA and a TGFβ receptor inhibitor in cultured astrocytes that resulted in the reversion of the activation of IL17A-stimulated TGFβ/Smad activation and Aβ1–42 expression [205].

The ***MAPT*** gene is known to encode, through an alternative splicing, a protein named Tau. This protein belongs to the microtubule-associated proteins family and is chiefly expressed in neurons mostly in axons. During Alzheimer disease and other tau-associated pathologies called tauopathies, hyper/abnormal phosphorylation of tau protein leads to its detachment from microtubules and consequently increase in intracellular levels soluble free tau protein [197]. These protein fragments end up aggregating forming intraneuronal Tau insoluble oligomeric structures called paired-helical filaments that constitute the neurofibrillary tangles that consequently can cause impairments in cell metabolism such as disruption of proteasome activity which may lead to neuronal death [206]. In Tauopathies pathological conditions, neurons can secrete Hyperphosphorylated pathological Tau species that are recognized and consequently activate microglial cells and astrocytes, triggering them to release cytokines or neurotoxic inflammatory molecules. Frontotemporal dementia patients carrying the P301S mutation show a sob reactivation of CD68 and hyper-phosphorylated Tau positive microglial cells around neurons along with an upregulation of IL1β through inflammasome activation, and Ciclo-oxigenase-2 [207].

In Formalin-fixed brain specimens from sporadic cases with frontotemporal dementia positive for positive Pick bodies (formed by tau protein), it was registered an activation of Microglial and reactive GFAP astrocytes [208] and in patients with Progressive Supranuclear Palsy tauopathy it was observed the production of IL-1β by microglia in the substantia nigra [209]. Furthermore, microglial cultures exposure to misfolded truncated Tau triggered a cytokine inflammatory response that included IL-6, IL-1β and TNFα through the NF-κB and MAPK signaling pathways [210]. In this particular study Kovac emphasizes an association between the MAPK signaling pathway and the neuroinflammation response supporting our results obtained through the GO Term Bioprocess enrichment analysis for P4T (**Figure 18**). Microglia is then involved in several tau inducing pathological steps such as the Tau phosphorylation, aggregation, propagation and synaptic alteration, for example through the modulation of Tau kinases such as p38, cdk5 [211]. In a study performed by [212] in two different models of Tauopathy: P301S mice and adeno-associated virus expressing mutated P301L Tau, it was revealed that microglial cells possessed a phagocytic capacity towards aggregated Tau structures. This capacity is possible through the G-protein coupled receptor 13 (CX3CR1) that can bind to hyper-phosphorylated Tau. In later stages of Alzheimer disease the over expression of chemokine (C-X3-C motif) ligand 1 (CX3CL1) causes competition between this chemokine and the hyperphosphorylated tau, slowly impairing microglial tau-

phagocytic capacity [213]. Curiously [214] reports a p38 MAPK upregulation in *hTau CX3CR1*−/− mice, especially at an early stage and that extracted and purified microglia from *hTau CX3CR1*−/−mice showed to be incapable to trigger Tau hyper-phosphorylation upon inhibition of IL-1β/p38 signaling pathway. Furthermore, it was demonstrated that microglial cells were able to transmit the phagocytized tau to neuronal cells through exosomal secretion [214].

Neuroinflammatory response is also seen to impact Tau pathogenesis in several studies upon LPS stimulation, through the myeloid receptor TLR4 capacity for microglial activation in the conditional rTg4510 mice model [215], through the exasperation of Tau pathology via CDK5 activation in the *APP*, *PS1* and *tau* mutated genes 3xTg- Alzheimer disease mice model [216] and through the impairment of tau hyper-phosphorylation in mice deficient for IL-1 receptor [217]. Together these evidences confirm the strict relationship between the innate immune system and the development of tau pathology suggested by our results.

Alpha-synuclein protein, coded by *SNCA* has been extensively correlated with Parkinson's disease in literature. This pathology is characterized by the development of aggregated alpha-synuclein constituted Lewy bodies and Lewy neurites in the substantia nigra, structures involved in its degeneration. Some variants of familial Parkinson's disease have also been shown to be correlated to point mutations or triplication of the alpha-synuclein gene, *SNCA* [218]. Alpha-synuclein aggregates have been shown to activate astrogliosis and microgliosis along with the increase in the intracellular inclusions of alpha-synuclein in the astrocytes and microglia cells suggesting phagocytic intervention by these cells [219] which according to Bjorkqvist, seems to depend on the activation state of microglia and on whether alpha-synuclein is in monomeric or oligomeric [220]. Parkinson's disease has also been correlated with chronic inflammation and innate immune leading to increase levels of IL-2, IL-4, IL-6, IL-10, TNF-α, and IFN-γ in the serum of Parkinson's disease patients [221]. Also, Lastres-Becker reveals that despite showing pro-inflammatory signals such as NF-κB, alpha-synuclein is also reported to be able to induce long-term anti-inflammatory signals in glia via NF-E2-related factor 2 (Nrf2) [222]. Other studies reveal that extracellular alpha-synuclein induces a pro-inflammatory profile in microglia with an increase in IL-1β, Ciclo-oxigenase-2 and nitric oxide synthase with, in general, an increase in reactive oxygen or nitrogen species that might be associated with cell toxicity [223].

Further studies reveal that extracellular alpha-synuclein not only alters immune cell behavior in the brain, but also circulating macrophages, T-cells and B cells; especially if the aggregates are initiated

in the digestive system or the mucosa in the nose [224]. A relation between SNCA/ Parkinson's disease and the IL-17 is approached throughout the literature particularly in a study performed by Reynolds. Neurodegenerative process triggered by Nitrated alpha-synuclein immunization in 1-methyl-4-phenyl-1,2,3,6-tetrahydropyridine (MPTP) mice model of Parkinson's disease is mediated by Th17 cells along with the suppression of $CD4^+$ $CD25^+$ regulatory T cell (Treg) that lacked the functional capacity of suppression of effector T-cells proliferation [225]. This comes as no surprise given that the signals that induce Th17 to differentiate also inhibit Treg differentiation.

The ***HTT*** gene codes for the huntingtin protein that when suffers specific expansion of its PolyQ tract leads to the coding of additional glutamine residues and consequently to the pathological development of Huntington's disease. Wildtype Huntingtin protein display between 6 and 35 glutamine residues whether mutant forms contains 36 or more. Evidences of the active role of the immune system in the pathophysiological development of Huntington's disease have been unveiled including the upregulation of cytokines such as IL-6, IL-8 and tumor necrosis factor (TNF)-α in the CSF of Huntington's disease patients [226] and a correlation between the increase in the levels of several proteins produced by cells from the innate immune system such as transforming growth factor (TGF)-1β, chemokines vascular endothelial growth factor (VEGF), (CCL4, 11, 13 and 26) in the blood Huntington's disease patients, and the progression the disease [227]. Also, it has been observed the upregulation of oxidative stress markers along with protein carbonyls in Huntington's disease brains [228] and an increase in the levels of 3-nitrotyrosine, a reactive nitrogen species biomarker, in Huntington's disease cortex and striatum [229]. In fact, mutant HTT aggregates have been proved to induce the production of free radicals [230] both in neuronal and non-neuronal cells [231]. Unusual accumulation of iron has been reported in Huntington's disease brains [232] and although Iron is strictly necessary for the normal functioning of mitochondria, excessive accumulation can lead to unmanageable production of ROS. Also, Iron possesses a regulating role towards HTT [233] and mutant HTT inclusions are iron-dependent centers of oxidative stress [234]. A study performed by Giorgini in a yeast suppressor screen, revealed that attenuation of the cell toxicity associated with mutant HTT was induced by the genetic deletion of kynurenine 3-monooxygenase, an enzyme present mainly in microglia, that converts kynurenine into 3-hydroxykynurenine known to be an agonist of NMDA receptors, generating free radicals and quinolinic acid in microglia but not in neurons [235].

Huntington's disease patients plasma levels reveled a decrease in the levels of IL-18 [227], a cytokine involved in the activation of cell-mediated immunity, thioredoxin reductase-1 and thioredoxin-1, with the last two being also decreased in erythrocytes from Huntington's disease patients [236]. Furthermore, mutant HTT levels in peripheral monocytes and T-cells from Huntington's disease patients were directly correlated with both with disease burden score and caudate atrophy rates [237]. Two studies report that, although found to express mutant HTT, monocytes and macrophages collected from Huntington's disease patients' blood samples did not displayed increased proinflammatory cytokines expression and/or production in comparison with monocytes collected from healthy donors [220] [238] and were found to be hyperactive when exposed to external proinflammatory stimulation. Particularly, upon LPS stimulation *in vitro*, mutant HTT in myeloid cells binds IKKγ leading to increased degradation of IκB and subsequent nuclear translocation of RelA (increasing NF-κB activity) triggering the production of excessive inflammatory cytokines. Reduction in HTT monocytes/macrophages levels from Huntington's disease patients by the administration of Glucan-encapsulated RNAi towards HTT showed a reversal of HTT induced elevated cytokine production and transcriptional changes [238]. Furthermore, mutant HTT was shown to be associated with impairment in macrophage migration to inflammatory stimulus [239] suggesting being the cause of absence of periphery innate immune cells infiltration detected in Huntington's disease.

Representatives from the innate immune system in the brain have been found to be reactive in the brains from Huntington's disease patients microglia and astrocytes [240]. In fact, reactive microglial cells can even be found in pre-symptomatic Huntington's disease gene carriers coincidentally with the increase in IL-6 levels in the plasma, up to 15 years before predicted age of onset [241] [220]. A genome wide associated study showed evidences that the microglia expression of mutant HTT is sufficient factor to induce a cell-autonomous increase in proinflammatory gene expression, particularly the mutant HTT inducing increase in the expression and transcriptional functions of myeloid lineage-determining factors PU.1 and CCAAT/enhancer-binding protein (C/EBP)-α,β being highly correlated with increased expression of both IL-6 and TNFα [242]. Several studies also show evidences of Complement system associated factors role in Huntington's disease, such as the deposition of C1q, C4, and C3, iC3b and C9 in the surface of astrocytes, neuron and myelin from the striatum of Huntington's disease patients contrasting with the absence in the control group. The same study also depicts the increase of astrogliosis and microgliosis in Huntington's disease caudate and the internal capsule samples compared to the control group along with the increase in mRNA of C1r ,C1q C chain, C4 and C3, known complement activating proteins of the classical pathway

along with the complement regulators, MCP, C1 inhibitor, DAF, CD59, clusterin in Huntington's disease brains compared to the control. Huntington's disease affected caudate also showed high expression of Complement anaphylatoxin receptor mRNAs (C5a and C3a receptors) and in-situ hybridization assay revealed the expression of C3 and C9 mRNA by reactive microglial cells in Huntington's disease internal capsule [243]. Several studies reveal that the presence of mutant HTT in astrocytes coincides with their incapacity to perform their supporting function towards neurons. In fact, compared to wildtype, mutant HTT expressing mice solely on astrocytes displayed body weight loss, motor function deficits, and decreased lifespans [244]. Neurons from the striatum are connected by cortex glutamatergic neurons. According to Lievens [245] glutamate uptake in primary astrocytes is impaired by mutant HTT which might contribute to neuronal excitotoxicity observed in Huntington's disease [246] and are for this reason particularly susceptible to an excess of extracellular glutamate. In another study, mutant HTT was also found to be responsible for the reduction of CCL5 transcription by NF-κB and protein secretion in astrocytes, which might contribute to neurons functional dysfunction in Huntington's disease.

The JAK/STAT3 pathway was found to be activated in reactive astrocytes in a mouse and a nonhuman primate lentiviral vector-based model of Huntington's disease [247]. JAK/STAT3 is known to be activated through IL-6 stimulation [248], that upon mutant HTT stimulated microglia secretion, as verified earlier, might exacerbate immune reactivity through astrocyte activation. Taken together, this collected data present strong evidences of the neuroinflammation process during the Huntington's disease pathophysiology depicting HTT as the mediating protein, as suggested by cross results from parameter and enrichment analysis

4.5.FK866 effect on neuroblastoma cells (SH-SY5Y)

Several distinct organisms, including human, display a significant reduction in the cellular NAD levels during aging. Therefore, in order to simulate those conditions in SH-SY5Y cells, used an NAMPT inhibitor FK866.

4.5.1. FK866 effect on SH-SY5Y cell viability

As described in the literature, disruption of the salvage pathway by the addition of FK866 to a wide variety of cells results in a decrease in cell viability [249] [250] [251] [252] [134] [253]. In order to test these results, SH-SY5Y (Passage 14 to 16) were cultured in MEM-F12 10% FBS with 10nM and

100nM FK866 for 24h, 48h and 72h. Cell viability was measured at each time using the Trypan blue method as described in the Methods and Materials section. Live cells cannot be dyed by trypan blue because this compound is not able to pass through its intact membrane, however when cells die, their membrane gets compromised allowing Trypan Blue to enter inside the cell giving it a blue tonality which allows its distinction from living cells.

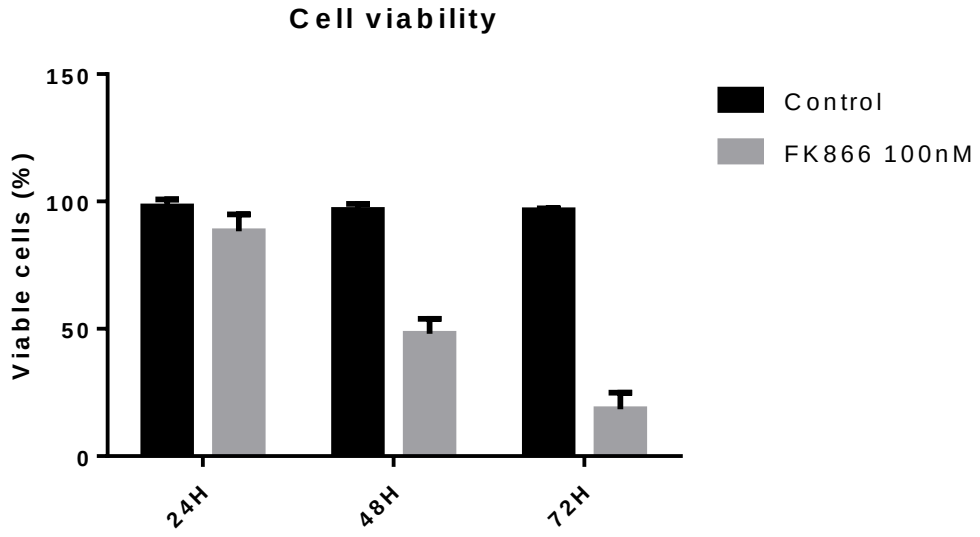

***Figure 22**- Cell viability assay using Trypan blue exclusion method performed at 24h, 48h and 72h timepoints in SH SY5Y cells cultured in 35mm plates exposed to FK866 100 nM for 3 days. Trypsin was inactivated with MEM-F12 containing suspended dead cells, collected previously from the same plates. n=3*

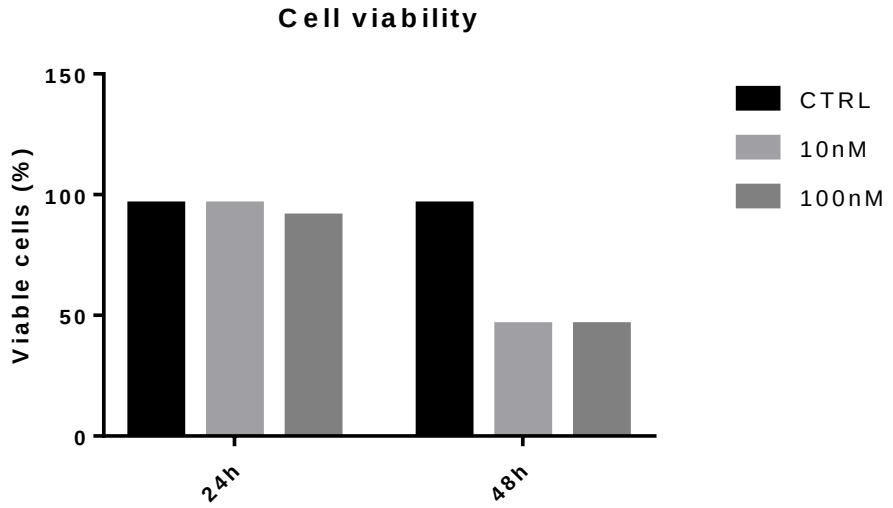

***Figure 23**- Cell viability assay using Trypan blue exclusion method performed at 24h and 48h timepoints in SH SY5Y cells cultured in 35mm plates exposed to FK866 10nM and 100 nM for 2 days. Trypsin was inactivated with MEM-F12 containing suspended dead cells, collected previously from the same plates.*

As represented in **Figure 22** and **Figure 23**, this experiment reveals no alterations in cell viability in cells exposed to both 10 nM and 100 nM FK866 for 24h compared to the control group. This contrasts with reports by Schuster in Huh7 and Hep3B cells treated with 10 nM FK866 that display a 50% decrease in cell viability [249]. This indicates that different cells have different sensibility to FK866. Furthermore, in another study performed in SH-SY5Y cells by Galli it is described how cell viability varies with FK866 concentration at 72h timepoint [254]. Gali reports that SH-SY5Y cultures treated with FK866 concentration between 10 nM and 10000 nM display a similar cell viability (20%) after 72h, which complies with the results obtained in this study (**Figure 22**). Similarly, after treating SH-SY5Y cells with a range of FK866 between 0,01 nM and 100 nM for 24h, Billington reported more than 70% of cells remained viable even at 100 nM concentration [134]. Both these studies indicate no difference in cell viability between 10 nM and 100 nM FK866 treatments at 24h and 72h in SH-SY5Y which meets the results obtained in this study (**Figure 23**). Furthermore, both SH-SY5Y cells treated with 10 nM and 100 nM FK866 for 48h displayed a decrease down to ± 50% cell viability (**Figure 22**) (**Figure 23**) compared to the ± 96% displayed by control group. A similar decrease in cell viability of 293T cells cultures submitted to the same treatment for 48h has been observed by Thakur [255], however it another study performed by the same author [253] is reported no alterations in cell viability of NB-4, OCI-AML3 and MOLM-13 cell lines treated with 10 nM FK866 for 48h. Curiously in the Billington study it was registered a softer decrease (around 70%) in cell viability upon SH-SY5Y cells had received 10 nM and 100 nM FK866 treatments for 48h. Billington also suggest increase in autophagy as the cause of SH-SY5Y cell death augmentation upon FK866 treatment. Indeed, another study performed with FK866 by Sharif, described NAMPT as a main regulator of autophagy in cancer stem cells (CSC) and also a main determinant of its level of pluripotency [256]. As suggested by the authors, NAMPT could play a positive and negative regulatory role at the same time where any alteration in its levels have direct effect on autophagy levels. Sharif also registered increased expression of senescence markers (CDKN2A, CDKN1A, CDKN1B) upon autophagy stimulating treatments such as serum starvation and rapamicyn treatment were applied to CSC cells. These treatments inhibit cells pluripotency without promoting their differentiation while leading to cell senescence. This suggests that basal levels of NAMPT and consequently of autophagy are required to prevent cells senescence giving an additional explanation besides the drop in NAD^+ levels to cell viability decline upon SH-SY5Y FK866 treatment during 48h registered in our study (**Figure 22**). Overall, our results suggest that 10 nM and 100 nM Fk866 treatment to SH-SY5Y cells induces considerable cell death when cultured for 48h hours or

more and shows no difference in the effect on cell viability between the two concentrations at both 24h and 48h.

4.5.2.FK866 effect in NAMPT and NAPRT protein expression

FK866 is an inhibitor of NAMPT activity whose effect has been confirmed in several cancer cell lines including in SH-SY5Y cells. NAMPT inhibition by FK866 leads to intracellular NAD^+ depletion in SH-SY5Y cells which has a direct correlation with decrease in cell viability [257] [258] [254]. In this experiment we intend to clarify how NAMPT and NAPRT protein expression is affected in SH-SY5Y cells by FK866 exposure during 8h, 24h and 48h. SH-SY5Y cells were therefore cultured on 60mm plates in MEM-F12 10% FBS with 10 nM and 100 nM FK866 for 8h, 24h and 48h, lysed with RIPA and quantified using the BCA kit. Proteins were separated by SDS-PAGE and detected by Western Blot analysis, using anti-rabbit NAMPT or NAPRT primary and HRP-linked secondary antibodies and revealed using ECL Prime mixture. To normalize results, Actin signal was measured.

NAMPT quantification revealed no differences between 10 nM and 100 nM FK866 treated cells and the control group at 8h, 24h and 48h (**Figure 24**). These results are in agreement with Grohmann who also did not find any difference in NAMPT protein expression between Molt-4 cells treated with 10 nM FK866 for 24h and its control group [259]. Also, after treating Jurkat cells

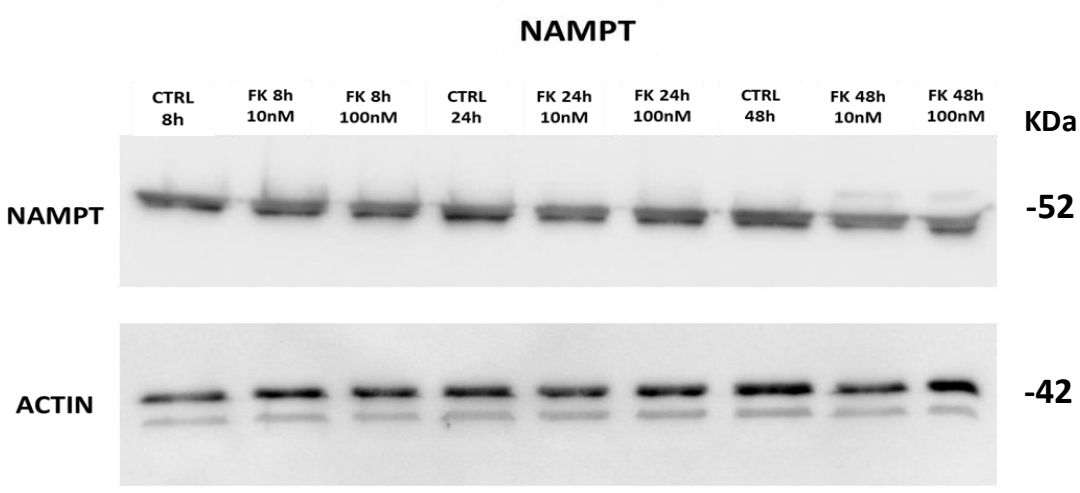

Figure 24- *SDS-PAGE Western Blot analysis of 15µg protein samples extracted from SH SY5Y cells treated with 10 nM and 100 nM FK866 for 8h, 24h and 48h and respective controls. NAMPT rabbit and Actin mouse primary antibodies were diluted at 1:2000 and 1:10000 proportions respectively and incubated for 2h at 4ºC. Detection was performed under ECL Prime kit.*

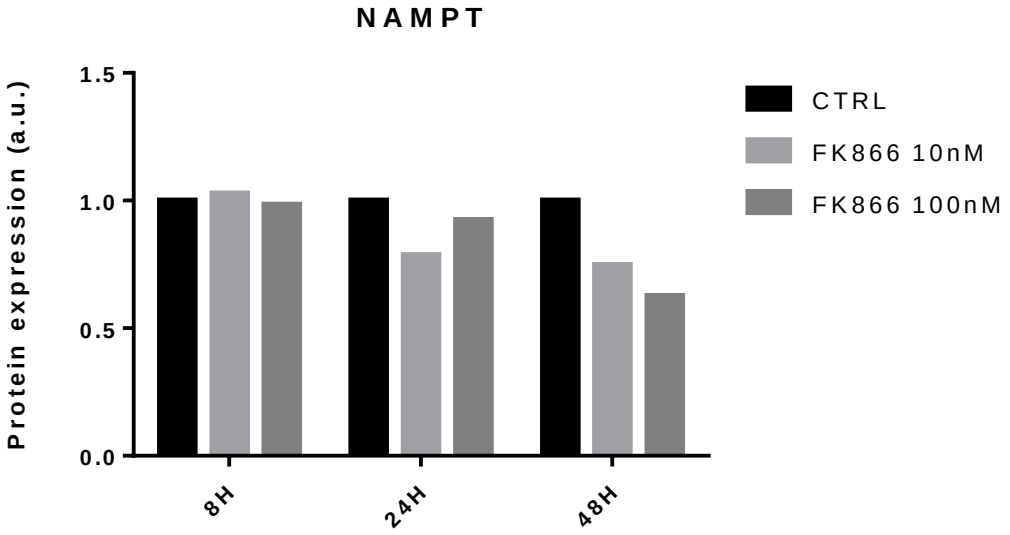

***Figure 25**- Quantification of NAMPT protein expression levels from FK866 treated SH SY5Y cells evaluated through SDS-PAGE Western Blot assay (Control normalized).*

with 100 nM FK866 for 48h, Zucal still did not find any significant differences in NAMPT protein expression comparatively to the control group [260]. In agreement with both these studies we did not find any difference in NAMPT protein expression between the two different concentration treatments.

NAPRT has been shown to be amplified and overexpressed in several common types of cancer, including ovarian, pancreatic, prostate, and breast cancer [261], although both NAPRT mRNA and protein expression levels have been reported to be reduced in some glioblastomas and neuroblastoma cell lines [262]. Therefore, we sought to elucidate SH-SY5Y cells NAPRT protein expression profile upon treatment with 100 nM FK866 for 8h, 24h and 48h.

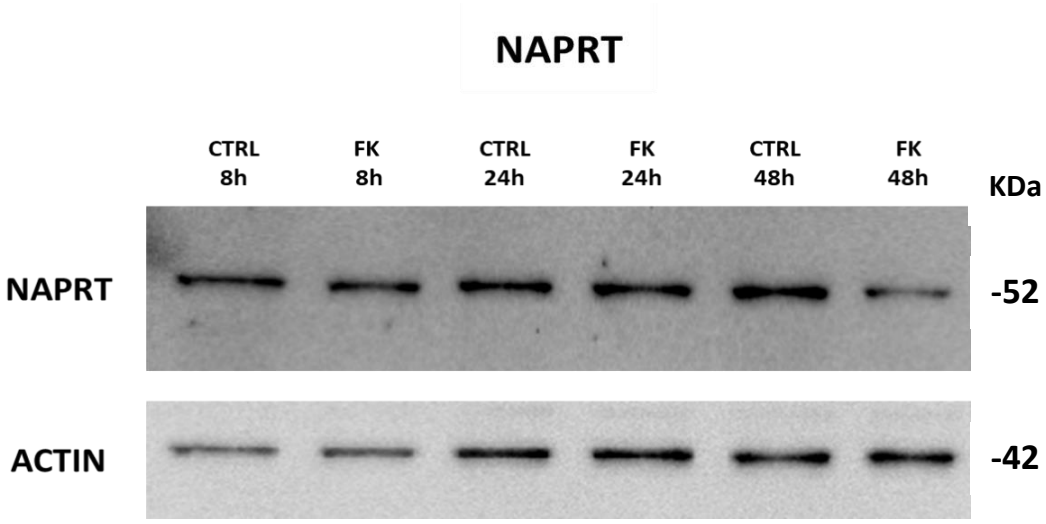

***Figure 26**- SDS-PAGE Western Blot analysis of 15µg protein samples extracted from SH SY5Y cells treated with 100 nM FK866 for 8h, 24h and 48h and respective controls. NAPRT rabbit and Actin mouse primary antibodies were diluted at 1:2000 and 1:10000 proportions respectively and incubated for 2h at 4ºC. Detection was performed under EC L Prime kit.*

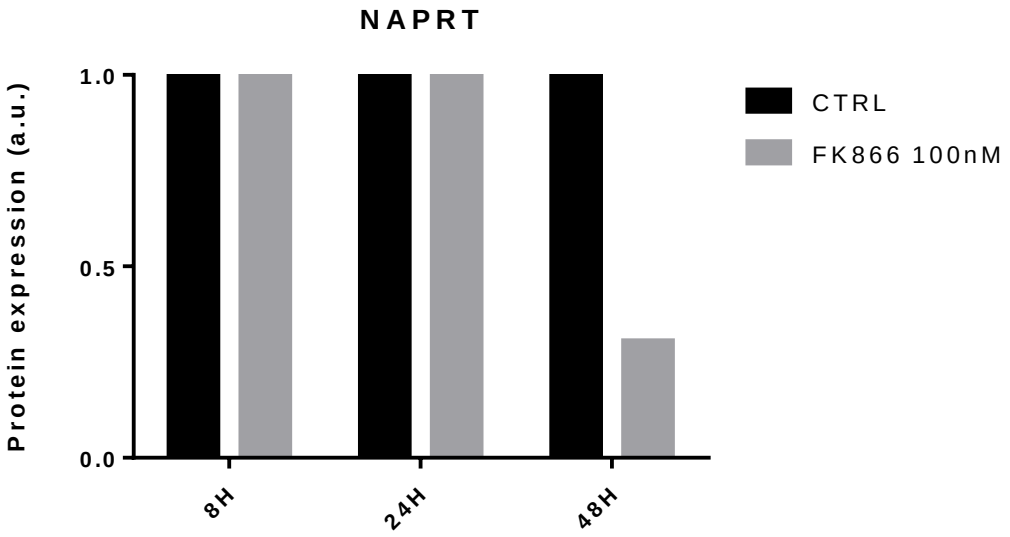

Figure 27- *Quantification of NAPRT protein expression levels from FK866 treated SH SY5Y cells evaluated through SDS-PAGE Western Blot assay (Control Normalized).*

As **Figure 25** shows, cells treated with FK866 for both 8h and 24h did not show any alterations relatively to the control group, although its expression at considerable levels in this type of cell line has been confirmed. On the other hand, FK866 treatment for 48h proved to have a decreasing effect on NAPRT protein expression compared to the control group. Despite our evidences of NAPRT protein expression in SH-SY5Y cells, it remains to be determined if it is indeed active. Some evidences in literature suggest an explanation for both lack of NAPRT expression and inactivity in some cell tissues and cancer cell lines that both include neuronal tissue [263] [264]. Our cell viability results (**Figure 22**) are strong indicators for brain tissue capacity for using the NR or the novo pathway to form NAD^+ which would explain SH-SY5Y cells capacity to remain viable during 24h of FK866 treatment. This conclusion can also be supported by the fact that cancer cells that are not able to generate NAD^+ via the Press handler suffer a large drop in NAD^+ levels and viability at 24h [265] and the ones who can are resistant to NAMPT inhibitors such as FK866 [133] [266] [267].

5. Conclusions & Future Perspectives

FK866 cytotoxic effect is evaluated in this work, showing 50% cell viability in cultured SH-SY5Y cells after a 48h incubation period at both 10nM and 100nM. NAMPT protein expression levels remain unaltered throughout the 48h treatment while NAPRT protein expression levels although maintained during the first 24h, suffer a decrease at 48h timepoint. It remains to be determined whether the simultaneous decline in cell viability and NAPRT protein expression at 48h are directly correlated and if so, what vital cellular processes are affected by NAPRT decline. Also, in order to completely establish a fully functional SH-SY5Y aging model is still necessary to describe the molecular mechanisms behind these cells' response to FK866 induced NAD^+ depletion that match the described cell viability featuring the NAMPT and NAPRT protein expression profile. This include questions such as how does NAMPT activity inhibition is related to NAPRT decline at 48h? Does it prevent NAD^+ decline given that NAPRT expressing tumors are reported to be more resistance to NAMPT inhibitors including FK866 [133] [266] [267]? Why does NAMPT Protein levels remain constant during 48h? Do its mRNA levels are also maintained during the 48h treatment or does it suffer alterations? Furthermore, in future studies it would be interesting to evaluate the if the remaining NAD^+ producing pathways (NR Salvage and de novo pathways) have any role in SH-SY5Y response to NAMPT activity inhibition by FK866.

From the results obtained in Network Analysis chapter we were able to emphasize the strait relationship between the immune system and the proteostasis, aging and aging-related metabolic, cardiovascular and neurodegenerative diseases. According to the parameter analysis, the more evident relation described in the 1500 articles data base is the neurodegenerative diseases-immune system. Cancer associated cell-cycle regulatory functions and pathways mainly the MAPK signaling pathway, were also highly associated with gene clusters suggesting a possible role in proteostasis, aging and aging-related metabolic, cardiovascular or neurodegenerative diseases. It was also verified that the suggested representative number of reviewed articles (200) does not provide an accurate sample for enrichment analysis representative of the total number articles employed. However, similar analysis using different enrichment parameters should be subject to future works in order to find more relevant correlations within this dataset. It would also be interesting to see this bioinformatic approach be applied to different datasets of different subjects in order to test its dataset text-mining protein network extraction and analyzing capacity.

6. References

1. Harden A, Young WJ. The alcoholic ferment of yeast-juice. Proceedings of the Royal Society of London Series B-Containing Papers of a Biological Character. 1906 Apr;77(519):405-20.
2. von Euler H, Myrback K. Co-zynase, XVII. Hoppe-Seylers Zeitschrift Fur Physiologische Chemie. 1930;190:93-100.
3. Warburg O, Christian W. Pyridine, the hydrogen transfusing component of fermentative enzymes. Helvetica Chimica Acta. 1936;19:79-88.
4. Pollak N, Dolle C, Ziegler M. The power to reduce: pyridine nucleotides - small molecules with a multitude of functions. Biochemical Journal. 2007 Mar;402:205-18.
5. Bogan KL, Brenner C. Nicotinic acid nicotinamide and nicotinamide riboside: A molecular evaluation of NAD(+) precursor vitamins in human nutrition. Annual Review of Nutrition. 2008;28:115-30.
6. Elvehjem CA, Madden RJ, Strong FM, Woolley DW. The isolation and identification of the anti- black tongue factor. Journal of Biological Chemistry. 1938 Mar;123(1):137-49.
7. Bieganowski P, Brenner C. Discoveries of nicotinamide riboside as a nutrient and conserved NRK genes establish a Preiss-Handler independent route to NAD(+) in fungi and humans. Cell. 2004 May;117(4):495-502.
8. Belenky P, Bogan KL, Brenner C. NAD(+) metabolism in health and disease. Trends in Biochemical Sciences. 2007 Jan;32(1):12-19.
9. Houtkooper RH, Canto C, Wanders RJ, Auwerx J. The Secret Life of NAD(+): An Old Metabolite Controlling New Metabolic Signaling Pathways. Endocrine Reviews. 2010 Apr;31(2):194-223.
10. Taylor MW, Feng GS. RELATIONSHIP BETWEEN INTERFERON-GAMMA, INDOLEAMINE 2,3-DIOXYGENASE, AND TRYPTOPHAN CATABOLISM. Faseb Journal. 1991 Aug;5(11):2516-22.
11. Heyes MP, Saito K, Jacobowitz D, Markey SP, Takikawa O, Vickers JH. POLIOVIRUS INDUCES INDOLEAMINE-2,3-DIOXYGENASE AND QUINOLINIC ACID SYNTHESIS IN MACAQUE BRAIN. Faseb Journal. 1992 Aug;6(11):2977-89.
12. Salter M, Pogson CI. THE ROLE OF TRYPTOPHAN 2,3-DIOXYGENASE IN THE HORMONAL-CONTROL OF TRYPTOPHAN-METABOLISM IN ISOLATED RAT-LIVER CELLS - EFFECTS OF GLUCOCORTICOIDS AND EXPERIMENTAL DIABETES. Biochemical Journal. 1985;229(2):499-504.
13. Comings DE, Muhleman D, Dietz G, Sherman M, Forest GL. SEQUENCE OF HUMAN TRYPTOPHAN 2,3-DIOXYGENASE (TDO2) - PRESENCE OF A GLUCOCORTICOID RESPONSE-LIKE ELEMENT COMPOSED OF A GTT REPEAT AND AN INTRONIC CCCCT REPEAT. Genomics. 1995 Sep;29(2):390-96.
14. Yamazaki F, Kuroiwa T, Takikawa O, Kido R. HUMAN INDOLYLAMINE 2,3-DIOXYGENASE - ITS TISSUE DISTRIBUTION, AND CHARACTERIZATION OF THE PLACENTAL ENZYME. Biochemical Journal. 1985;230(3):635-38.
15. Kudo Y, Boyd CAR. Human placental indoleamine 2,3-dioxygenase: cellular localization and characterization of an enzyme preventing fetal rejection. Biochimica Et Biophysica Acta-Molecular Basis of Disease. 2000 Jan;1500(1):119-24.
16. Bender DA. BIOCHEMISTRY OF TRYPTOPHAN IN HEALTH AND DISEASE. Molecular Aspects of Medicine. 1983;6(2):101-97.
17. Rongvaux A, Shea RJ, Mulks MH, Gigot D, Urbain J, Leo O, et al. Pre-B-cell colony-enhancing factor, whose expression is up-regulated in activated lymphocytes, is a nicotinamide phosphoribosyltransferase, a cytosolic enzyme involved in NAD biosynthesis. European Journal of Immunology. 2002 Nov;32(11):3225-34.
18. Werner E, Ziegler M, Lerner F, Schweiger M, Muller YA, Heinemann U. Crystallization and preliminary X-ray analysis of human nicotinamide mononucleotide adenylyltransferase

(NMNAT). Acta Crystallographica Section D-Biological Crystallography. 2002 Jan;58:140-42.
19. Zhou TJ, Kurnasov O, Tomchick DR, Binns DD, Grishin NV, Marquez VE, et al. Structure of human nicotinamide/nicotinic acid mononucleotide adenylyltransferase - Basis for the dual substrate specificity and activation of the oncolytic agent tiazofurin. Journal of Biological Chemistry. 2002 Apr;277(15):13148-54.
20. Ali YO, Li-Kroeger D, Bellen HJ, Zhai RG, Lu HC. NMNATs, evolutionarily conserved neuronal maintenance factors. Trends in Neurosciences. 2013 Nov;36(11):632-40.
21. Yalowitz JA, Xiao SH, Biju MP, Antony AC, Cummings OW, Deeg MA, et al. Characterization of human brain nicotinamide 5 '-mononucleotide adenylyltransferase-2 and expression in human pancreas. Biochemical Journal. 2004 Jan;377:317-26.
22. Berger F, Lau C, Dahlmann M, Ziegler M. Subcellular compartmentation and differential catalytic properties of the three human nicotinamide mononucleotide adenylyltransferase isoforms. Journal of Biological Chemistry. 2005 Oct;280(43):36334-41.
23. Preiss J, Handler P. BIOSYNTHESIS OF DIPHOSPHOPYRIDINE NUCLEOTIDE .1. IDENTIFICATION OF INTERMEDIATES. Journal of Biological Chemistry. 1958;233(2):488-92.
24. Gingrich W, Schlenk F. Codehydrogenase I and other pyridinium compounds as V-factor for hemophilus influenzae and H parainfluenzae. Journal of Bacteriology. 1944 Jun;47(6):535-50.
25. Leder IG, Handler P. SYNTHESIS OF NICOTINAMIDE MONONUCLEOTIDE BY HUMAN ERYTHROCYTES INVITRO. Journal of Biological Chemistry. 1951;189(2):889-99.
26. Shifrine M, Biberstein EL. GROWTH FACTOR FOR HAEMOPHILUS SPECIES SECRETED BY A PSEUDOMONAD. Nature. 1960;187(4737):623-23.
27. Rine J, Herskowitz I. 4 GENES RESPONSIBLE FOR A POSITION EFFECT ON EXPRESSION FROM HML AND HMR IN SACCHAROMYCES-CEREVISIAE. Genetics. 1987 May;116(1):9-22.
28. De Flora A, Zocchi E, Guida L, Franco L, Bruzzone S. Autocrine and paracrine calcium signaling by the CD38 NAD(+) cyclic ADP-ribose system. In: Bradlow HL, Castagnetta L, Massimo L, Zaenker K, editors. Signal Transduction and Communication in Cancer Cells. Annals of the New York Academy of Sciences. 2004. p. 176-91.
29. Sinclair DA, Guarente L. Extrachromosomal rDNA circles - A cause of aging in yeast. Cell. 1997 Dec;91(7):1033-42.
30. Kaeberlein M, McVey M, Guarente L. The SIR2/3/4 complex and SIR2 alone promote longevity in Saccharomyces cerevisiae by two different mechanisms. Genes & Development. 1999 Oct;13(19):2570-80.
31. Kennedy BK, Austriaco NR, Zhang JS, Guarente L. MUTATION IN THE SILENCING GENE SIR4 CAN DELAY AGING IN SACCHAROMYCES-CEREVISIAE. Cell. 1995 Feb;80(3):485-96.
32. Sinclair DA, Guarente L. Unlocking the secrets of longevity genes. Scientific American. 2006 Mar;294(3):48-+.
33. Sauve AA, Wolberger C, Schramm VL, Boeke JD. The biochemistry of sirtuins. Annual Review of Biochemistry. 2006;75:435-65.
34. Imai S, Guarente L. NAD(+) and sirtuins in aging and disease. Trends in Cell Biology. 2014 Aug;24(8):464-71.
35. Michan S, Sinclair D. Sirtuins in mammals: insights into their biological function. Biochemical Journal. 2007 May;404:1-13.
36. Finkel T, Deng CX, Mostoslavsky R. Recent progress in the biology and physiology of sirtuins. Nature. 2009 Jul;460(7255):587-91.
37. Westphal CH, Dipp MA, Guarente L. A therapeutic role for sirtuins in diseases of aging? Trends in Biochemical Sciences. 2007 Dec;32(12):555-60.
38. Imai S, Guarente L. It takes two to tango: NAD(+) and sirtuins in aging/longevity control. Npj Aging and Mechanisms of Disease. 2016 Aug;2.

39. Haigis MC, Guarente LP. Mammalian sirtuins - emerging roles in physiology, aging, and calorie restriction. Genes & Development. 2006 Nov;20(21):2913-21.
40. Haigis MC, Sinclair DA. Mammalian Sirtuins: Biological Insights and Disease Relevance. Annual Review of Pathology-Mechanisms of Disease. 2010;5:253-95.
41. Imai S, Armstrong CM, Kaeberlein M, Guarente L. Transcriptional silencing and longevity protein Sir2 is an NAD-dependent histone deacetylase. Nature. 2000 Feb;403(6771):795-800.
42. Cao Y, Jiang XL, Ma HJ, Wang YL, Xue P, Liu Y. SIRT1 and insulin resistance. Journal of Diabetes and Its Complications. 2016 Jan-Feb;30(1):178-83.
43. Chen D, Bruno J, Easlon E, Lin SJ, Cheng HL, Alt FW, et al. Tissue-specific regulation of SIRT1 by calorie restriction. Genes & Development. 2008 Jul;22(13):1753-57.
44. Bordone L, Guarente L. Calorie restriction, SIRT1 and metabolism: Understanding longevity. Nature Reviews Molecular Cell Biology. 2005 Apr;6(4):298-305.
45. Qin WP, Yang TL, Ho L, Zhao Z, Wang J, Chen LH, et al. Neuronal SIRT1 activation as a novel mechanism underlying the prevention of Alzheimer disease amyloid neuropathology by calorie restriction. Journal of Biological Chemistry. 2006 Aug;281(31):21745-54.
46. Civitarese AE, Carling S, Heilbronn LK, Hulver MH, Ukropcova B, Deutsch WA, et al. Calorie restriction increases muscle mitochondrial biogenesis in healthy humans. Plos Medicine. 2007 Mar;4(3):485-94.
47. Kume S, Uzu T, Horiike K, Chin-Kanasaki M, Isshiki K, Araki S, et al. Calorie restriction enhances cell adaptation to hypoxia through Sirt1-dependent mitochondrial autophagy in mouse aged kidney. Journal of Clinical Investigation. 2010 Apr;120(4):1043-55.
48. Baur JA, Pearson KJ, Price NL, Jamieson HA, Lerin C, Kalra A, et al. Resveratrol improves health and survival of mice on a high-calorie diet. Nature. 2006 Nov;444(7117):337-42.
49. Milne JC, Lambert PD, Schenk S, Carney DP, Smith JJ, Gagne DJ, et al. Small molecule activators of SIRT1 as therapeutics for the treatment of type 2 diabetes. Nature. 2007 Nov;450(7170):712-16.
50. Hasler P, Zouali M. Immune receptor signaling, aging, and autoimmunity. Cellular Immunology. 2005 Feb;233(2):102-08.
51. Larbi A, Fulop T, Pawelec G. Immune Receptor Signaling, Aging and Autoimmunity. In: Sigalov AB, editor. Multichain Immune Recognition Receptor Signaling: from Spatiotemporal Organization to Human Disease. Advances in Experimental Medicine and Biology. 2008. p. 312-24.
52. Aw D, Silva AB, Palmer DB. Immunosenescence: emerging challenges for an ageing population. Immunology. 2007 Apr;120(4):435-46.
53. Jonsson H, Peng SL. Forkhead transcription factors in immunology. Cellular and Molecular Life Sciences. 2005 Feb;62(4):397-409.
54. Vanfleteren JR, Braeckman BP. Mechanisms of life span determination in Caenorhabditis elegans. Neurobiology of Aging. 1999 Sep-Oct;20(5):487-502.
55. Lin L, Hron JD, Peng SL. Regulation of NF-kappa B, Th activation, and autoinflammation by the forkhead transcription factor Foxo3a. Immunity. 2004 Aug;21(2):203-13.
56. Yang XF, Fang P, Meng S, Jan M, Xiong XY, Yin Y, et al. The Forkhead Transcription Factors Play Important Roles in Vascular Pathology and Immunology. In: Maiese K, editor. Forkhead Transcription Factors: Vital Elements in Biology and Medicine. Advances in Experimental Medicine and Biology. 2009. p. 90-105.
57. Henderson ST, Bonafe M, Johnson TE. daf-16 protects the nematode Caenorhabditis elegans during food deprivation. Journals of Gerontology Series a-Biological Sciences and Medical Sciences. 2006 May;61(5):444-60.

58. Brunet A, Sweeney LB, Sturgill JF, Chua KF, Greer PL, Lin YX, et al. Stress-dependent regulation of FOXO transcription factors by the SIRT1 deacetylase. Science. 2004 Mar;303(5666):2011-15.
59. Salminen A, Huuskonen J, Ojala J, Kauppinen A, Kaarniranta K, Suuronen T. Activation of innate immunity system during aging: NF-kappa B signaling is the molecular culprit of inflamm-aging. Ageing Research Reviews. 2008 Apr;7(2):83-105.
60. Bai P, Canto C. The Role of PARP-1 and PARP-2 Enzymes in Metabolic Regulation and Disease. Cell Metabolism. 2012 Sep;16(3):290-95.
61. Morales JC, Li LS, Fattah FJ, Dong Y, Bey EA, Patel M, et al. Review of Poly (ADP-ribose) Polymerase (PARP) Mechanisms of Action and Rationale for Targeting in Cancer and Other Diseases. Critical Reviews in Eukaryotic Gene Expression. 2014;24(1):15-28.
62. Gibson BA, Kraus WL. New insights into the molecular and cellular functions of poly(ADP-ribose) and PARPs. Nature Reviews Molecular Cell Biology. 2012 Jul;13(7):411-24.
63. Bai P, Canto C, Oudart H, Brunyanszki A, Cen YN, Thomas C, et al. PARP-1 Inhibition Increases Mitochondrial Metabolism through SIRT1 Activation. Cell Metabolism. 2011 Apr;13(4):461-68.
64. Rottenberg S, Jaspers JE, Kersbergen A, van der Burg E, Nygren AOH, Zander SAL, et al. High sensitivity of BRCA1-deficient mammary tumors to the PARP inhibitor AZD2281 alone and in combination with platinum drugs. Proceedings of the National Academy of Sciences of the United States of America. 2008 Nov;105(44):17079-84.
65. Bey EA, Bentle MS, Reinicke KE, Dong Y, Yang CR, Girard L, et al. An NQO1-and PARP-1-mediated cell death pathway induced in non-small-cell lung cancer cells by beta-lapachone. Proceedings of the National Academy of Sciences of the United States of America. 2007 Jul;104(28):11832-37.
66. Seimiya H, Muramatsu Y, Ohishi T, Tsuruo T. Tankyrase 1 as a target for telomere-directed molecular cancer therapeutics. Cancer Cell. 2005 Jan;7(1):25-37.
67. Seimiya H. The telomeric PARP, tankyrases, as targets for cancer therapy. British Journal of Cancer. 2006 Feb;94(3):341-45.
68. Malavasi F, Deaglio S, Funaro A, Ferrero E, Horenstein AL, Ortolan E, et al. Evolution and function of the ADP ribosyl cyclase/CD38 gene family in physiology and pathology. Physiological Reviews. 2008 Jul;88(3):841-86.
69. Quarona V, Zaccarello G, Chillemi A, Brunetti E, Singh VK, Ferrero E, et al. CD38 and CD157: A long journey from activation markers to multifunctional molecules. Cytometry Part B-Clinical Cytometry. 2013 Jul-Aug;84B(4):207-17.
70. Barbosa MTP, Soares SM, Novak CM, Sinclair D, Levine JA, Aksoy P, et al. The enzyme CD38 (a NAD glycohydrolase, EC 3.2.2.5) is necessary for the development of diet-induced obesity. Faseb Journal. 2007 Nov;21(13):3629-39.
71. Malavasi F, Deaglio S, Damle R, Cutrona G, Ferrarini M, Chiorazzi N. CD38 and chronic lymphocytic leukemia: a decade later. Blood. 2011 Sep;118(13):3470-78.
72. Deaglio S, Capobianco A, Bergui L, Durig J, Morabito F, Duhrsen U, et al. CD38 is a signaling molecule in B-cell chronic lymphocytic leukemia cells. Blood. 2003 Sep;102(6):2146-55.
73. Ikehata F, Satoh J, Nata K, Tohgo A, Nakazawa T, Kato I, et al. Autoantibodies against CD38 (ADP ribosyl cyclase cyclic ADP ribose hydrolase) that impair glucose-induced insulin secretion in noninsulin-dependent diabetes patients. Journal of Clinical Investigation. 1998 Jul;102(2):395-401.
74. Aksoy P, White TA, Thompson M, Chini EN. Regulation of intracellular levels of NAD: A novel role for CD38. Biochemical and Biophysical Research Communications. 2006 Jul;345(4):1386-92.

75. Aksoy P, Escande C, White TA, Thompson M, Soares S, Benech JC, et al. Regulation of SIRT 1 mediated NAD dependent deacetylation: A novel role for the multifunctional enzyme CD38. Biochemical and Biophysical Research Communications. 2006 Oct;349(1):353-59.
76. Braidy N, Guillemin GJ, Mansour H, Chan-Ling T, Poljak A, Grant R. Age Related Changes in NAD plus Metabolism Oxidative Stress and Sirt1 Activity in Wistar Rats. Plos One. 2011 Apr;6(4).
77. Mouchiroud L, Houtkooper RH, Moullan N, Katsyuba E, Ryu D, Canto C, et al. The NAD(+)/Sirtuin Pathway Modulates Longevity through Activation of Mitochondrial UPR and FOXO Signaling. Cell. 2013 Jul;154(2):430-41.
78. Camacho-Pereira J, Tarrago MG, Chini CCS, Nin V, Escande C, Warner GM, et al. CD38 Dictates Age-Related NAD Decline and Mitochondrial Dysfunction through an SIRT3-Dependent Mechanism. Cell Metabolism. 2016 Jun;23(6):1127-39.
79. Ramsey KM, Mills KF, Satoh A, Imai SI. Age-associated loss of Sirt1-mediated enhancement of glucose-stimulated insulin secretion in beta cell-specific Sirt1-overexpressing (BESTO) mice. Aging Cell. 2008 Feb;7(1):78-88.
80. Yoshino J, Baur JA, Imai SI. NAD(+) Intermediates: The Biology and Therapeutic Potential of NMN and NR. Cell Metabolism. 2018 Mar;27(3):513-28.
81. Yoshino J, Mills KF, Yoon MJ, Imai SI. Nicotinamide Mononucleotide, a Key NAD(+) Intermediate, Treats the Pathophysiology of Diet- and Age-Induced Diabetes in Mice. Cell Metabolism. 2011 Oct;14(4):528-36.
82. Beneke S, Bukle A. Poly(ADP-ribosyl)ation in mammalian ageing. Nucleic Acids Research. 2007 Dec;35(22):7456-65.
83. Burkle A. DNA repair and PARP in aging. Free Radical Research. 2006 Dec;40(12):1295-302.
84. Imai S, Yoshino J. The importance of NAMPT/NAD/SIRT1 in the systemic regulation of metabolism and ageing. Diabetes Obesity & Metabolism. 2013 Sep;15:26-33.
85. Stein LR, Imai S. Specific ablation of Nampt in adult neural stem cells recapitulates their functional defects during aging. Embo Journal. 2014 Jun;33(12):1321-40.
86. Imai S. Nicotinamide Phosphoribosyltransferase (Nampt): A Link Between NAD Biology, Metabolism, and Diseases. Current Pharmaceutical Design. 2009 Jan;15(1):20-28.
87. Zheng CX, Lu M, Guo YB, Zhang FX, Liu H, Guo F, et al. Electroacupuncture Ameliorates Learning and Memory and Improves Synaptic Plasticity via Activation of the PKA/CREB Signaling Pathway in Cerebral Hypoperfusion. Evidence-Based Complementary and Alternative Medicine. 2016:11.
88. de Picciotto NE, Gano LB, Johnson LC, Martens CR, Sindler AL, Mills KF, et al. Nicotinamide mononucleotide supplementation reverses vascular dysfunction and oxidative stress with aging in mice. Aging Cell. 2016 Jun;15(3):522-30.
89. Williams PA, Harder JM, Foxworth NE, Cardozo BH, Cochran KE, John SWM. Nicotinamide and WLDS Act Together to Prevent Neurodegeneration in Glaucoma. Frontiers in Neuroscience. 2017 Apr;11.
90. Gariani K, Menzies KJ, Ryu D, Wegner CJ, Wang X, Ropelle ER, et al. Eliciting the Mitochondrial Unfolded Protein Response by Nicotinamide Adenine Dinucleotide Repletion Reverses Fatty Liver Disease in Mice. Hepatology. 2016 Apr;63(4):1190-204.
91. Trammell SAJ, Weidemann BJ, Chadda A, Yorek MS, Holmes A, Coppey LJ, et al. Nicotinamide Riboside Opposes Type 2 Diabetes and Neuropathy in Mice. Scientific Reports. 2016 May;6.
92. Gariani K, Ryu D, Menzies KJ, Yi HS, Stein S, Zhang H, et al. Inhibiting poly ADP-ribosylation increases fatty acid oxidation and protects against fatty liver disease. Journal of Hepatology. 2017 Jan;66(1):132-41.

93. Bordone L, Motta MC, Picard F, Robinson A, Jhala US, Apfeld J, et al. Sirt1 regulates insulin secretion by repressing UCP2 in pancreatic beta cells. Plos Biology. 2006 Feb;4(2):210-20.
94. Pfluger PT, Herranz D, Velasco-Miguel S, Serrano M, Tschop MH. Sirt1 protects against high-fat diet-induced metabolic damage. Proceedings of the National Academy of Sciences of the United States of America. 2008 Jul;105(28):9793-98.
95. Friedman SL, Neuschwander-Tetri BA, Rinella M, Sanyal AJ. Mechanisms of NAFLD development and therapeutic strategies. Nature Medicine. 2018 Jul;24(7):908-22.
96. Kalus P, Slotboom J, Gallinat J, Mahlberg R, Cattapan-Ludewig K, Wiest R, et al. Examining the gateway to the limbic system with diffusion tensor imaging: The perforant pathway in dementia. Neuroimage. 2006 Apr;30(3):713-20.
97. Kandan NM, Pigino GF, Brady ST, Lazarov O, Binder LI, Morfini GA. Axonal degeneration in Alzheimer's disease: When signaling abnormalities meet the axonal transport system. Experimental Neurology. 2013 Aug;246:44-53.
98. Martin LJ, Pan Y, Price AC, Sterling W, Copeland NG, Jenkins NA, et al. Parkinson's disease alpha-synuclein transgenic mice develop neuronal mitochondrial degeneration and cell death. Journal of Neuroscience. 2006 Jan;26(1):41-50.
99. Dutta R, McDonough J, Yin XG, Peterson J, Chang A, Torres T, et al. Mitochondrial dysfunction as a cause of axonal degeneration in multiple sclerosis patients. Annals of Neurology. 2006 Mar;59(3):478-89.
100. Mack TGA, Reiner M, Beirowski B, Mi WQ, Emanuelli M, Wagner D, et al. Wallerian degeneration of injured axons and synapses is delayed by a Ube4b/Nmnat chimeric gene. Nature Neuroscience. 2001 Dec;4(12):1199-206.
101. Samsam M, Mi WQ, Wessig C, Zielasek R, Toyka KV, Coleman MP, et al. The Wld(s) mutation delays robust loss of motor and sensory axons in a genetic model for myelin-related axonopathy. Journal of Neuroscience. 2003 Apr;23(7):2833-39.
102. Conforti L, Wilbrey A, Morreale G, Janeckova L, Beirowski B, Adalbert R, et al. Wld(S) protein requires Nmnat activity and a short N-terminal sequence to protect axons in mice. Journal of Cell Biology. 2009 Feb;184(4):491-500.
103. Conforti L, Gilley J, Coleman MP. Wallerian degeneration: an emerging axon death pathway linking injury and disease. Nature Reviews Neuroscience. 2014 Jun;15(6):394-409.
104. Wang G, Han T, Nijhawan D, Theodoropoulos P, Naidoo J, Yadavalli S, et al. P7C3 Neuroprotective Chemicals Function by Activating the Rate-Limiting Enzyme in NAD Salvage. Cell. 2014 Sep;158(6):1324-34.
105. Pieper AA, Xie SH, Capota E, Estill SJ, Zhong JN, Long JM, et al. Discovery of a Proneurogenic, Neuroprotective Chemical. Cell. 2010 Jul;142(1):39-51.
106. Yin TC, Britt JK, De Jesus-Cortes H, Lu Y, Genova RM, Khan MZ, et al. P7C3 Neuroprotective Chemicals Block Axonal Degeneration and Preserve Function after Traumatic Brain Injury. Cell Reports. 2014 Sep;8(6):1731-40.
107. Katsyuba E, Auwerx J. Modulating NAD(+) metabolism, from bench tobedside. Embo Journal. 2017 Sep;36(18):2670-83.
108. De Jesus-Cortes H, Xu P, Drawbridge J, Estill SJ, Huntington P, Tran S, et al. Neuroprotective efficacy of aminopropyl carbazoles in a mouse model of Parkinson disease. Proceedings of the National Academy of Sciences of the United States of America. 2012 Oct;109(42):17010-15.
109. Tesla R, Wolf HP, Xu P, Drawbridge J, Estill SJ, Huntington P, et al. Neuroprotective efficacy of aminopropyl carbazoles in a mouse model of amyotrophic lateral sclerosis. Proceedings of the National Academy of Sciences of the United States of America. 2012 Oct;109(42):17016-21.

110. Sasaki Y, Nakagawa T, Mao XR, DiAntonio A, Milbrandt J. NMNAT1 inhibits axon degeneration via blockade of SARM1-mediated NAD(+) depletion. Elife. 2016 Oct;5.
111. Schoenmann Z, Assa-Kunik E, Tiomny S, Minis A, Haklai-Topper L, Arama E, et al. Axonal Degeneration Is Regulated by the Apoptotic Machinery or a NAD(+)-Sensitive Pathway in Insects and Mammals. Journal of Neuroscience. 2010 May;30(18):6375-86.
112. Araki T, Sasaki Y, Milbrandt J. Increased nuclear NAD biosynthesis and SIRT1 activation prevent axonal degeneration. Science. 2004 Aug;305(5686):1010-13.
113. Yan TT, Feng Y, Zhai QW. Axon degeneration: Mechanisms and implications of a distinct program from cell death. Neurochemistry International. 2010 Mar;56(4):529-34.
114. Kim D, Nguyen MD, Dobbin MM, Fischer A, Sananbenesi F, Rodgers JT, et al. SIRT1 deacetylase protects against neurodegeneration in models for Alzheimer's disease and amyotrophic lateral sclerosis. Embo Journal. 2007 Jul;26(13):3169-79.
115. Donmez G, Arun A, Chung CY, McLean PJ, Lindquist S, Guarente L. SIRT1 Protects against alpha-Synuclein Aggregation by Activating Molecular Chaperones. Journal of Neuroscience. 2012 Jan;32(1):124-32.
116. Jiang ML, Wang JW, Fu JR, Du L, Jeong H, West T, et al. Neuroprotective role of Sirt1 in mammalian models of Huntington's disease through activation of multiple Sirt1 targets. Nature Medicine. 2012 Jan;18(1):153-58.
117. Jeong H, Cohen DE, Cui LB, Supinski A, Savas JN, Mazzulli JR, et al. Sirt1 mediates neuroprotection from mutant huntingtin by activation of the TORC1 and CREB transcriptional pathway. Nature Medicine. 2012 Jan;18(1):159-65.
118. Brown KD, Maqsood S, Huang JY, Pan Y, Harkcom W, Li W, et al. Activation of SIRT3 by the NAD(+) Precursor Nicotinamide Riboside Protects from Noise-Induced Hearing Loss. Cell Metabolism. 2014 Dec;20(6):1059-68.
119. Scheibye-Knudsen M, Mitchell SJ, Fang EF, Iyama T, Ward T, Wang J, et al. A High-Fat Diet and NAD(+) Activate Sirt1 to Rescue Premature Aging in Cockayne Syndrome. Cell Metabolism. 2014 Nov;20(5):840-55.
120. Fang EF, Kassahun H, Croteau DL, Scheibye-Knudsen M, Marosi K, Lu HM, et al. NAD(+) Replenishment Improves Lifespan and Healthspan in Ataxia Telangiectasia Models via Mitophagy and DNA Repair. Cell Metabolism. 2016 Oct;24(4):566-81.
121. Lakatta EG. So! What's aging? Is cardiovascular aging a disease? Journal of Molecular and Cellular Cardiology. 2015 Jun;83:1-13.
122. Warboys CM, de Luca A, Amini N, Luong L, Duckles H, Hsiao S, et al. Disturbed Flow Promotes Endothelial Senescence via a p53-Dependent Pathway. Arteriosclerosis Thrombosis and Vascular Biology. 2014 May;34(5):985-95.
123. Gorenne I, Kumar S, Gray K, Figg N, Yu HX, Mercer J, et al. Vascular Smooth Muscle Cell Sirtuin 1 Protects Against DNA Damage and Inhibits Atherosclerosis. Circulation. 2013 Jan;127(3):386-+.
124. Wallace DC. Mitochondrial defects in cardiomyopathy and neuromuscular disease. American Heart Journal. 2000 Feb;139(2):S70-S85.
125. Winnik S, Auwerx J, Sinclair DA, Matter CM. Protective effects of sirtuins in cardiovascular diseases: from bench to bedside. European Heart Journal. 2015 Dec;36(48):3404-U120.
126. Wallace DC. Mitochondrial diseases in man and mouse. Science. 1999 Mar;283(5407):1482-88.
127. Pillai VB, Sundaresan NR, Jeevanandam V, Gupta MP. Mitochondrial SIRT3 and heart disease. Cardiovascular Research. 2010 Nov;88(2):250-56.
128. Khan JA, Forouhar F, Tao X, Tong L. Nicotinamide adenine dinucleotide metabolism as an attractive target for drug discovery. Expert Opinion on Therapeutic Targets. 2007 May;11(5):695-705.

129. Bi TQ, Che XM. Nampt/PBEF/visfatin and cancer. Cancer Biology & Therapy. 2010 Jul;10(2):119-25.
130. Bi TQ, Che XM, Liao XH, Zhang DJ, Long HL, Li HJ, et al. Overexpression of Nampt in gastric cancer and chemopotentiating effects of the Nampt inhibitor FK866 in combination with fluorouracil. Oncology Reports. 2011 Nov;26(5):1251-57.
131. Lee YC, Yang YH, Su JH, Chang HL, Hou MF, Yuan SSF. High Visfatin Expression in Breast Cancer Tissue Is Associated with Poor Survival. Cancer Epidemiology Biomarkers & Prevention. 2011 Sep;20(9):1892-901.
132. Wang B, Hasan MK, Alvarado E, Yuan H, Wu H, Chen WY. NAMPT overexpression in prostate cancer and its contribution to tumor cell survival and stress response. Oncogene. 2011 Feb;30(8):907-21.
133. Hasmann M, Schemainda I. FK866, a highly specific noncompetitive inhibitor of nicotinamide phosphoribosyltransferase, represents a novel mechanism for induction of tumor cell apoptosis. Cancer Research. 2003 Nov;63(21):7436-42.
134. Billington RA, Genazzani AA, Travelli C, Condorelli F. NAD depletion by FK866 induces autophagy. Autophagy. 2008 Apr;4(3):385-87.
135. Billington RA, Travelli C, Ercolano E, Galli U, Roman CB, Grolla AA, et al. Characterization of NAD uptake in mammalian cells. Journal of Biological Chemistry. 2008 Mar;283(10):6367-74.
136. Cagnetta A, Cea M, Calimeri T, Acharya C, Fulciniti M, Tai YT, et al. Intracellular NAD(+) depletion enhances bortezomib-induced anti-myeloma activity. Blood. 2013 Aug;122(7):1243-55.
137. Holen K, Saltz LB, Hollywood E, Burk K, Hanauske AR. The pharmacokinetics, toxicities, and biologic effects of FK866, a nicotinamide adenine dinucleotide biosynthesis inhibitor. Investigational New Drugs. 2008 Feb;26(1):45-51.
138. Garten A, Petzold S, Korner A, Imai S, Kiess W. Nampt: linking NAD biology, metabolism and cancer. Trends in Endocrinology and Metabolism. 2009 Apr;20(3):130-38.
139. He JY, Tu C, Li MJ, Wang SL, Guan XM, Lin JF, et al. Nampt/Visfatin/PBEF: A Functionally Multi-faceted Protein with a Pivotal Role in Malignant Tumors. Current Pharmaceutical Design. 2012 Dec;18(37):6123-32.
140. Sharif T, Ahn DG, Liu RZ, Pringle E, Martell E, Dai C, et al. The NAD(+) salvage pathway modulates cancer cell viability via p73. Cell Death and Differentiation. 2016 Apr;23(4):669-80.
141. Labbadia J, Morimoto RI. Huntington's disease: underlying molecular mechanisms and emerging concepts. Trends in Biochemical Sciences. 2013 Aug;38(8):378-85.
142. Krstic D, Knuesel I. Deciphering the mechanism underlying late-onset Alzheimer disease. Nature Reviews Neurology. 2013 Jan;9(1):25-34.
143. Trinh J, Farrer M. Advances in the genetics of Parkinson disease. Nature Reviews Neurology. 2013 Aug;9(8):445-54.
144. Robberecht W, Philips T. The changing scene of amyotrophic lateral sclerosis. Nature Reviews Neuroscience. 2013 Apr;14(4):248-64.
145. Ron D, Hubbard SR. How IRe1 reacts to ER stress. Cell. 2008 Jan;132(1):24-26.
146. Lee AH, Heidtman K, Hotamisligil GS, Glimcher LH. Dual and opposing roles of the unfolded protein response regulated by IRE1 alpha and XBP1 in proinsulin processing and insulin secretion. Proceedings of the National Academy of Sciences of the United States of America. 2011 May;108(21):8885-90.
147. Yoshida H, Matsui T, Yamamoto A, Okada T, Mori K. XBP1 mRNA is induced by ATF6 and spliced by IRE1 in response to ER stress to produce a highly active transcription factor. Cell. 2001 Dec;107(7):881-91.

148. Calfon M, Zeng HQ, Urano F, Till JH, Hubbard SR, Harding HP, et al. IRE1 couples endoplasmic reticulum load to secretory capacity by processing the XBP-1 mRNA. Nature. 2002 Jan;415(6867):92-96.
149. Needham PG, Brodsky JL. How early studies on secreted and membrane protein quality control gave rise to the ER associated degradation (ERAD) pathway: The early history of ERAD. Biochimica Et Biophysica Acta-Molecular Cell Research. 2013 Nov;1833(11):2447-57.
150. Smith MH, Ploegh HL, Weissman JS. Road to Ruin: Targeting Proteins for Degradation in the Endoplasmic Reticulum. Science. 2011 Nov;334(6059):1086-90.
151. Walter P, Ron D. The Unfolded Protein Response: From Stress Pathway to Homeostatic Regulation. Science. 2011 Nov;334(6059):1081-86.
152. Haze K, Yoshida H, Yanagi H, Yura T, Mori K. Mammalian transcription factor ATF6 is synthesized as a transmembrane protein and activated by proteolysis in response to endoplasmic reticulum stress. Molecular Biology of the Cell. 1999 Nov;10(11):3787-99.
153. Yamamoto K, Sato T, Matsui T, Sato M, Okada T, Yoshida H, et al. Transcriptional induction of mammalian ER quality control proteins is mediated by single or combined action of ATF6 alpha and XBP1. Developmental Cell. 2007 Sep;13(3):365-76.
154. Hetz C, Papa FR. The Unfolded Protein Response and Cell Fate Control. Molecular Cell. 2018 Jan;69(2):169-81.
155. Glickman MH, Ciechanover A. The ubiquitin-proteasome proteolytic pathway: Destruction for the sake of construction. Physiological Reviews. 2002 Apr;82(2):373-428.
156. da Cunha FM, Demasi M, Kowaltowski AJ. Aging and calorie restriction modulate yeast redox state, oxidized protein removal, and the ubiquitin-proteasome system. Free Radical Biology and Medicine. 2011 Aug;51(3):664-70.
157. Strucksberg KH, Tangavelou K, Schroder R, Clemen CS. Proteasomal activity in skeletal muscle: A matter of assay design, muscle type, and age. Analytical Biochemistry. 2010 Apr;399(2):225-29.
158. Cavo M. Proteasome inhibitor bortezomib for the treatment of multiple myeloma. Leukemia. 2006 Aug;20(8):1341-52.
159. Keller JN, Hanni KB, Markesbery WR. Impaired proteasome function in Alzheimer's disease. Journal of Neurochemistry. 2000 Jul;75(1):436-39.
160. Thibaudeau TA, Smith DM. A Practical Review of Proteasome Pharmacology. Pharmacological Reviews. 2019 Apr;71(2):170-97.
161. Doyle SM, Genest O, Wickner S. Protein rescue from aggregates by powerful molecular chaperone machines. Nature Reviews Molecular Cell Biology. 2013 Oct;14(10):617-29.
162. Labbadia J, Morimoto RI. The Biology of Proteostasis in Aging and Disease. In: Kornberg RD, editor. Annual Review of Biochemistry, Vol 84. Annual Review of Biochemistry. Palo Alto: Annual Reviews; 2015. p. 435-64.
163. Yang ZF, Klionsky DJ. Mammalian autophagy: core molecular machinery and signaling regulation. Current Opinion in Cell Biology. 2010 Apr;22(2):124-31.
164. Laskey RA, Honda BM, Mills AD, Finch JT. NUCLEOSOMES ARE ASSEMBLED BY AN ACIDIC PROTEIN WHICH BINDS HISTONES AND TRANSFERS THEM TO DNA. Nature. 1978;275(5679):416-20.
165. Ellis J. PROTEINS AS MOLECULAR CHAPERONES. Nature. 1987 Jul;328(6129):378-79.
166. Kim YE, Hipp MS, Bracher A, Hayer-Hartl M, Hartl FU. Molecular Chaperone Functions in Protein Folding and Proteostasis. In: Kornberg RD, editor. Annual Review of Biochemistry, Vol 82. Annual Review of Biochemistry. Palo Alto: Annual Reviews; 2013. p. 323-55.
167. Taipale M, Jarosz DF, Lindquist S. HSP90 at the hub of protein homeostasis: emerging mechanistic insights. Nature Reviews Molecular Cell Biology. 2010 Jul;11(7):515-28.

168. Matos S, Campos D, Pinho R, Silva RM, Mort M, Cooper DN, et al. Mining clinical attributes of genomic variants through assisted literature curation in Egas. Database-the Journal of Biological Databases and Curation. 2016 Jun.
169. Campos D, Lourenço J, Matos S, Oliveira JL. Egas: a collaborative and interactive document curation platform. Database (Oxford). 2014;2014.
170. Chen YM, Huang XW, Zhang YW, Rockenstein E, Bu GJ, Golde TE, et al. Alzheimer's beta-Secretase (BACE1) Regulates the cAMP/PKA/CREB Pathway Independently of beta-Amyloid. Journal of Neuroscience. 2012 Aug;32(33):11390-95.
171. Tang YS, Shao SJ, Guo Y, Zhou Y, Cao J, Xu AP, et al. Electroacupuncture Mitigates Hippocampal Cognitive Impairments by Reducing BACE1 Deposition and Activating PKA in APP/PS1 Double Transgenic Mice. Neural Plasticity. 2019:12.
172. Haass C, Selkoe DJ. CELLULAR PROCESSING OF BETA-AMYLOID PRECURSOR PROTEIN AND THE GENESIS OF AMYLOID BETA-PEPTIDE. Cell. 1993 Dec;75(6):1039-42.
173. Mockett BG, Richter M, Abraham WC, Muller UC. Therapeutic Potential of Secreted Amyloid Precursor Protein APPs alpha. Frontiers in Molecular Neuroscience. 2017 Feb;10:14.
174. Mockett BG, Guevremont D, Elder MK, Parfitt KD, Peppercorn K, Morrissey J, et al. Glutamate Receptor Trafficking and Protein Synthesis Mediate the Facilitation of LTP by Secreted Amyloid Precursor Protein-Alpha. Journal of Neuroscience. 2019 Apr;39(17):3188-203.
175. Wyss-Coray T, Yan FR, Lin AHT, Lambris JD, Alexander JJ, Quigg RJ, et al. Prominent neurodegeneration and increased plaque formation in complement-inhibited Alzheimer's mice. Proceedings of the National Academy of Sciences of the United States of America. 2002 Aug;99(16):10837-42.
176. Yin CJ, Ackermann S, Ma Z, Mohanta SK, Zhang CK, Li YF, et al. ApoE attenuates unresolvable inflammation by complex formation with activated C1q. Nature Medicine. 2019 Mar;25(3):496-+.
177. Zamolodchikov D, Renne T, Strickland S. The Alzheimer's disease peptide beta-amyloid promotes thrombin generation through activation of coagulation factor XII. Journal of Thrombosis and Haemostasis. 2016 May;14(5):995-1007.
178. Lanna A, Gomes DCO, Muller-Durovic B, McDonnell T, Escors D, Gilroy DW, et al. A sestrin-dependent Erk-Jnk-p38 MAPK activation complex inhibits immunity during aging. Nature Immunology. 2017 Mar;18(3):354-63.
179. Di Mitri D, Azevedo RI, Henson SM, Libri V, Riddell NE, Macaulay R, et al. Reversible Senescence in Human CD4(+)CD45RA(+)CD27(-) Memory T Cells. Journal of Immunology. 2011 Sep;187(5):2093-100.
180. Veng LM, Mesches MH, Browning MD. Age-related working memory impairment is correlated with increases in the L-type calcium channel protein alpha(1D) (Ca(v)1.3) in area CA1 of the hippocampus and both are ameliorated by chronic nimodipine treatment. Molecular Brain Research. 2003 Feb;110(2):193-202.
181. Foster TC, Sharrow KM, Masse JR, Norris CM, Kumar A. Calcineurin links Ca2+ dysregulation with brain aging. Journal of Neuroscience. 2001 Jun;21(11):4066-73.
182. Abraham WC, Logan B, Greenwood JM, Dragunow M. Induction and experience-dependent consolidation of stable long-term potentiation lasting months in the hippocampus. Journal of Neuroscience. 2002 Nov;22(21):9626-34.
183. Ryan MM, Guevremont D, Luxmanan C, Abraham WC, Williams JM. Aging alters long-term potentiation-related gene networks and impairs synaptic protein synthesis in the rat hippocampus. Neurobiology of Aging. 2015 May;36(5):1868-80.
184. Glass C, Singla DK. MicroRNA-1 transfected embryonic stem cells enhance cardiac myocyte differentiation and inhibit apoptosis by modulating the PTEN/Akt pathway in the

infarcted heart. American Journal of Physiology-Heart and Circulatory Physiology. 2011 Nov;301(5):H2038-H49.
185. Morissette MR, Cook SA, Foo S, McKoy G, Ashida N, Novikov M, et al. Myostatin regulates cardiomyocyte growth through modulation of Akt signaling. Circulation Research. 2006 Jul;99(1):15-24.
186. Gutkind JS. The pathways connecting G protein-coupled receptors to the nucleus through divergent mitogen-activated protein kinase cascades. Journal of Biological Chemistry. 1998 Jan;273(4):1839-42.
187. Daud A, Bastian BC. Beyond BRAF in Melanoma. In: Mellinghoff IK, Sawyers CL, editors. Therapeutic Kinase Inhibitors. Current Topics in Microbiology and Immunology. Berlin: Springer-Verlag Berlin; 2012. p. 99-117.
188. Land H, Parada LF, Weinberg RA. TUMORIGENIC CONVERSION OF PRIMARY EMBRYO FIBROBLASTS REQUIRES AT LEAST 2 COOPERATING ONCOGENES. Nature. 1983;304(5927):596-602.
189. Tang ZJ, Dai SY, He YS, Doty RA, Shultz LD, Sampson SB, et al. MEK Guards Proteome Stability and Inhibits Tumor-Suppressive Amyloidogenesis via HSF1. Cell. 2015 Feb;160(4):729-44.
190. Mulholland DJ, Kobayashi N, Ruscetti M, Zhi A, Tran LM, Huang JT, et al. Pten Loss and RAS/MAPK Activation Cooperate to Promote EMT and Metastasis Initiated from Prostate Cancer Stem/Progenitor Cells. Cancer Research. 2012 Apr;72(7):1878-89.
191. Yang JB, Price MA, Neudauer CL, Wilson C, Ferrone S, Xia H, et al. Melanoma chondroitin sulfate proteoglycan enhances FAK and ERK activation by distinct mechanisms. Journal of Cell Biology. 2004 Jun;165(6):881-91.
192. Chen WS, Xu PZ, Gottlob K, Chen ML, Sokol K, Shiyanova T, et al. Growth retardation and increased apoptosis in mice with homozygous disruption of the akt1 gene. Genes & Development. 2001 Sep;15(17):2203-08.
193. Wright GL, Maroulakou IG, Eldridge J, Liby TL, Sridharan V, Tsichlis PN, et al. VEGF stimulation of mitochondrial biogenesis: requirement of AKT3 kinase. Faseb Journal. 2008 Sep;22(9):3264-75.
194. Turner KM, Sun YT, Ji P, Granberg KJ, Bernard B, Hu LM, et al. Genomically amplified Akt3 activates DNA repair pathway and promotes glioma progression. Proceedings of the National Academy of Sciences of the United States of America. 2015 Mar;112(11):3421-26.
195. Xu YX, Li N, Xiang R, Sun PQ. Emerging roles of the p38 MAPK and PI3K/AKT/mTOR pathways in oncogene-induced senescence. Trends in Biochemical Sciences. 2014 Jun;39(6):268-76.
196. Heneka MT, Kummer MP, Latz E. Innate immune activation in neurodegenerative disease. Nature Reviews Immunology. 2014 Jul;14(7):463-77.
197. Laurent C, Buee L, Blum D. Tau and neuroinflammation: What impact for Alzheimer's Disease and Tauopathies? Biomedical Journal. 2018 Feb;41(1):21-33.
198. Sanchez-Guajardo V, Tentillier N, Romero-Ramos M. THE RELATION BETWEEN alpha-SYNUCLEIN AND MICROGLIA IN PARKINSON'S DISEASE: RECENT DEVELOPMENTS. Neuroscience. 2015 Aug;302:47-58.
199. Crotti A, Glass CK. The choreography of neuroinflammation in Huntington's disease. Trends in Immunology. 2015 Jun;36(6):364-73.
200. Stewart CR, Stuart LM, Wilkinson K, van Gils JM, Deng JS, Halle A, et al. CD36 ligands promote sterile inflammation through assembly of a Toll-like receptor 4 and 6 heterodimer. Nature Immunology. 2010 Feb;11(2):155-U75.

201. Fellner L, Irschick R, Schanda K, Reindl M, Klimaschewski L, Poewe W, et al. Toll-like receptor 4 is required for alpha-synuclein dependent activation of microglia and astroglia. Glia. 2013 Mar;61(3):349-60.
202. Udan MLD, Ajit D, Crouse NR, Nichols MR. Toll-like receptors 2 and 4 mediate A beta(1-42) activation of the innate immune response in a human monocytic cell line. Journal of Neurochemistry. 2008 Jan;104(2):524-33.
203. Latz E, Xiao TS, Stutz A. Activation and regulation of the inflammasomes. Nature Reviews Immunology. 2013 Jun;13(6):397-411.
204. Tang Y, Le WD. Differential Roles of M1 and M2 Microglia in Neurodegenerative Diseases. Molecular Neurobiology. 2016 Mar;53(2):1181-94.
205. Tian A, Ma H, Zhang RW, Tan WF, Wang XL, Wu BY, et al. Interleukin17A Promotes Postoperative Cognitive Dysfunction by Triggering beta-Amyloid Accumulation via the Transforming Growth Factor-beta (TGF beta)/Smad Signaling Pathway. Plos One. 2015 Oct;10(10):18.
206. Opattova A, Cente M, Novak M, Filipcik P. The ubiquitin proteasome system as a potential therapeutic target for treatment of neurodegenerative diseases. General Physiology and Biophysics. 2015 Oct;34(4):337-52.
207. Bellucci A, Bugiani O, Ghetti B, Spillantini MG. Presence of Reactive Microglia and Neuroinflammatory Mediators in a Case of Frontotemporal Dementia with P301S Mutation. Neurodegenerative Diseases. 2011;8(4):221-29.
208. Schofield E, Kersaitis C, Shepherd CE, Kril JJ, Halliday GM. Severity of gliosis in Pick's disease and frontotemporal lobar degeneration: tau-positive glia differentiate these disorders. Brain. 2003 Apr;126:827-40.
209. Fernandez-Botran R, Ahmed Z, Crespo FA, Gatenbee C, Gonzalez J, Dickson DW, et al. Cytokine expression and rnicroglial activation in progressive supranuclear palsy. Parkinsonism & Related Disorders. 2011 Nov;17(9):683-88.
210. Kovac A, Zilka N, Kazmerova Z, Cente M, Zilkova M, Novak M. Misfolded Truncated Protein tau Induces Innate Immune Response via MAPK Pathway. Journal of Immunology. 2011 Sep;187(5):2732-39.
211. Li YK, Liu L, Barger SW, Griffin WST. Interleukin-1 mediates pathological effects of microglia on tau phosphorylation and on synaptophysin synthesis in cortical neurons through a p38-MAPK pathway. Journal of Neuroscience. 2003 Mar;23(5):1605-11.
212. Asai H, Ikezu S, Tsunoda S, Medalla M, Luebke J, Haydar T, et al. Depletion of microglia and inhibition of exosome synthesis halt tau propagation. Nature Neuroscience. 2015 Nov;18(11):1584-93.
213. Bolos M, Llorens-Martin M, Perea JR, Jurado-Arjona J, Rabano A, Hernandez F, et al. Absence of CX3CR1 impairs the internalization of Tau by microglia. Molecular Neurodegeneration. 2017 Aug;12:14.
214. Maphis N, Xu GX, Kokiko-Cochran ON, Jiang S, Cardona A, Ransohoff RM, et al. Reactive microglia drive tau pathology and contribute to the spreading of pathological tau in the brain. Brain. 2015 Jun;138:1738-55.
215. Lee DC, Rizer J, Selenica ML, Reid P, Kraft C, Johnson A, et al. LPS-Induced Inflammation Exacerbates Phospho-Tau Pathology in rTg4510 Mice. Cell Transplantation. 2010;19(3):347-47.
216. Kitazawa M, Oddo S, Yamasaki TR, Green KN, LaFerla FM. Lipopolysaccharide-induced inflammation exacerbates tau pathology by a cyclin-dependent kinase 5-mediated pathway in a transgenic model of Alzheimer's disease. Journal of Neuroscience. 2005 Sep;25(39):8843-53.

217. Bhaskar K, Konerth M, Kokiko-Cochran ON, Cardona A, Ransohoff RM, Lamb BT. Regulation of Tau Pathology by the Microglial Fractalkine Receptor. Neuron. 2010 Oct;68(1):19-31.
218. Obi T, Nishioka K, Ross OA, Terada T, Yamazaki K, Sugiura A, et al. Clinicopathologic study of a SNCA gene duplication patient with Parkinson disease and dementia. Neurology. 2008 Jan;70(3):238-41.
219. Sacino AN, Brooks M, McKinney AB, Thomas MA, Shaw G, Golde TE, et al. Brain Injection of alpha-Synuclein Induces Multiple Proteinopathies, Gliosis, and a Neuronal Injury Marker. Journal of Neuroscience. 2014 Sep;34(37):12368-78.
220. Bjorkqvist M, Wild EJ, Thiele J, Silvestroni A, Andre R, Lahiri N, et al. A novel pathogenic pathway of immune activation detectable before clinical onset in Huntington's disease. Journal of Experimental Medicine. 2008 Aug;205(8):1869-77.
221. Brodacki B, Staszewski J, Toczylowska B, Kozlowska E, Drela N, Chalimoniuk M, et al. Serum interleukin (IL-2, IL-10, IL-6, IL-4), TNF alpha, and INF gamma concentrations are elevated in patients with atypical and idiopathic parkinsonism. Neuroscience Letters. 2008 Aug;441(2):158-62.
222. Lastres-Becker I, Ulusoy A, Innamorato NG, Sahin G, Rabano A, Kirik D, et al. alpha-Synuclein expression and Nrf2 deficiency cooperate to aggravate protein aggregation, neuronal death and inflammation in early-stage Parkinson's disease. Human Molecular Genetics. 2012 Jul;21(14):3173-92.
223. Su XM, Maguire-Zeiss KA, Giuliano R, Prifti L, Venkatesh K, Federoff HJ. Synuclein activates microglia in a model of Parkinson's disease. Neurobiology of Aging. 2008 Nov;29(11):1690-701.
224. Holmqvist S, Chutna O, Bousset L, Aldrin-Kirk P, Li W, Bjorklund T, et al. Direct evidence of Parkinson pathology spread from the gastrointestinal tract to the brain in rats. Acta Neuropathologica. 2014 Dec;128(6):805-20.
225. Reynolds AD, Stone DK, Hutter JAL, Benner EJ, Mosley RL, Gendelman HE. Regulatory T Cells Attenuate Th17 Cell-Mediated Nigrostriatal Dopaminergic Neurodegeneration in a Model of Parkinson's Disease. Journal of Immunology. 2010 Mar;184(5):2261-71.
226. Wild EJ, Bjorkqvist M, Thiele J, Silvestroni A, Andre R, Lahiri N, et al. A novel pathogenic pathway of immune activation detectable before clinical onset in Huntington's disease. Journal of Neurology Neurosurgery and Psychiatry. 2008 Oct;79:A4-A4.
227. Chang KH, Wu YR, Chen YC, Chen CM. Plasma inflammatory biomarkers for Huntington's disease patients and mouse model. Brain Behavior and Immunity. 2015 Feb;44:121-27.
228. Sorolla MA, Reverter-Branchat G, Tamarit J, Ferrer I, Ros JQ, Cabiscol E. Proteomic and oxidative stress analysis in human brain samples of Huntington disease. Free Radical Biology and Medicine. 2008 Sep;45(5):667-78.
229. Browne SE, Bowling AC, MacGarvey U, Baik MJ, Berger SC, Muqit MMK, et al. Oxidative damage and metabolic dysfunction in Huntington's disease: Selective vulnerability of the basal ganglia. Annals of Neurology. 1997 May;41(5):646-53.
230. Hands S, Sajjad MU, Newton MJ, Wyttenbach A. In Vitro and in Vivo Aggregation of a Fragment of Huntingtin Protein Directly Causes Free Radical Production. Journal of Biological Chemistry. 2011 Dec;286(52):44512-20.
231. Wyttenbach A, Sauvageot O, Carmichael J, Diaz-Latoud C, Arrigo AP, Rubinsztein DC. Heat shock protein 27 prevents cellular polyglutamine toxicity and suppresses the increase of reactive oxygen species caused by huntingtin. Human Molecular Genetics. 2002 May;11(9):1137-51.
232. van den Bogaard SJA, Dumas EM, Roos RAC. The Role of Iron Imaging in Huntington's Disease. In: Bhatia KP, Schneider SA, editors. Metal Related Neurodegenerative Disease.

International Review of Neurobiology. San Diego: Elsevier Academic Press Inc; 2013. p. 241-50.
233. Hilditch-Maguire P, Trettel F, Passani LA, Auerbach A, Persichetti F, MacDonald ME. Huntingtin: an iron-regulated protein essential for normal nuclear and perinuclear organelles. Human Molecular Genetics. 2000 Nov;9(19):2789-97.
234. Firdaus WJJ, Wyttenbach A, Giuliano P, Kretz-Remy C, Currie RW, Arrigo AP. Huntingtin inclusion bodies are iron-dependent centers of oxidative events. Febs Journal. 2006 Dec;273(23):5428-41.
235. Giorgini F, Guidetti P, Nguyen QV, Bennett SC, Muchowski PJ. A genomic screen in yeast implicates kynurenine 3-monooxygenase as a therapeutic target for Huntington disease. Nature Genetics. 2005 May;37(5):526-31.
236. Sanchez-Lopez F, Tasset I, Aguera E, Feijoo M, Fernandez-Bolanos R, Sanchez FM, et al. Oxidative stress and inflammation biomarkers in the blood of patients with Huntington's disease. Neurological Research. 2012 Sep;34(7):721-24.
237. Weiss A, Trager U, Wild EJ, Grueninger S, Farmer R, Landles C, et al. Mutant huntingtin fragmentation in immune cells tracks Huntington's disease progression. Journal of Clinical Investigation. 2012 Oct;122(10):3731-36.
238. Trager U, Andre R, Lahiri N, Magnusson-Lind A, Weiss A, Grueninger S, et al. HTT-lowering reverses Huntington's disease immune dysfunction caused by NF kappa B pathway dysregulation. Brain. 2014 Mar;137:819-33.
239. Kwan W, Trager U, Davalos D, Chou A, Bouchard J, Andre R, et al. Mutant huntingtin impairs immune cell migration in Huntington disease. Journal of Clinical Investigation. 2012 Dec;122(12):4737-47.
240. Rosas HD, Lee SY, Bender AC, Zaleta AK, Vangel M, Yu P, et al. Altered white matter microstructure in the corpus callosum in Huntington's disease: Implications for cortical "disconnection". Neuroimage. 2010 Feb;49(4):2995-3004.
241. Tai YF, Pavese N, Gerhard A, Tabrizi SJ, Barker RA, Brooks DJ, et al. Microglial activation in presymptomatic Huntington's disease gene carriers. Brain. 2007 Jul;130:1759-66.
242. Crotti A, Benner C, Kerman BE, Gosselin D, Lagier-Tourenne C, Zuccato C, et al. Mutant Huntingtin promotes autonomous microglia activation via myeloid lineage-determining factors. Nature Neuroscience. 2014 Apr;17(4):513-U58.
243. Singhrao SK, Neal JW, Morgan BP, Gasque P. Increased complement biosynthesis by microglia and complement activation on neurons in Huntington's disease. Experimental Neurology. 1999 Oct;159(2):362-76.
244. Bradford J, Shin JY, Roberts M, Wang CE, Li XJ, Li S. Expression of mutant huntingtin in mouse brain astrocytes causes age-dependent neurological symptoms. Proceedings of the National Academy of Sciences of the United States of America. 2009 Dec;106(52):22480-85.
245. Lievens JC, Woodman B, Mahal A, Spasic-Boscovic O, Samuel D, Goff LKL, et al. Impaired glutamate uptake in the R6 Huntington's disease transgenic mice. Neurobiology of Disease. 2001 Oct;8(5):807-21.
246. Shin JY, Fang ZH, Yu ZX, Wang CE, Li SH, Li XJ. Expression of mutant huntingtin in glial cells contributes to neuronal excitotoxicity. Journal of Cell Biology. 2005 Dec;171(6):1001-12.
247. Ben Haim L, Ceyzeriat K, Carrillo-de Sauvage MA, Aubry F, Auregan G, Guillermier M, et al. The JAK/STAT3 Pathway Is a Common Inducer of Astrocyte Reactivity in Alzheimer's and Huntington's Diseases. Journal of Neuroscience. 2015 Feb;35(6):2817-29.
248. Dominguez E, Rivat C, Pommier B, Mauborgne A, Pohl M. JAK/STAT3 pathway is activated in spinal cord microglia after peripheral nerve injury and contributes to neuropathic pain development in rat. Journal of Neurochemistry. 2008 Oct;107(1):50-60.

249. Schuster S, Penke M, Gorski T, Gebhardt R, Weiss TS, Kiess W, et al. FK866-induced NAMPT inhibition activates AMPK and downregulates mTOR signaling in hepatocarcinoma cells. Biochemical and Biophysical Research Communications. 2015 Mar;458(2):334-40.
250. Barraud M, Garnier J, Loncle C, Gayet O, Lequeue C, Vasseur S, et al. A pancreatic ductal adenocarcinoma subpopulation is sensitive to FK866, an inhibitor of NAMPT. Oncotarget. 2016 Aug;7(33):53783-96.
251. Ju HQ, Zhuang ZN, Li H, Tian T, Lu YX, Fan XQ, et al. Regulation of the Nampt-mediated NAD salvage pathway and its therapeutic implications in pancreatic cancer. Cancer Letters. 2016 Aug;379(1):1-11.
252. Cea M, Cagnetta A, Acharya C, Acharya P, Tai YT, Yang C, et al. Dual NAMPT and BTK Targeting Leads to Synergistic Killing of Waldenstrom Macroglobulinemia Cells Regardless of MYD88 and CXCR4 Somatic Mutation Status. Clinical Cancer Research. 2016 Dec;22(24):6099-109.
253. Thakur BK, Dittrich T, Chandra P, Becker A, Kuehnau W, Klusmann JH, et al. Involvement of p53 in the cytotoxic activity of the NAMPT inhibitor FK866 in myeloid leukemic cells. International Journal of Cancer. 2013 Feb;132(4):766-74.
254. Galli U, Ercolano E, Carraro L, Roman CRB, Sorba G, Canonico PL, et al. Synthesis and biological evaluation of isosteric analogues of FK866, an inhibitor of NAD salvage. Chemmedchem. 2008 May;3(5):771-79.
255. Thakur BK, Dittrich T, Chandra P, Becker A, Lippka Y, Selvakumar D, et al. Inhibition of NAMPT pathway by FK866 activates the function of p53 in HEK293T cells. Biochemical and Biophysical Research Communications. 2012 Aug;424(3):371-77.
256. Sharif T, Martell E, Dai C, Kennedy BE, Murphy P, Clements DR, et al. Autophagic homeostasis is required for the pluripotency of cancer stem cells. Autophagy. 2017;13(2):264-84.
257. Theeramunkong S, Galli U, Grolla AA, Caldarelli A, Travelli C, Massarotti A, et al. Identification of a novel NAMPT inhibitor by combinatorial click chemistry and chemical refinement. Medchemcomm. 2015;6(10):1891-97.
258. Hara H, Sueyoshi S, Taniguchi M, Kamiya T, Adachi T. Differences in intracellular mobile zinc levels affect susceptibility to plasma-activated medium-induced cytotoxicity. Free Radical Research. 2017 Mar;51(3):306-15.
259. Grohmann T, Penke M, Petzold-Quinque S, Schuster S, Richter S, Kiess W, et al. Inhibition of NAMPT sensitizes MOLT4 leukemia cells for etoposide treatment through the SIRT2-p53 pathway. Leukemia Research. 2018 Jun;69:39-46.
260. Zucal C, D'Agostino VG, Casini A, Mantelli B, Thongon N, Soncini D, et al. EIF2A-dependent translational arrest protects leukemia cells from the energetic stress induced by NAMPT inhibition. Bmc Cancer. 2015 Nov;15.
261. Cerami E, Gao JJ, Dogrusoz U, Gross BE, Sumer SO, Aksoy BA, et al. The cBio Cancer Genomics Portal: An Open Platform for Exploring Multidimensional Cancer Genomics Data. Cancer Discovery. 2012 May;2(5):401-04.
262. Watson M, Roulston A, Belec L, Billot X, Marcellus R, Bedard D, et al. The Small Molecule GMX1778 Is a Potent Inhibitor of NAD(+) Biosynthesis: Strategy for Enhanced Therapy in Nicotinic Acid Phosphoribosyltransferase 1-Deficient Tumors. Molecular and Cellular Biology. 2009 Nov;29(21):5872-88.
263. Lee J, Kim H, Lee JE, Shin SJ, Oh S, Kwon G, et al. Selective Cytotoxicity of the NAMPT Inhibitor FK866 Toward Gastric Cancer Cells With Markers of the Epithelial-Mesenchymal Transition, Due to Loss of NAPRT. Gastroenterology. 2018 Sep;155(3):799-+.
264. Duarte-Pereira S, Pereira-Castro I, Silva SS, Correia MG, Neto C, da Costa LT, et al. Extensive regulation of nicotinate phosphoribosyltransferase (NAPRT) expression in human tissues and tumors. Oncotarget. 2016 Jan;7(2):1973-83.

265. Zerp SF, Vens C, Floot B, Verheij M, van Triest B. NAD(+) depletion by APO866 in combination with radiation in a prostate cancer model, results from an in vitro and in vivo study. Radiotherapy and Oncology. 2014 Feb;110(2):348-54.
266. Tolstikov V, Nikolayev A, Dong S, Zhao G, Kuo MS. Metabolomics Analysis of Metabolic Effects of Nicotinamide Phosphoribosyltransferase (NAMPT) Inhibition on Human Cancer Cells. Plos One. 2014 Dec;9(12).
267. Piacente F, Caffa I, Ravera S, Sociali G, Passalacqua M, Vellone VG, et al. Nicotinic Acid Phosphoribosyltransferase Regulates Cancer Cell Metabolism, Susceptibility to NAMPT Inhibitors, and DNA Repair. Cancer Research. 2017 Jul;77(14):3857-69.